Mapping Stream Channel Head Locations in the State of Alabama

by

Burak Avcioglu

A thesis submitted to the Graduate Faculty of
Auburn University
in partial fulfillment of the
requirements for the Degree of
Master of Science in Natural Resources

Auburn, Alabama
December 12, 2015

Keywords: channel head, channel initiation, slope-area method,
Alabama, physiographic regions, Headwaters

Approved by

Christopher J. Anderson, Chair, Associate Professor of Forestry and Wildlife Sciences
Latif Kalin, Professor of Forestry and Wildlife Sciences
Eve Brantley, Associate Professor of Crop, Soil and Environmental Sciences

Abstract

This study focuses on assessing the utility of the slope-area method for predicting channel head locations in forested areas in Alabama under different physiographic regions, improving this method by evaluating the other landscape parameters related to channel initiation, and lastly comparing the results to the widely used National Hydrographic Dataset. To achieve these objectives, the models developed and evaluated in this study, included three region-specific multi-variable models, a comprehensive state multi-variable model, and the slope-area model. A total of 163 stream channel head locations across three physiographic regions of Alabama, including Southwestern Appalachians (*n*=51), Piedmont (*n*=61), and Coastal Plains (*n*=51), were mapped with extensive field work using a GPS device. The field data were collected in national forests within each physiographic region, namely William B. Bankhead National Forest, Talladega National Forest, and Conecuh National Forest of Alabama, to capture the least disturbed (i.e. reference) conditions. The local slope and the drainage area had an inverse and strong correlation in the Piedmont/Ridge and Valley region (r^2=0.71) and the Southwestern Appalachian region (r^2=0.61). Among the three physiographic regions, the weakest correlation was observed in the Coastal Plain region (r^2=0.45). Overall, calculated reliability and sensitivity indices indicated that model accuracy and reliance were weak to moderate; however, the slope-area method gave a much better estimation on the channel head locations compared to NHD. The region-specific multi-variable models provided the best predictions of stream channel head locations mapped in the field at each region. A comprehensive state-model was less accurate at locating the actual stream

channel head locations compared to the region-specific models. However, the comprehensive model was comparable to the slope-area model, showing that it could be applied in regions where no field mapped stream channel head location data is available.

Acknowledgement

I would like to express my deepest gratitude to my advisors Dr. Christopher J. Anderson and Dr. Latif Kalin for the infinite support of my MS thesis and research, for their patience, motivation, and encouragement. I appreciate their immense knowledge and skills in many areas, and all their assistance in writing my proposal, conference abstracts, and this thesis. Sincere thanks go to Dr. Eve Brantley, who was also one of my committee members, for her encouragement, insightful comments, and all the assistance she provided whenever I needed.

I must also acknowledge Prof. Larry Teeter and John Gilbert for their suggestions and supports for providing the necessary equipment (GPS device) for my thesis research. Many thanks to Hanna Schurman, Megan Bartholomew, Guleser Sufraci, and Rajesh Sawant for helping me collect stream channel head location data from the field. My research would not have been possible without their helps. I recognize that this research would not have been possible without the financial assistance of the Turkish General Directorate of Combating Desertification and Erosion.

Last but not the least, I would like to thank my parents, elder sister, and little brother, always supporting me and encouraging me with their best wishes. Finally, I would like to thank my wife, Guleser Sufraci who was always there cheering me up and stood by me.

Table of Contents

Abstract ii

Acknowledgement iv

Table of Contents v

List of Tables vii

Table of Figures viii

Chapter 1: 1

INTRODUCTION 1

LITERATURE REVIEW 6

THESIS ORGANIZATION 12

LITERATURE CITED 13

Chapter 2: 20

ABSTRACT 20

INTRODUCTION 22

METHODOLOGY 26

RESULTS 32

DISCUSSION 35

LITERATURE CITED 56

Chapter 3: 61

ABSTRACT 61

INTRODUCTION 63

METHODOLOGY 67

RESULTS 73

DISCUSSION 76

LITERATURE CITED 92

Chapter 4: Summary 97

List of Tables

Table 2.1: 51

Table 2.2: 52

Table 2.3: 53

Table 2.4 : 54

Table 2.5: 55

Table 3.1: 88

Table 3.2: 89

Table 3.3: 90

Table 3.4: 91

Table of Figures

Figure 2.1: 40

Figure 2.2: 41

Figure 2.3: 42

Figure 2.4: 43

Figure 2.5: 44

Figure 2.6: 45

Figure 2.7: 46

Figure 2.8: 47

Figure 2.9: 48

Figure 2.10: 49

Figure 2.11: 50

Figure 3.1: 81

Figure 3.2:. 82

Figure 3.3: 83

Figure 3.4: 84

Figure 3.5: 85

Figure 3.6: 86

Figure 3.7: 87

Chapter 1: Mapping Stream Channel Head Locations

INTRODUCTION

Channel heads represent the beginning of a stream channel. They are the transitional area between the hillslope and the stream channel domain of a drainage basin (Montgomery and Dietrich, 1988, Gomi et al., 2002). Stream channel heads are important boundaries in the stream network and therefore understanding and precisely determining their location is important for watershed integrity and sustaining stream and river ecosystems (Doppelt et al., 1993). Headwater streams are intimately connected with downstream ecosystems (Pringle, 1997) and any change or degradation in these streams can impact downstream conditions. For example, since they play a significant role in sediment transport from hillslopes to stream channel domains, estimating the exact location of the stream channel heads is an important task for assessing watershed contributions. Because of their importance, channel heads have been the focus of several studies (Montgomery and Dietrich, 1988 and 1989; Dietrich and Dunne, 1993; Istanbulluoglu et al., 2002; Heine et al., 2004; Arave, 2008; Henkle et al., 2011; Julian et al., 2012; and Clubb et al., 2014); however there remains several important questions related to their location and function.

The definition of ‘channel head’ by Dietrich and Dunne (1993) has been widely accepted and used by most researchers (Hancock and Evans, 2005, Julian et al., 2012; Prosser et al., 1995; Clubb et al., 2014; Orlandini et al., 2011; Istanbulluoglu et al., 2002). They defined a channel head as the upstream boundary of concentrated water flow and sediment transport between definable banks (Dietrich and Dunne, 1993). Definable banks include a bedrock step or narrow zone of gradient steeper than both the adjacent hillslope and transverse slope of the channel bed. Therefore, the bank can be defined as the morphological feature independent of flow (Dietrich and Dunne, 1993). Dietrich and Dunne (1993) mentioned some typology of channel heads based on their field experience and showed that channel heads are distinct morphological features. Despite the formation of channel heads, which is commonly a distinct steep or head cut, the crossing from the upstream to a channel is not in need of a remarkable topographic break.

Channel head location ultimately determines watershed drainage density which is an important basin characteristic. Position of channel heads affects the channel length in the stream network and the drainage density which eventually impacts water and sediment transportation rates to the river system (Montgomery and Dietrich, 1989; Jefferson and McGee 2013). Drainage density has been shown to influence the rapidity of flow to an outlet and as stream length in a drainage basin increases so should the drainage density (Knighton, 2014). According to Novotny (2002), the location of channel heads determines how fast pollutants enter water bodies based on its proximity to human influenced land uses such as construction, manufacturing, industry or mining. Consequently, accurately determining channel head locations is important for estimating and managing discharge, pollution in water bodies, prediction of ecosystem functions, and overall landscape condition. Precisely predicting the channel head location is necessary for determining threshold points where erosion begins due to changing surface flow accumulation (Montgomery and Dietrich, 1988) in addition to hydrologic modeling and other watershed analyses. Channel initiation normally occurs as the threshold shear stress is exceeded (Vandekerckhove et al., 1998). In other words, channels tend to initiate where the shear stress caused by flowing water at the bed has exceeded the critical shear strength required for sediment transport resulting in erosion.

Channel heads are basically formed by three runoff processes, including overland flow, sub-aerial erosion (seepage or where subsurface water intersects the land surface) and mass failure (Dietrich and Dunne, 1993; Dietrich et al., 1992; Montgomery and Dietrich, 1994; and Prosser and Abernethy, 1996; Montgomery and Foufoula-Georgiou, 1993). They are most often formed by overland flows occurring at topographic convergences where runoff exceeds the sediment erosion threshold. The location of channel heads by seepage erosion is harder to predict; however, subsurface flow convergence is understood to be the explanatory mechanism (Julian et al., 2012). Mass failure locations are also influenced by topographic convergence where colluvium accumulates and eventually reaches a critical depth where mass failure occurs (Julian et al., 2012).

The location of a channel head can be easily identified in the field using a morphologic criteria: "the upstream boundary of concentrated water flow and sediment transport between definable banks" (Dietrich and Dunne, 1993). Even though identification of individual channel heads in the field is easy, mapping numerous channel heads would be extremely time-consuming and unrealistic. For these reasons, several methods have been developed to estimate the location of channel heads using elevation maps and related data. These include geometric techniques developed by Passalacqua et al. (2010) and Pelletier (2013) that uses the geometric characteristics of high resolution-DEM to locate stream channel heads and process-based techniques developed by Montgomery and Dietrich (1988) and Royden et al. (2000) (e.g. slope-area method) (for further information refer to Clubb et al. (2014) and Heine et al. (2004)). Geographic information systems (GIS) and current watershed models, such as SWAT, BASIN, WEPP, are commonly used to delineate watersheds from DEM and have become an essential tool in geomorphology because of the availability of high-resolution DEMs. These delineated watersheds are used to extract a channel network by setting a unique source area threshold value for the area contributing to all channel heads.

The slope-area threshold relationship is a widely used method to extract the position of channel heads from digital elevation models (Hancock and Evans, 2006). The slope-area relationship is the relationship between the area draining to a channel head and the slope at that point. Using a DEM, slope can be defined as the change in elevation per unit distance and be calculated as the maximum slope between the pixel and its eight surrounding neighbors in the DEM. Drainage area is the sum of all pixels along a connected flow path to the pixel of interest multiplied by the area of a pixel. Drainage area is also calculated by using the D∞ (D-infinity or multidirectional) flow algorithm method (Tarboton, 1997). Even though the slope-area method is widely used, the accuracy and validity of the method can vary and remains uncertain across many regions (Montgomery and Dietrich, 1989; Dietrich and Dunne, 1993; Prosser and Abernethy, 1996; Julian et al, 2012).

Channel Head Formation

In order to understand channel head formation, it is necessary to understand the hydrologic processes that can contribute to their formation. Infiltration excess overland flow occurs when the amount of water from rainfall accumulating on the land surface exceeds the infiltration capacity of the soil, and surface runoff begins. The excess water from rainfall can increase shear stress resulting in the transition from hillslope to a channel network. Areas with low permeable soils and high rainfall rates are more susceptible to overland flow. When water flows along the ground, it can pick up sediments or contaminants and lead to increased suspended solids or related water pollution in nearby streams. In other words, overland flow increases shear stress to the particles at the soil surface and can transport sediment eventually causing incision and channel formation (Dietrich and Dunne, 1993).

Saturation overland flow and Horton overland flow are two types of overland flow presented in the literature. Saturation overland flow is a common runoff generation mechanism where water tables are near or close to the soil surface (Dunne and Black, 1970). Horton overland flow can be defined as the part of rainfall that exceeds the infiltration capacity of soil, flows overland, and contributes to storm flow (Horton, 1933). Saturation overland flow is usually observed in gentle-slope areas (Montgomery and Dietrich, 1989), and studies have proposed that Horton overland flow is mostly non-existent in forested lands (Sidle et al., 2007). The two types of overland flow, saturation and Horton overland flow, have other distinctions. Saturation overland flow does not extend to the drainage divide and is generally independent of rainfall intensity while Horton overland flow is more dependent on rainfall intensity. Another distinction is that the erosive effects of saturation overland flow, unlike Horton overland flow, do not depend on the raindrop impact which leads to sediment transportation (Moss, et al., 1979).

Seepage erosion can also contribute to channel head formation and can be described as the process of sediment transport out of the streambank face by entraining soil particles in which case instability results in erosion. Seepage erosion is dominant in steeper topography (Montgomery and Dietrich, 1989) and occurs at ground water springs located at breaks in topography where they are often covered up by dense vegetation. Continuous discharge from the springs forms channels that support perennial streams (McNamara et al., 2006). Some studies have been done to show under which conditions seepage erosion occurs (Dunne, 1990; Howard and MacLane, 1988; Iverson and Major, 1986). The studies showed that it is necessary to have a hydraulic gradient of sufficient size and direction to affect erosion. The angle of the hillslope and the density and frictional resistance of material also is a factor in the tendency for erosion to occur. However, plant roots give extra strength to the materials to resist separation and, therefore, protect the materials against the seepage erosion (Dietrich and Dunne, 1993).

Mass failure is the third way in which a channel head may form and includes bank collapse where large amounts of bank material become unstable and is transported into the stream or river. Mass failure dominantly occurs in the lower reaches of large streams and results in scouring of the lower banks. Bare and near-vertical banks or areas of collapsed bank materials are obvious signs of these processes which are mostly caused by natural and human factors. Mass failure represents an important form of channel morphology changes and a significant source of sediment (Moran et al., 2014).

Hollows located on steep slopes can be affected by periodic excavation of bedrock (Woodruff, 1971). High pore pressures caused by storms and the shear strength of colluvium regulate the critical state which leads to the transportation of colluvium to the unchanneled valleys/hollows. The magnitude of the shallow colluvial landslides in the hallows is often controlled by lateral root strength (Reneau and Dietrich, 1987). After mass failure, the remaining colluvium often becomes eroded through gullying and subsequent failure. The tendency for mass failure is often dictated by the steepness of topography (Montgomery and Dietrich, 1989).

LITERATURE REVIEW

Because the location of channel heads is important to watershed management, several attempts have been done to delineate them from digital elevation models. Horton (1945) pointed out the importance of the channel head location for better understanding of catchment development and channel network. A number of methods and theories have been proposed on the subject of channel initiation. The most common method to delineate the stream channel heads from DEMs using a single direction flow algorithm is the unique source area threshold method suggested by O'Callaghan and Mark (1984). However, more recent research has demonstrated that the unique source area threshold method which assumes a common drainage area size is not a good assumption to estimate the location of the channel heads because the drainage area is not the same for each stream channel heads even in a single catchment (Bischetti et al. 1998, Heine et al., 2004).

Slope and drainage area are significantly related to erosional processes, and they can influence the distribution of a variety of erosional activities (McNamara et al., 2006). It has been found that the slope of stream channel heads is normally scaled by drainage area (Flint, 1974).

The representation of this relation can be shown as:

$$A \sim S^{-\theta} \quad (1.1)$$

where *A* and *S* stand for drainage area and the slope, respectively, and θ is a constant.

Additionally, according to various studies, the mathematical representation of this relation, used to simulate the channel heads, can be demonstrated by the following equation (Montgomery and Dietrich, 1989, 1992):

$$A = C * S^{-\theta} \quad (1.2)$$

where *C* represents the threshold value to initiate the channel heads. The relationship between the local slope and the drainage area varies depending on whether the channel tends to initiate by landsliding (i.e., on steeper slopes), or the channel initiation tends to occur by seepage erosion and saturation overland flow (i.e., on more gradual slopes) (Montgomery and Dietrich, 1989). It is suggested that the exponent of the slope is ~2 for gradual slopes where overland flow initiates channels and >2 for steeper slopes where landsliding is the dominant factor to initiate channels (Montgomery and Dietrich, 1994). Additionally, Montgomery and Dietrich (1994) suggested that the channel initiation for the areas where slope is greater than 0.5 can often be explained by landsliding. A study conducted in northern Italy (Bischetti et al., 1998) supported Montgomery and Dietrich (1994) for one catchment but not for all. Their inconsistent results might be explained by some experimental factors such as low number of samples and sampling the channel heads too close to the forest roads.

Montgomery and Dietrich (1988) studied 184 channel heads in three study areas of the western U.S. to demonstrate what factors initiated and maintained a channel. Topographic variables – slope and drainage area – were found as the main mechanism that initiated and maintained the stream channel heads on their sites. In other words, channel heads occurred when the topographic threshold to create enough accumulation was exceeded. As soon as the topographic threshold was reached, the scouring began. Their results showed an inverse relationship between the source area and local valley gradient where landsliding is a common initiator of channel networks with steep (5-45 degrees) humid landscapes. They also deduced that aridity of the region contributed to the higher drainage areas necessary to initiate channel heads even though the slopes were generally the same.

Montgomery and Dietrich (1989) further analyzed channel heads from the southwest United States. In this study, they obtained a significant inverse relationship between drainage area and local valley gradient as well as source basin length and local slope. Their observations supported their previous work (Montgomery and Dietrich, 1988) by demonstrating that subsurface flow was the main activator of channel initiation on steep slopes; whereas, seepage and saturation overland flow initiated the channels (abruptly and gradually, respectively) on more gradual slopes.

The source area that accumulates enough flow to initiate the stream channel head is typically related to the local slope (Montgomery and Dietrich 1988, 1989). However, a weak relationship between the local slope and drainage area was observed in the areas where the channel initiation is controlled by bedrock close to soil surface (Montgomery and Dietrich, 1994). Anderson et al. (1997) demonstrated that bedrock had a substantial influence on water movement and was the dominant factor to initiate the stream channel heads in the northwestern US. Where bedrock is important, the slope-area relationship may not apply for channel head locations since the flow accumulation does not depend as much on the source area (Jaeger et al., 2007). Dietrich et al. (1987) observed no significant relationship between slope and drainage area in areas where the bedrock rapidly forces groundwater to the surface.

In other research, Jaeger et al. (2007) studied channel head locations in forested areas of the northwest U.S. while considering variations in local lithology (sandstone and basalt). In their study, the source area of each mapped channel head was delineated using both DEM and a GPS device and their results showed no evidence of a slope-area relationship for the sandstone or basalt lithology. The DEM derived source area did not match their GPS derived source area which could have an effect on their results. They also concluded that bedrock was a controlling influence on the initiation of the channel heads in this area.

The slope-area method which accounts for the topographic variables to locate stream channel head locations has shown variable reliability and sensitivity over different drainage areas (Orlandini et al., 2011; Sofia et al., 2011). This suggest that in some cases other variables, such as climate, land use, and soil depth, rather than just slope and drainage area might be more effective for modeling the initiation of stream channel heads. Later works have also pointed out the need to study the effects of the land use and climatic variability on the processes that controls the location of the channel head (Montgomery and Dietrich, 1992; Prosser and Abernethy, 1996; McGlynn and McDonnel, 2003).

Research has also been conducted to evaluate how slope-area method and other estimations of stream channel head initiation compare. In their study, Heine et al. (2004) compared seven methods of identification of stream channel heads, including available maps (DOQs and existing blue lines), constant flow accumulation area method, slope-area threshold method, and two new methods developed in the study. These two new methods used other topographic variables derived from DEMs besides slope and drainage area in order to improve the accuracy of the existing methods. They found that the slope-area method resulted in better estimates of stream channel heads compared to the constant drainage area threshold method. They also demonstrated that the variable drainage area estimated by logistic regression was the best method to accurately generate the stream channel head locations from DEM data. However, since they only focused on the variables generated from DEM data, other variables, such as soil, climate, and landuse, were not considered even though they could further improve the estimation of the stream channel head locations.

Variation in results may also be related to physiographic differences. Julian et al. (2012) studied 253 channel head locations across five physiographic regions in the mid-Atlantic US. They analyzed topographic, geologic, climatic, and land cover variables to demonstrate the statistical relationship these variables had in each physiographic region. They found no relationship between the local slope and the drainage area in any of their study sites. As suggested by others (Dietrich and Dunne, 1993), they concluded that the slope-area method is only applicable in areas where the channels are initiated by overland flow. The best correlation to the drainage area of the stream channel head was also found as the topographic attributes, i.e., local plan curvature in a site, average profile curvature in tree sites and local slope in a site.

In another study located in the Appalachian Coalfields of eastern Kentucky, Villines et al. (2015) analyzed the headwater stream origins along with their topographical and geological/soil characteristics. They found that geological and soil variables were not effective for predicting the initiation of stream channel head locations, and drainage area and local slope were the primary predictors of the stream channel head locations in this area.

Despite several studies on the identification of channel head locations, only a few of them have focused on how relationships may shift across physiographic changes within a region. Likewise, few studies have examined how other landscape variables may affect the origin of stream network under these contrasting physiographic regions (Julian et al., 2012). For this study, it was important to discover if and how the slope-area relationship method was viable in Alabama and if it could be improved by considering other variables, such as climate, soil, or land cover properties, under different physiographic regions.

The overall goal of this project is to assess the utility of slope-area method for predicting channel head locations in forested areas of Alabama under different physiographic regions.

The specific objectives of this study include:

I. Assess the slope-area model's ability to locate channel heads under a variety of physiographic regions

II. Define what other topographic variables may improve the model's explanatory capability for each physiographic region.

For this study, the slope-area method for locating stream channel heads was examined across three physiographic regions in Alabama (the Coastal Plain, the Piedmont/Ridge and Valley, and the Southwest Appalachian). Data were collected from three national forests (Bankhead National Forest, Talladega National Forest, and Conecuh National Forest) representing different physiographic regions and then used to determine and possibly improve the capability of this method to predict channel head locations across the state.

THESIS ORGANIZATION

Chapter 1 includes the introduction of the thesis. It consists of background information on the stream channel head locations, available literature introducing the methods to automatically identify the stream channel head locations, and thesis objectives. Chapter 2, first part of the thesis project, focuses on the slope-area method and its accuracy to locate the stream channel head locations across the state of Alabama along with the methodology and procedures, results, and conclusions. Chapter 3, the second part of the thesis project, mainly presents the applicability of utilizing other landscape variables to accurately locate the stream channel head locations across a variety of physiographic regions of Alabama. Finally, Chapter 4 discusses the overall conclusions highlighting main findings of this study and future research opportunities.

LITERATURE CITED

Anderson, S. P., Dietrich, W. E., Montgomery, D. R., Torres, R., Conrad, M. E., & Loague, K., 1997. Subsurface flow paths in a steep, unchanneled catchment. Water Resources Research, 33(12), 2637-2653.

Arave, N., 2008. Locating channel heads with digital elevation models, geology, soils, and spectral data in a geographic information systems. Thesis in Idaho State University.

Bischetti, G. B., Gandolfi, C., & Whelan, M. J., 1998. The definition of stream channel head location using digital elevation data. IAHS Publications-Series of Proceedings and Reports-Intern Assoc Hydrological Sciences, 248, 545-552.

Clubb, F. J., Mudd, S. M., Milodowski, D. T., Hurst, M. D., and Slater, L. J., 2014. Objective extraction of channel heads from high-resolution topographic data. Water Resour. Res., 50, 4283–4304, DOI: 10.1002/ 2013WR015167.

Die Moran, A., El kadi Abderrezzak, K., Tassi, P., & Herouvet, J. M., 2014, May. Modeling river bank erosion processes and mass failure mechanisms using 2-D depth averaged numerical model. In EGU General Assembly Conference Abstracts (Vol. 16, p. 10857).

Dietrich, W. E., and Dunne T., 1993. The channel head. In: Channel Network Hydrology, edited by K. Beven and M. J. Kirkby, pp. 175–219, John Wiley, N. Y.

Dietrich, W.E., Reneau, S.L., Wilson, C.J., 1987. Overview: “zero-order basins” and problems of drainage density, sediment transport and hillslope morphology. Int. Assoc. Hydrol. Sci. Bull. 165, 27–37.

Doppelt, B., Scurlock, M., Frissell, C. & Karr, 1993. Entering the Watershed. Island Press, Washington DC.

Dunne, T., & Black, R. D., 1970. Partial area contributions to storm runoff in a small New England watershed. Water resources research, 6(5), 1296-1311.

Dunne, T., 1990. Geomorphic significance of subsurface flow. Groundwater geomorphology: the role of subsurface water in earth-surface processes and landforms, (252), 1.

Flint, J. J., 1974. Stream gradient as a function of order, magnitude, and discharge. Water Resources Research, 10(5), 969-973.

Gomi, T., Sidle, R. C., & Richardson, J. S., 2002. Understanding Processes and Downstream Linkages of Headwater Systems Headwaters differ from downstream reaches by their close coupling to hillslope processes, more temporal and spatial variation, and their need for different means of protection from land use. BioScience, 52(10), 905-916.

Hancock GR, Evans KG., 2006. Gully position, characteristics and geomorphic thresholds in an undisturbed catchment in Northern Australia. Hydrological Processes.

Heine, R.A., Lant, C.L., and Sengupta, R.R., 2004. Development and comparison of approaches for automated mapping of stream channel networks. Annals of the Association of American Geographers, 94(3), pp. 477-490.

Henkle, J. E., Wohl, E., and Beckman, N., 2011. Locations of channel heads in the semiarid Colorado Front Range, USA. Geomorphology, 129(3–4), 309–319, DOI:10.1016/j.geomorph.2011.02.026.

Horton, R. E., 1933. The role of infiltration in the hydrologic cycle. Eos, Transactions American Geophysical Union, 14(1), 446-460.

Horton, R. E., 1945. Erosional development of streams and their drainage basins; hydrophysical approach to quantitative morphology. Geological society of America bulletin, 56(3), 275-370.

Howard, A. D., & McLane, C. F., 1988. Erosion of cohesionless sediment by groundwater seepage. Water Resources Research, 24(10), 1659-1674.

Istanbulluoglu, E., Tarboton, D. G., Pack, R. T., and Luce, C., 2002. A probabilistic approach for channel initiation. Water Resour. Res., 38(12), 1325, DOI: 10.1029/2001WR000782.

Iverson, R. M., & Major, J. J., 1986. Groundwater seepage vectors and the potential for hillslope failure and debris flow mobilization. Water Resources Research, 22(11), 1543-1548.

Jaeger, K. L., Montgomery, D. R., & Bolton, S. M., 2007. Channel and perennial flow initiation in headwater streams: management implications of variability in source-area size. Environmental Management, 40(5), 775-786.

Jefferson, A. J., and McGee, R. W., 2013. Channel network extent in the context of historical land use, flow generation processes, and landscape evolution in the North Carolina Piedmont. Earth Surf. Processes Landforms, 38(6), 601–613, DOI:10.1002/esp.3308.

Julian J.P., Elmore A.J., Guinn S.M., 2012. Channel head locations in forested watersheds across the mid-Atlantic United States: A physiographic analysis. Geomorphology 177-178, pp. 194-203.

Knighton, D., 2014. Drainage Networks. In: Fluvial forms and processes: a new perspective. Routledge, pp. 9-56.

McGlynn, B. L., McDonnell, J. J., 2003. Role of discrete landscape units in controlling catchment dissolved organic carbon dynamics. Water Resources Research, 39(4).

McNamara, J. P., Ziegler, A. D., Wood, S. H., & Vogler, J. B., 2006. Channel head locations with respect to geomorphologic thresholds derived from a digital elevation model: A case study in northern Thailand. Forest Ecology and Management, 224(1), 147-156.

Montgomery DR, Dietrich WE., 1988. Where do channels begin? Nature, 336, 232–234, DOI: 10.1038/336232a0.

Montgomery DR, Dietrich WE., 1989. Source areas, drainage density and channel initiation. Wat. Res. Res., 25, 1907-18.

Montgomery DR, Dietrich WE., 1994. Landscape dissection and drainage area–slope thresholds. In Process Models I Theoretical Geomorphology, Kirkby M (ed.). Wiley: Chichester; 221–246.

Montgomery DR, Foufoula-Georgiou E., 1993. Channel network source representation using digital elevation models. Water Resources Research 29: 3925–3934.

Montgomery, D. R., & Dietrich, W. E., 1992. Channel initiation and the problem of landscape scale. Science 255(5046): 826-830.

Moss, A. J., Walker, P. H., & Hutka, J., 1979. Raindrop-stimulated transportation in shallow water flows: an experimental study. Sedimentary Geology, 22(3), 165-184.

Novotny, V., 2002. Water Quality: Diffuse Pollution and Watershed Management. John Wiley, N. Y.

O'Callaghan, J. F., and Mark, D. M., 1984. The extraction of drainage networks from digital elevation data. Comput. Vis. Graph. Image Process, 28(3), 323–344, DOI: 10.1016/S0734-189X (84)80011-0.

Orlandini, S., Tarolli, P., Moretti, G., and Fontana D.G., 2011. On the prediction of channel heads in a complex alpine terrain using gridded elevation data. Water Resour. Res., 47(2), W02538, DOI: 10.1029/2010WR009648.

Passalacqua, P., Trung, D.T., Foufoula-Georgiou, E., Sapiro, G., and Dietrich, W. E., 2010. A geometric framework for channel network extraction from lidar: Nonlinear diffusion and geodesic paths. J. Geophys. Res., 115, F01002, DOI: 10.1029/2009JF001254.

Pelletier, J. D., 2013. A robust, two-parameter method for the extraction of drainage networks from high-resolution digital elevation models (DEMs): Evaluation using synthetic and real-world DEMs. Water Resour. Res., 49, 75–89, DOI: 10.1029/2012WR012452.

Pringle, C. M., 1997. Exploring how disturbance is transmitted upstreams: going against the flow. Journal of the North American Benthological Society 16,425-438.

Prosser IP, Abernethy B., 1996. Predicting the topographic limits to a gully network using a digital elevation and process thresholds. Water Resources Research 32(7): 2289–2298.

Prosser IP, Dietrich W, Stevenson J., 1995. Flow resistance and sediment transport by concentrated overland flow in a grassland valley. Geomorphology 13: 71–86.

Reneau, S. L., & Dietrich, W. E., 1987. The importance of hollows in debris flow studies; examples from Marin County, California. Reviews in engineering geology, 7, 165-180.

Royden, L. H., Clark, M. K., & Whipple, K. X., 2000. Evolution of river elevation profiles by bedrock incision: Analytical solutions for transient river profiles related to changing uplift and precipitation rates. Eos Trans. AGU, 81, 48.

Sidle, R. C., Hirano, T., Gomi, T., & Terajima, T., 2007. Hortonian overland flow from Japanese forest plantations—an aberration, the real thing, or something in between? Hydrological Processes, 21(23), 3237-3247.

Sofia, G., Tarolli, P., Cazorzi, F., and Fontana, D.G., 2011. An objective approach for feature extraction: Distribution analysis and statistical descriptors for scale choice and channel network identification. Hydrol. Earth Syst. Sci., 15(5), 1387–1402, DOI: 10.5194/hess-15-1387-2011.

Tarboton D. G., 1997. A new method for the determination of flow directions and upslope areas in grid digital elevation models. Water Resources Research 33: 309–319.

Vandekerckhove, L., Poesen, J., Wijdenes, D. O., & De Figueiredo, T., 1998. Topographical thresholds for ephemeral gully initiation in intensively cultivated areas of the Mediterranean. Catena, 33(3), 271-292.

Villines, Jonathan A., Carmen T. Agouridis, Richard C. Warner, and Christopher D. Barton, 2015. Using GIS to Delineate Headwater Stream Origins in the Appalachian Coalfields of Kentucky. Journal of the American Water Resources Association (JAWRA) 1-21. DOI: 10.1111/1752-1688.12350

Woodruff, J. F., 1971. Debris avalanches as an erosional agent in the Appalachian Mountains. Journal of Geography, 70(7), 399-406.

Chapter 2: Evaluating the slope-area method to accurately identify channel heads in the State of Alabama

ABSTRACT

Channel heads represent the beginning of a stream channel. Estimation of the stream channel head locations is an important task for managing watersheds since they play a significant role in the sediment transport from hillslope to downstream. Identification of individual channel heads in the field is straightforward but extremely time consuming. The slope-area method utilizes digital elevation maps and related information to develop slope–area threshold relationships that are used to estimate the position of channel heads from digital elevation models. A total of 162 stream channel heads were located in the field and mapped across the three physiographic regions of Alabama, including the Southwestern Appalachians (*n*=51), Piedmont/Ridge and Valley (*n*=61), and Coastal Plains (*n*=51). Using Geographic Information System (GIS) and Digital Elevation Models (DEMs), local slope and drainage area for each mapped channel head was calculated and region specific models were developed and evaluated for accuracy and reliance. The results demonstrated that the local slope and the drainage area had an inverse and strong correlation in the Piedmont/Ridge and Valley region ($r^2 = 0.71$) and the Southwestern Appalachian region ($r^2 = 0.61$). Among three physiographic regions, the weakest correlation was observed in the Coastal Plain region ($r^2 = 0.45$). Overall, the r and s indices indicated that model accuracy and reliance were weak to moderate; however, the slope-area method gave a much better estimation on the channel head locations compared to NHD. The NHD significantly underestimated the

drainage densities in all three physiographic regions and omitted most headwater streams (1^{st}-3^{rd} order streams).

INTRODUCTION

A channel head is defined as "the upstream boundary of concentrated water flow and sediment transport between definable banks" (Dietrich and Dunne, 1993). The location of channel heads is the transitional area of water and sediment movement from the hillslope to the stream of drainage basins (Montgomery and Dietrich, 1988, Gomi et al., 2002). Locations of channel heads in a drainage basin are important because they determine the drainage density defined as the unit length of stream channel for a unit area. Drainage density is an important watershed characteristic and has been shown to influence sediment and water transportation rates to the stream network (Jefferson and McGee, 2013).

Headwater streams can consist of up to 85% of the total stream network in a drainage basin and are the major source of water and nutrients for larger streams (Peterson et al., 2001). Headwater streams are defined as 1st-3rd order streams including streams with ephemeral, intermittent, and perennial flow regimes (Vannote et al., 1980). Despite the importance of headwater streams, they are often absent from stream and topographic maps. It is accepted that the use of topographic maps may omit smaller headwater streams from mapping efforts. These streams are often denoted as zero-order streams, instead of first or second order, because they do not appear on topographic maps (Storey et al., 2009).

The National Hydrographic Dataset (NHD) (USGS, 2000), the digital representation of USGS 1:24,000 scale topographic maps, consists of flowline shapefiles representing the streams in the United States. The NHD is the most commonly used dataset for watershed modeling and to locate and map streams for planning and regulatory purposes (Colson et al., 2008). The NHD is considered a digital representation of the surface waters of the entire United States; however, most studies have proved that the NHD consistently underestimates the number of streams and their length (Montgomery and Foufoula-Georgiou, 1993; Heine et al., 2004; Colson et al., 2008; Julian et al., 2012), since the flowlines in the NHD were not proposed to depict headwater streams (Mark *et al.,* 1993). Simley (2007) reported that the streams identified in the NHD were perennial and intermittent streams that were large enough to be displayed on a 1:24000 USGS quadrangle topographic map. Colson et al. (2008) investigated the NHD in 9 watersheds in North Carolina. Their results indicated that USGS maps underestimated the stream network by 35-55%. Similarly, Julian et al. (2012) compared their field surveyed stream channel heads from a variety of physiographic regions across the mid-Atlantic U.S. with the NHD. They found that the NHD often did not include first, second, even third order streams. They also noted that the NHD significantly underestimated modeled stream networks where overland flow was the main factor initiating stream channel head locations. However, the NHD was better matched with the modeled stream network in areas where stream valleys could be easily defined in the field and located with topographic maps and were initiated by springs.

Because Digital Elevation Models (DEMs) cover the entire U.S. and their accuracy and resolution are continually getting better, the utilization of Geographic Information Systems (GIS) for watershed modeling (e.g., SWAT, WEPP) and locating streams has become more common (Arave, 2008). In contrast to the easy identification of individual channel heads in the field, mapping the vast number of channel heads across the landscape would be extremely time consuming and unrealistic (sometimes impossible). As an alternative, several attempts have been carried out to locate channel heads using GIS and DEMs (Montgomery and Dietrich, 1989, 1992; Montgomery and Foufoula-Georgiou, 1993; Bischetti et al., 1998; Heine et al., 2004; Orlandini et al., 2009; Sofia et al., 2011; Jefferson and McGee, 2013; Clubb et al., 20014). Single source area threshold method (O'Callaghan and Mark, 1984) is the most common method for extracting stream channel head location from DEMs by defining a source area threshold, yet the source area of each stream channel head is not the same even in a single catchment (Bischetti et al. 1998, Heine et al., 2004). Alternatively, it has been demonstrated that a threshold related to local slope (S) and drainage area (A) is often exceeded to initiate a stream channel (Montgomery and Dietrich, 1988, 1989, 1992, 1994; Montgomery and Foufoula-Georgiou, 1993; Istanbulluoglu et al., 2002; Jefferson and McGee, 2013). This relationship can be represented as Equation 1 below:

$$A \propto S^{-\theta} \tag{2.1}$$

where A represents the contributing area (L^2), S is the local slope at the point where the channel initiates (L/L), and θ is a constant. The contributing area can be defined as the total land area contributing to an outlet. As a GIS raster dataset, this is the area of cells draining to the outlet cell (Tarbaton, 1997). Slope is the change in elevation per unit distance. It is calculated from the DEM as the maximum slope found between the outlet cell and any of its eight surrounding neighbor cells in the DEM.

The slope-area threshold method is a widely used GIS method to locate channel head from DEM and incorporate this into related watershed models (Hancock and Evans, 2006). In spite of its acceptance, the accuracy and the validity of the slope-area method to locate stream channel heads varies and still remains uncertain across many regions. Since the method uses the drainage area and local slope, it is expected to be most reliable in areas where location of channel initiation can be readily detected from surface topography (Hasting and Kamph, 2014). However, derivatives of the slope and source area (and thus the threshold value) are significantly dependent on the resolution of the DEM (Orlandini et al, 2011) and it cannot be concluded that finer resolution DEM is best suited for extracting stream channel head location because it is dependent on the natural characteristics of the areas (Hasting and Kamph, 2014).

Several studies have examined the potential utility of the slope-area method. Hancock and Evans (2006) found the slope-area method accurately predicted the field surveyed channel heads that were located in a catchment in northern Australia. Others have had mixed success using the slope-area method and relating this to regional differences. In their study with two different catchments in Northern Italy, Bischetti et al. (1998) found an inverse relationship between the local slope and the drainage area for one catchment, but not another. They have found that θ (exponent of the slope) was close to 2 where slope was higher than 0.5 and increased with increasing slope. Some studies have demonstrated that slope-area method is not a reliable method to predict channel head locations from DEM (Heine et al., 2004; Julian et al., 2012). It is clear that the drainage density and predicted location of channel heads can vary between regions because of climate, landscape attributes, and land use impact and that these factors may contribute to the successful application of the slope-area method (Montgomery and Dietrich, 1988, 1989; Dietrich and Dunne, 1993; Prosser and Abernethy, 1996).

Only a few studies have focused on how the slope-area method's accuracy to locate the channel heads differs across the physiographic regions (however see Julian et al, 2012). Like many areas in the world, there is a need to better understand the extent of headwater streams in the southeast U.S. The main objective of this study was to demonstrate whether or not the slope-area method is applicable to accurately locate the stream channel heads across varying physiographic regions in the State of Alabama (USA) and whether slope-area relationships would be consistent across the regions. The goal of this research is to evaluate the utility of slope-area method in the forested areas across a variety of physiographic regions of Alabama and compare it to the commonly used NHD.

METHODOLOGY

Study Area

For this study, the slope-area method was applied for locating stream channel heads in three physiographic regions of Alabama: the Coastal Plain (CP), the Piedmont/Ridge and Valley (P/RV), and the Southwestern Appalachian (SWA). Field mapped stream channel head data were used to determine whether or not the slope-area threshold method is a suitable method to determine the channel head locations in each physiographic region. We selected these regions to capture the landscape variations across the state. In the interest of using forested, less disturbed sites and maximizing stream access, our study was conducted in three national forests, representative of each physiographic region: Conecuh National Forest (CP region), Talladega National Forest (P/RV region), and William B. Bankhead National Forest (SWA region) (Figure 2.1). A brief description of each study area is provided below.

Conecuh National Forest

Conecuh National Forest is located in the CP physiographic region of Alabama. Average annual precipitation at this national forest is approximately 1550 mm per year (PRISM, 2004). Based on available DEM, elevations at the Conecuh National Forest range from 24 to 104 m above sea level and the slope ranges from 0 to 29.7 degrees (Table 2.1). The CP region covers almost two-thirds of Alabama, including most of central and southern parts of the state (Figure 2.1). Soils in the CP are generally described as being well-drained and having loamy subsoils with sandy loam or loam surface layers (Mitchel, 2008). Forests in the CP of Alabama are often dominated by a mix of pine and oak forest as well as network of winding creeks and bottomlands.

Talladega National Forest

Talladega National Forest is located along the border of the Ridge and Valley and Piedmont physiographic regions (at the southern edge of the Appalachian Mountains). Based on mapped physiographic boundaries, our study was conducted on the Piedmont side of the forest; however, the area was considered a transitional zone. Average annual precipitation in this forest is approximately 1400 mm per year (PRISM, 2004). Based on available DEM, elevation and slope ranges in the Talladega National Forest are 115 to 734 m above sea level and 0 to 71.8 degrees, respectively (Table 2.1), and includes some of the highest elevations in Alabama (located further in the northern portions of the national forest). The Piedmont physiography is a plateau region located in central-east Alabama between the Coastal Plain and the Ridge and Valley region and is a transitional physiographic province from the Appalachian mountainous regions. Soils in this region often consist of some clayey subsoils with a sandy loam to clay loam surface layers (Mitchell, 2008). Forest vegetation in the Piedmont region of Alabama can include mesic and xeric upland forest communities (mixed oak, hickory, and pine) along with frequent stream bottom communities (mixed hardwoods) (Golden, 1979).

William B. Bankhead National Forest

The William Bankhead National Forest is located along the SWA physiographic region in northwestern Alabama, USA. The SWA region stretches from Kentucky to Alabama and is characterized by low, flat-topped mountains with steep slopes and high gradient streams. Average annual precipitation in the forest is approximately 1450 mm per year (PRISM, 2004). Based on available DEM, elevations at Bankhead National Forest are between 154 to 331 m above sea level and slopes range from 0 to 61.5 degrees (Table 2.1). The soil of this region is often moderately deep, well drained, and permeable and consists mostly of loamy subsoils and sandy loam surface layers (Mitchell, 2008). The Bankhead N.F. is almost entirely dominated by oak-hickory forest (McWilliams, 1991). Pines, especially loblolly pines (*Pinus taeda*), were also commonly planted in the region for commercial and reforestation purposes (Gaines and Creed, 2003).

Channel Head Field Mapping

The field mapping for this study was carried out in the designated national forests representing each studied physiographic region of Alabama. Between February and May 2015, approximately 50-60 channel heads in each region were located and mapped in the field as described below.

In order to represent these landscapes, multiple areas (3-4 different watersheds) within each national forest were visited. Aerial photographs from Google Earth Pro 7.1 were initially evaluated to identify prospective sites. Even though study sites were in a national forest, some private outparcels still existed and those areas were avoided during field work.

A map-grade global positioning system (GPS) - Forge 912 F4 device was used to map channel head locations in the field. The device was chosen because its accuracy under forested canopy is 1 to 3 m (f4devices.com). Channel heads from the study areas were located and mapped by repeating the following steps:

1) locate a stream previously identified,
2) walk up the stream until the channel head was identified,
3) mark the geographic position with the GPS,
4) walk back down the stream until the first confluence,
5) walk up the next stream to the next channel head.

Photographs and notes were taken for each stream channel head to better interpret the field data. Notes were taken on the form of stream initiation (i.e., gradual or abrupt), apparent bedrock condition, and flow conditions (dry or wet) during the visit.

Upon returning from the field, the location of each GPS position was plotted onto a GIS-DEM layer. Applying the assumption that all channel heads must be located on stream flow lines, we corrected our GPS-mapped data which often had some horizontal location errors due to both positional accuracy of the GPS and the accuracy of the DEM and DEM-based flow lines. Therefore, each mapped channel head was adjusted slightly by moving it to the largest flow accumulation cell within a certain distance determined by the accuracy of the GPS device and DEM used for analysis. After the field mapped channel heads were collected, the drainage basin (i.e. contributing area) of the each mapped channel head was determined along with its local slope (explained below). The area and the local slope of the mapped channel head in each physiographic region was plotted in logarithmic scale, and a linear regression was fitted. Potential differences in model regression slopes between the different physiographic regions were assessed using a one-way ANCOVA. The data from all sites were combined, plotted, and linear regression was applied to determine if a significant model could be developed for all regions. All the data used for analyses were tested for normality and homogeneity and all statistical test results were considered significant at $p<0.05$. STATISTICA® (StatSoft 2013) was used for all statistical procedures.

Data Source and Processing

Based on the results of the regression analyses, we used the models to simulate the channel networks in each study area and assess the model performance compared to observed (mapped) locations. Topographic variables for each region, including drainage area and local slope, were obtained using 10-m DEM acquired from the USGS National Elevation Dataset (NED). For DEM processing and further analysis, the TauDEM hydrology toolbox (version 5) for ArcGIS was used to estimate channel head locations that had been previously located in the field. The DEM processing can be categorized into four steps: removing the pits in the DEM, creating a flow direction raster, creating the contributing area raster, and creating the slope raster. Each step is briefly described below.

The first step of the DEM processing is removing the surface depressions (pits) in the DEM. A surface depression can be defined as a low elevation cell in the DEM completely surrounded by higher elevation cells. They were removed by raising their elevation to the point where they drain off the edge of the domain. The pits in the DEM are likely a result of inaccurate outputs to the flow algorithm (Senevirathne and Willgoose, 2013). Following DEM pit removal, the data were used to create a flow direction raster. The most widely used flow algorithm method, called the D8 flow direction method, creates the flow cells from DEM using the direction of the steepest downward slope towards one of the eight neighboring cells (O'Callaghan and Mark, 1984). Although it is a well suited method to identify the individual channels and drainage boundaries, there are some limitations which causes it to inaccurately reflect the divergent flow over hillslopes (Costa-Cabral and Burges, 1994). The limitations of the D8 flow method result from only having eight discrete flow angles and having a single flow direction in each pixel. As an alternative, the D∞ (D-infinity) flow algorithm method (suggested by Tarboton (1997), Figure 2.2) was used to capture the geometry of flow more accurately on divergent hillslopes. This method (also called Multi Flow Direction (MFD) algorithm) allowed for continuous flow angles (as opposed to only eight) and flow partitioning between one or two neighboring pixels. For this study, the slope for each cell was calculated as the steepest outwards slope on one of eight triangular facets centered at each grid cell using the D∞ method. The contributing area raster, created using the D∞ method, was calculated as the total area of cells which flow into the outlet cell and included area from the outlet cell itself.

Assessment of Model Performance

For each of the physiographic regions, the predicted channel heads were compared to the field mapped channel heads to assess the reliability and sensitivity of the slope-area model to accurately predict the number of channel heads at each study site. To assess the model's accuracy, a method performed by Orlandini et al. (2011) was used to quantify the reliability and sensitivity of the method. Around each mapped channel head, a 10-m buffer zone was created to define a reasonable neighborhood. Channel head locations were classified into three classes: true positives (*TP*), false positives (*FP*), and false negatives (*FN*). *TPs* were defined as occurring when a predicted channel head was found inside one of the circles around a mapped channel head location. *FPs* occurred when a predicted channel head fell outside of the circle drawn around the mapped channel head. *FNs* were defined when the buffer drawn around the observed channel heads do not include any of the predicted channel heads. Examples of each scenario are provided in Figure 2.3.

Using these classifications, the reliability (*r*) of the slope-area method was calculated as:

$$\mathbf{r} = \frac{\sum \mathbf{TP}}{\sum \mathbf{TP} + \sum \mathbf{FP}} \tag{2.2}$$

where $\sum$ TP and $\sum$ FP were the total numbers of true and false positives. This measured the model's capacity not to generate channel heads when there is no observed channel head.

The sensitivity (*s*) of the method was calculated as:

$$\mathbf{s} = \frac{\sum \mathbf{TP}}{\sum \mathbf{TP} + \sum \mathbf{FN}} \tag{1.3}$$

where $\sum$ TP and $\sum$ FN were the total numbers of true positives and false negatives. This measured the model's ability not to generate *FNs*, or to predict all mapped channel heads. The indices (r and s values) ranged from 0 to 1 with the higher values representing better performance.

National Hydrographic Dataset

National Hydrography Dataset used in this research was the high resolution (1:24,000 scale) topography. The NHD at 1:24,000 scale, digitally representing the USGS topographic map blue lines, were downloaded from http://nhd.usgs.gov/data.html for the whole State of Alabama. In order to compare slope-area modeled stream locations with NHD, a similar-sized watershed (10-11 km^2) was randomly located and delineated in the national forest of each physiographic region using ArcGIS. The slope-area model were applied to these watersheds to compare with the high resolution NHD. For each study site, the simulated stream network and the NHD were generated within the test watersheds. To compare methods, the stream length (km) and drainage density (km^{-1}) for each test watershed were calculated in order to determine the differences between the NHD and the simulated stream network.

RESULTS

A total of 162 channel heads from the three physiographic regions of Alabama were identified in the field (Table 2.2). Sixty channel heads were mapped in the P/RV physiographic region, 51 channel heads were located in SWA physiographic region and 51 in the CP physiographic region. The channel head locations were usually distinctive features and easily identifiable in the field. Abrupt channel banks were not always observed however, and in some areas, like the CP region, the initiation of the channel head was more gradual where the slope was flatter. Both the gradual and abrupt channel head formations occurred in all regions; however, most of the gradual channel heads were observed in the CP region. Nearly all the channel heads mapped were considered ephemeral or intermittent streams.

Using the mapped channel head locations, the minimum, maximum, average, and standard variation of the drainage area and slope per physiographic area were calculated and are provided in Table 2.2. The magnitude of drainage area of the channel heads varied significantly between the physiographic regions (ANOVA, $p<0.005$). However, the local slope did not significantly differ between the P/RV and the SWA, but varied with the CP region. Based on average slope, the P/RV and the SWA region had steeper topography than the CP region. Based on observations in the field and DEM analysis, the CP region was substantially flatter than the other regions and had the highest average source area and the lowest slope (Table 2.2). The results of the analysis showed that drainage area decreased when the slope was steeper. Regression results showed a strong and negative relationship between the local slope and the drainage area for the P/RV (r^2=0.702, $p<0.001$) and the SWA region (r^2=0.604, $p<0.001$) (Figures 2.4 and 2.5; Table 2.3). On the other hand, the weakest relationship between the local slope and the drainage area was observed for channel head locations in the CP (r^2 = 0.448, $p<0.001$) (Figure 2.6; Table 2.3). The overall model performance (all sites combined, n=162) was also significant (r^2=0.63, $p<0.001$) (Figure 2.7; Table 2.3). However, results from the ANCOVA for each physiographic region indicated significant differences in drainage area between all three regions after controlling for the local slope ($p<0.0001$) (Table 2.3).

Visual inspection of the simulated stream network confirmed that the slope-area model resulted in some feathering at the low order streams in steep areas, like PRV and SWA region (Figure 2.8). Feathering can be described as parallel running streams caused from the smaller threshold (Montgomery and Foufoula-Georgiou, 1993). The small thresholds derived from the linear regression equation for the P/RV and SWA regions performed extensive feathering. In these areas, adjusted threshold values were used to avoid the feathering effect. The appropriate threshold values were found as 400 – 600 m^2 ($A*S^{\theta} \geq 400 - 600$) in the P/RV and SWA regions.

Assessment of Model Performance

The reliability and sensitivity analysis was performed for each study area. The *r* and *s* indices demonstrated the reliability and the sensitivity of the results, respectively (Table 2.4). Even though there is no general guidance on what constitutes adequate *r* and *s* values, we compared the values calculated between each physiographic region and sites with values closer to one were better performing models. According to the index scores, all sites had values significantly less than 1 suggesting the simulation of the channel head locations by slope-area threshold method did not accurately depict the ones observed in the field. On the other hand, there was a range of scores and the reliability and the sensitivity of the models for each study area varied substantially. Overall, the P/RV region resulted in the most reliable prediction among the others with a relatively higher index score (r=0.70). The P/RV and SWA regions resulted the most sensitive predictions, with similar sensitivity scores (s=0.42 and s=0.41, respectively) relatively higher than the CP region (s=0.35) The reliability index scores were higher than the sensitivity index scores for the P/RV and SWA, but not in CP. Overall, the reliability and sensitivity analysis performed the poorest in the CP region, consistent with the linear regression analysis (Table 2.3).

Comparison with National Hydrography Dataset

The differences between the modeled stream network and the high resolution NHD were demonstrated for the CP, P/RV, and SWA regions (Figure 2.9, 2.10, and 2.11, respectively). Almost all the modeled mapped stream channel heads in the randomly selected watershed did not exist in the NHD for each region. According to the model, the drainage densities of the CP, P/RV and SWA region for the test watersheds were calculated as 6.5, 9.7 and 8.3, respectively (Table 2.5). However, the drainage densities of NHD in the CP, P/RV and SWA regions were found to be substantially lower than the actual stream network by 75%, 83%, and 80%, respectively. Additionally, the model again demonstrated that drainage densities varied in each physiographic region. The smallest drainage density was in the CP region while the P/RV and the SWA had a drainage density respectively higher than the CP region. Results from the NHD did not show any substantial differences in the drainage densities for all the three physiographic region (Table 2.5). All of the first-order and second-order streams and most of the third-order streams in the simulated stream networks were not present in the NHD.

DISCUSSION

The objective of this study was to assess the applicability of the slope-area method to accurately estimate the location of the stream channel heads across the three physiographic regions of Alabama using DEM. In all of the three study sites, an inverse relationship between the local slope and the drainage area was observed. These results support earlier works that found a strong inverse relationship between local slope and drainage area (Montgomery and Dietrich, 1988, 1989, 1992; Prosser and Abernethy, 1996; Jefferson and McGee, 2013). It has also been reported that the slope-area method is more suitable where the channel initiation is resulted from landsliding (Montgomery and Dietrich, 1994). Montgomery and Dietrich (1994) have suggested that landsliding is the dominant factor where the slope is higher than 0.5. In contrast to this finding, a strong relationship was found between the local slope and the drainage area for the P/RV region and the SWA region where the average slopes were 0.20 m/m and 0.18 m/m, respectively. These results demonstrated that the slope-area method may also be suitable on landscapes that do not have steeper slopes.

Results from this study also showed that as slope at the channel head gets steeper, the source area decreases which has been reported by others as well (Montgomery and Dietrich, 1988, 1989, 1992). Higher local slope values (and consequently lower drainage areas) were observed in P/RV region and SWA region; whereas, the slope values displayed in the CP region indicated a flatter topography that had a much larger drainage area to accumulate enough water flow to initiate the stream channel heads. Although there was a significant slope-area relationship when all data across the state were pooled, analyses indicated that there was a significant difference among the regional watershed areas after controlling for slope. It was not surprising that CP differed from both P/RV and SWA. However, it was somewhat surprising that the SWA and P/RV regions differed from each other in spite of their similar steep topography. These results suggest that other factors may be important to determine the relationship between slope, drainage area, and the resulting location of channel heads. Studies have found a weak correlation between the local slope and the drainage area in areas where bedrock was the controlling factor to initiate the stream channel heads (Dietrich et al., 1987; Montgomery and Dietrich, 1994). The soil characteristics, including the soil texture, hydraulic conductivity, and depth to restricted layer would also have some impacts on the drainage area by altering the infiltration capacity of the soils, creating a less permeable layer, and ultimately increasing/decreasing the overland flow (Dietrich et al., 1987; Dietrich and Dunne, 1993; Montgomery and Dietrich, 1994). Differences in soil depth between the P/RV and SWA regions have been documented and may be contributing to detected differences between regions where topography is similar.

The different relationship between the slope and drainage area can be observed depending on how steep or gradual the area is (Montgomery and Dietrich, 1994). Other studies have found the exponent of the slope would be ~2 (Montgomery and Dietrich, 1988; McNamara et al., 2006;

Imaizumu, 2010); however, our findings were significantly lower compared to these findings. This may be explained by the differences between our study areas and earlier studies which had a wider range of slopes. In our mapped channel heads across the State of Alabama, the local slopes in general were less than 0.5 while Montgomery and Dietrich (1988), for instance, had a wide range of slopes (0.1 to 1.0) in their stream channel heads across the western U.S. The exponent of the slope also shows an increasing trend as the local slope gets steeper. These results suggest that other variables, such as soil, climate, land use, or geology, are also important to the initiation of channel heads and become a more important factor if the slope is flatter, like in the CP areas.

The slope-area method has been demonstrated to have feathering effect along the low order streams in highly dissected topographies (Montgomery and Foufoula-Georgiou, 1993; Tarboton and Ames, 2001), consistent with our results. Feathering effect in stream network is resulted from the low threshold values due to steep slopes, and decreasing threshold causes the more feathering effect in these areas. The error could be eliminated by adjusting (increasing) the threshold until an acceptable stream network is obtained. However, one must also consider that the increase in the threshold would also cause the decrease in the ability of the model to generate the stream channel head locations observed in the field.

The reliability (*r*) and sensitivity (*s*) analysis results (Table 2.4) provided a view of the model performance over the three study sites. It is interesting to note that the sensitivity indices, which calculates the ability of the model to generate all the field mapped stream channel heads, indicated lower values than expected in contrast to the strong regression results. However, it is worth noting that these index scores were comparable to Orlandini et al. (2011) where similar *r* and *s* indices were obtained ($r = 0.26$ and $s = 0.47$) for stream channel heads in the eastern Italian Alps. Also consistent with other reports (Orlandini et al., 2011, Club et al., 2014), the reliable models were often relatively insensitive and vice versa. In other words, if a stream network was found to be reliable, it also tended to be insensitive. The reliability and the sensitivity scores were also strongly linked to the threshold. The increase in the threshold improved the reliability, not to generate FP, but also decreased the sensitivity of the model. The balance between the reliability and the sensitivity must be considered while adjusting the threshold value to avoid the feathering effect. These results also suggest that consideration of additional variables beyond slope and drainage area may be needed to improve the performance of the models used to locate channel head locations.

In all three physiographic regions of Alabama, the NHD severely underestimated total stream length (Table 2.5). These results demonstrate that the USGS topographic map blue lines, or NHD, have a noticeable omission in terms of horizontal accuracy and completeness of stream networks, especially in consideration of the headwater streams. Compared to the slope-area modeled stream network, the NHD did not include almost all first, second, and many third order streams within each of the physiographic regions that were studied here. If the mapped streams were included in the NHD, the stream orders would also be higher than now calculated in the NHD. In other words, if the actual stream networks were represented in the NHD, the first order streams would be second-order, second-order streams would be third-order. Since the headwater streams can comprise around 85% of the actual stream network (Peterson et al., 2001), their omission explains the large discrepancy between the slope-area model and NHD. The biggest discrepancies were found in the P/RV region and SWA region where there was the highest density of headwater streams (first-to third-order streams). It was interesting to note that NHD did not show any significant differences in the drainage densities calculated between the test watersheds in each physiographic regions. However, the modeled stream network in CP was relatively less than P/RV and SWA. The inability of NHD maps to depict the smallest streams and only focus on perennial streams (Simley, 2007) contributes to this large discrepancy. In addition to NHD, use of the single source area threshold method is commonly used by watershed managers. Findings from this study indicate that this method may also be inappropriate for some applications. The source areas of the mapped channel heads across the state of Alabama ranged from 270 to 75,000 m^2 and were shown to vary substantially even within a single catchment. Professionals utilizing NHD and single source threshold stream maps should understand that these products may not include the vast majority of the drainage network and consider whether the omission of headwaters is appropriate when applying these methods for planning or modeling purposes.

In conclusion, the results from this study show that the slope-area method, derivation of digital elevation models with 10-m resolution, produce a reliable estimation of stream channel head locations across the physiographic regions of Alabama. However, indices indicating model reliability and sensitivity were low to moderate and it is still worth considering how using other variables (e.g., soil, climate, and land use) may improve the slope-area method to more accurately place the stream channel head locations as observed in the field. Colson et al. (2008) stated that blue line streams from USGS topographic maps were commonly used to place headwater streams for federal and state planning purposes. Even though the reliability and the sensitivity of the model was marginal, the model had significant advantages for depicting headwater streams compared to topographic maps or NHD. We recommend the watershed modelers, and federal and state planners and other watershed professionals consider the slope-area model as an alternate approach to placing headwater streams rather than relying on NHD or single source area threshold method.

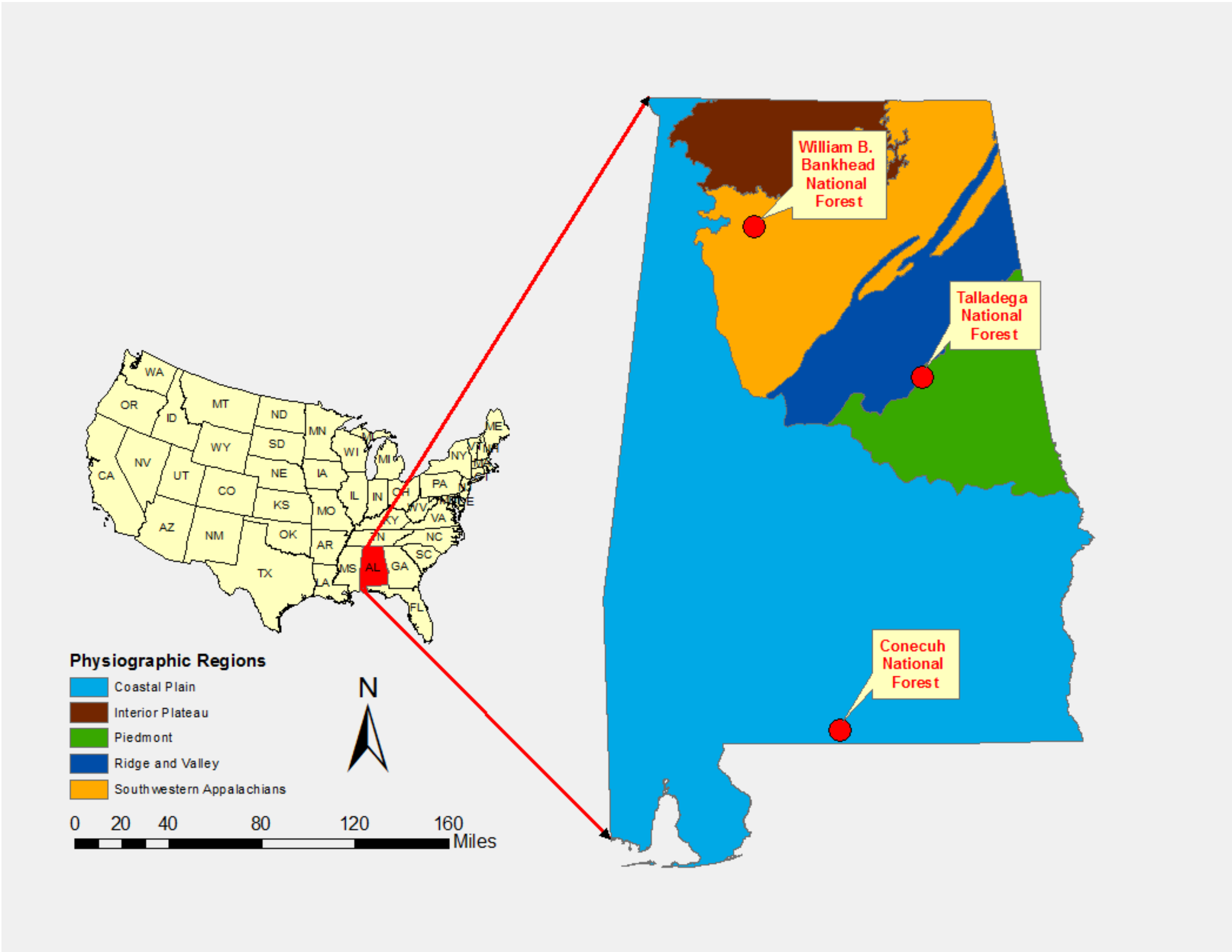

Figure 2.1: Locations of channel heads mapped in the watersheds across the physiographic regions of Southwestern Appalachian, Piedmont/Ridge and Valley, and Coastal Plain. (N.F: National Forest)

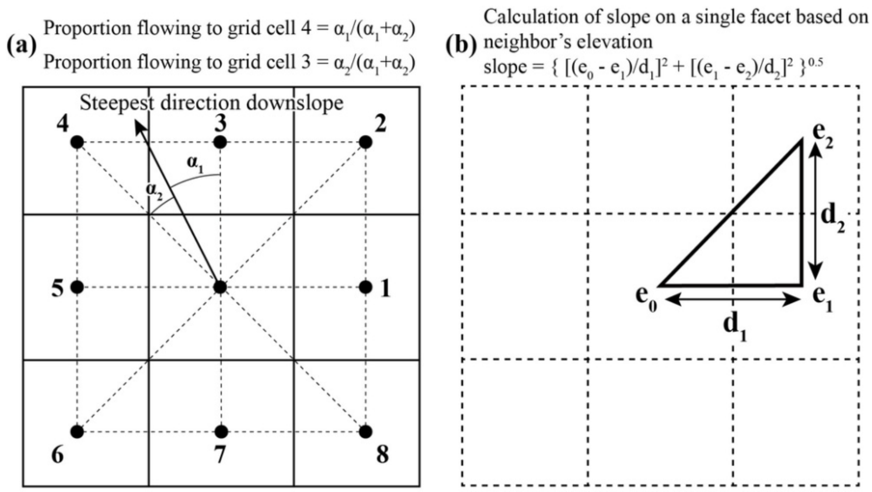

Figure 2.2: D∞ flow direction method (Tarboton, 1997). Calculation of flow direction (a) and slope (b) (Figure obtained from Yang et al., 2015).

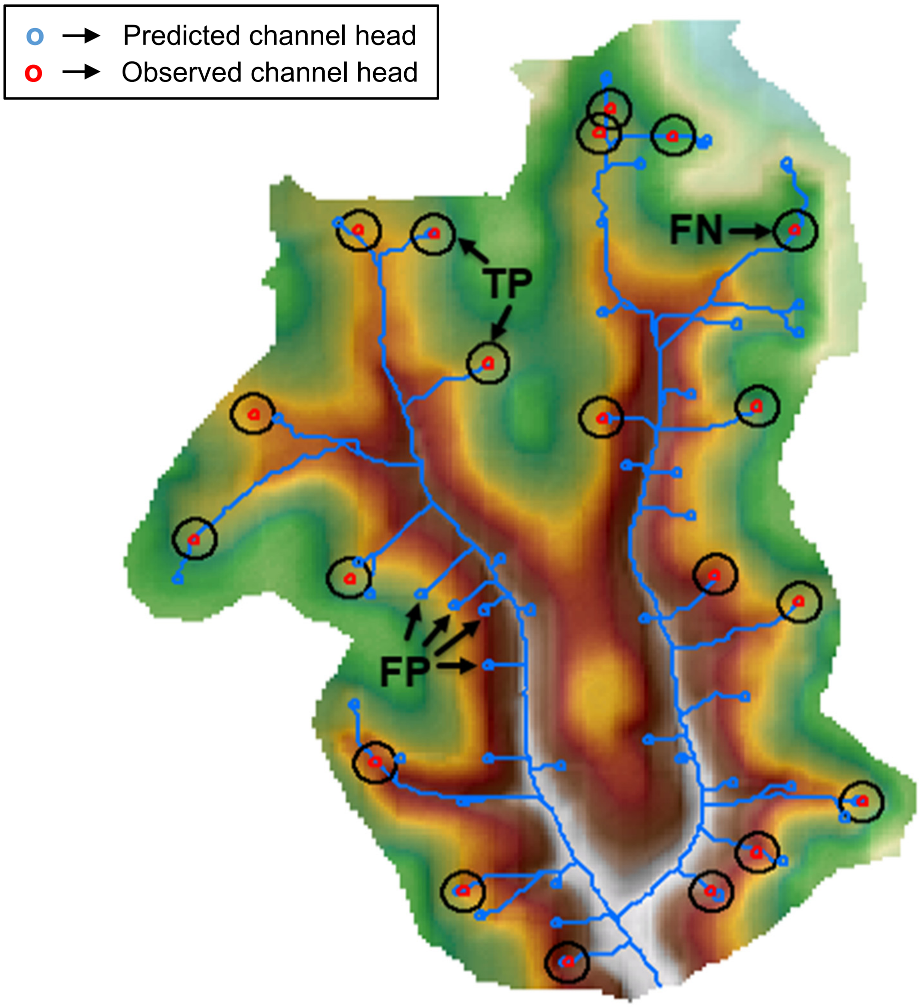

Figure 2.3: Methodology used to determine the reliability and sensitivity of the slope-area method. TP represents true positives, FN represents the false negatives, and FP also represents the false positives (Orlandini, 2011). TPs are the predicted stream channel heads that fall inside the buffer drawn around the observed stream channel heads. FPs are the predicted stream channels which do not fall into the buffer. FNs represents the buffers that do not contain any predicted stream channel heads.

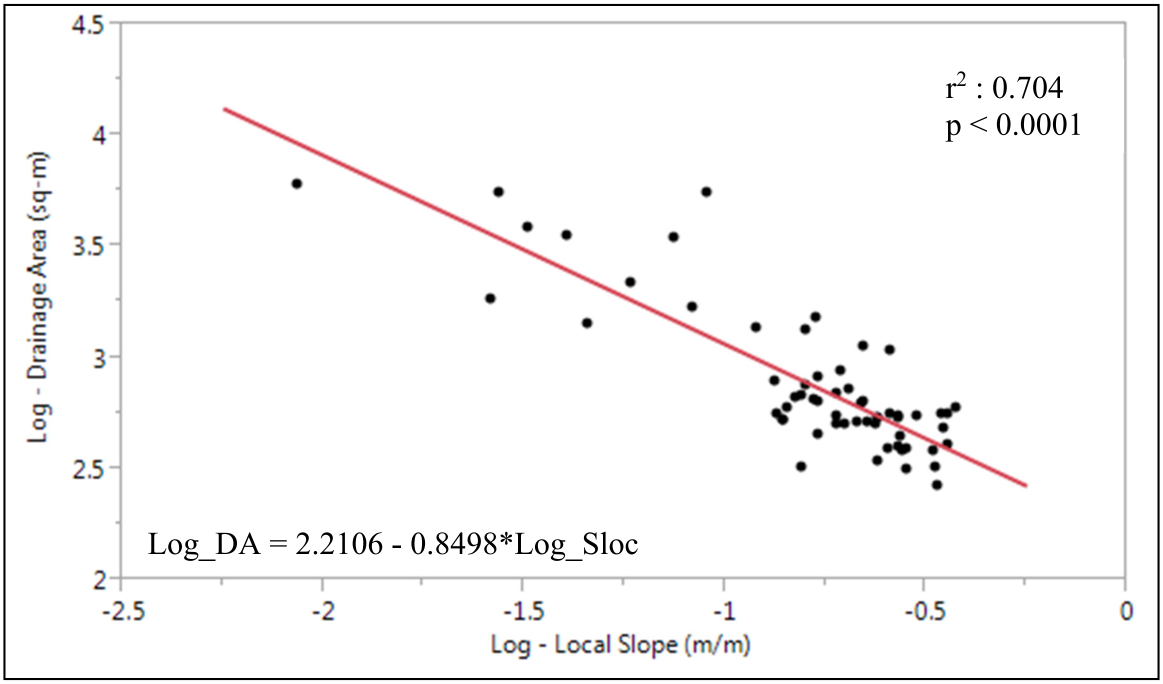

Figure 2.4: The slope-area scatterplot of P/RV Physiographic Region

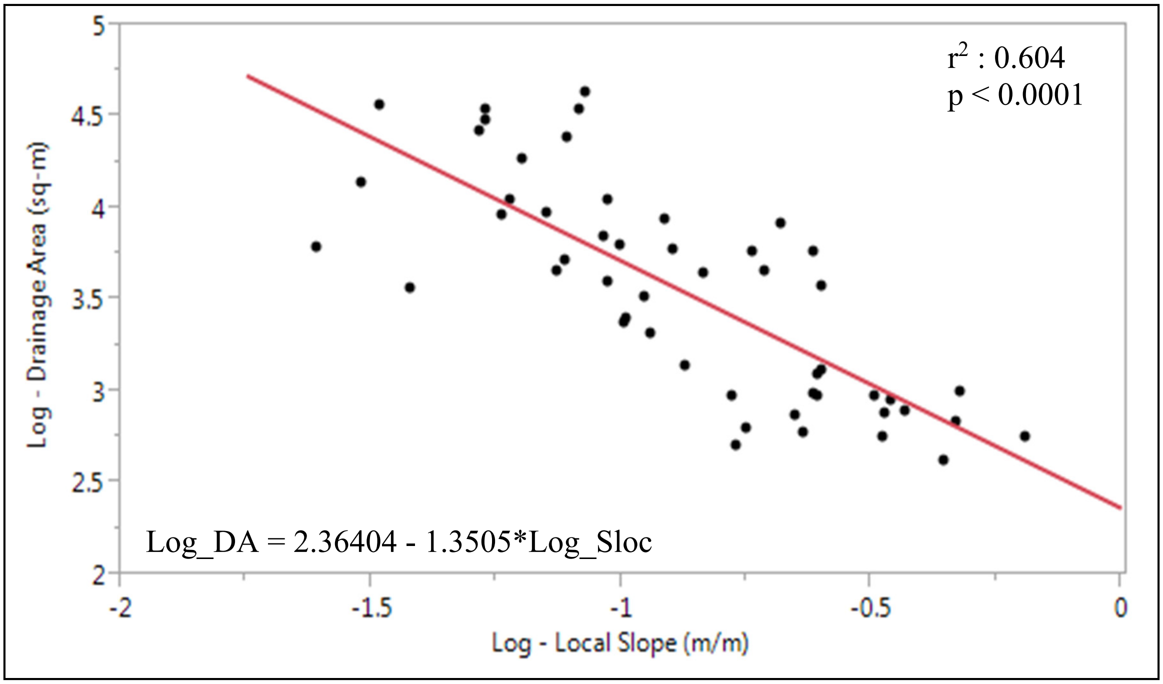

Figure 2.5: The slope-area scatterplot of SWA Physiographic Region

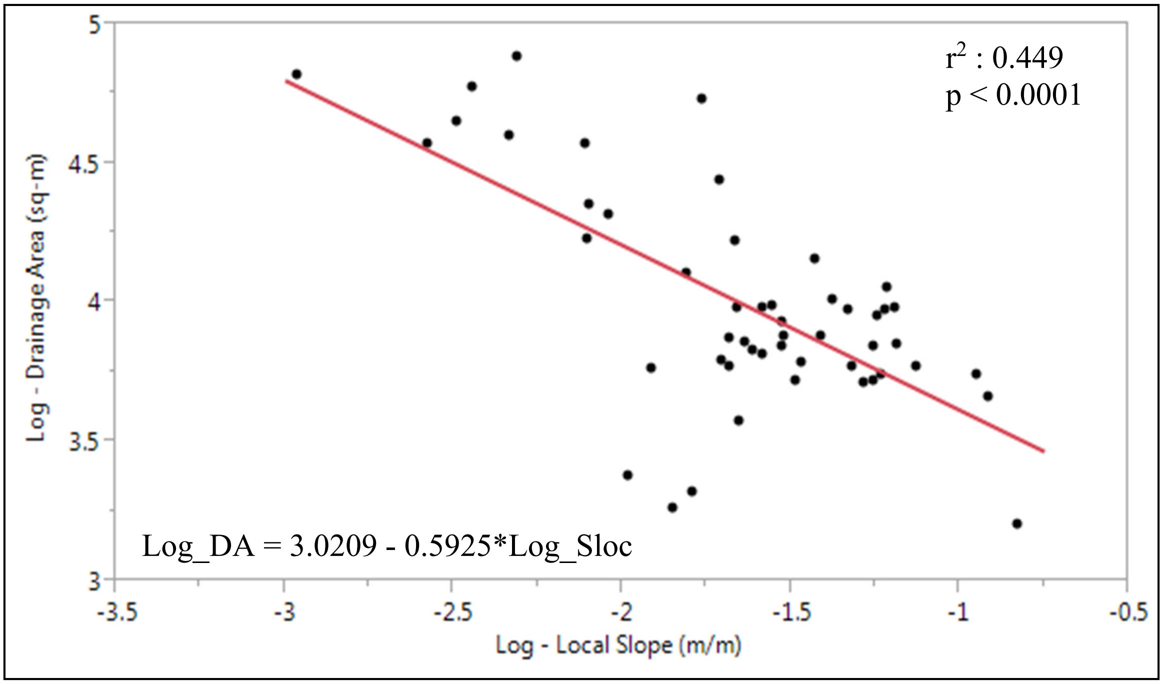

Figure 2.6: The slope-area scatterplot of CP Physiographic Region

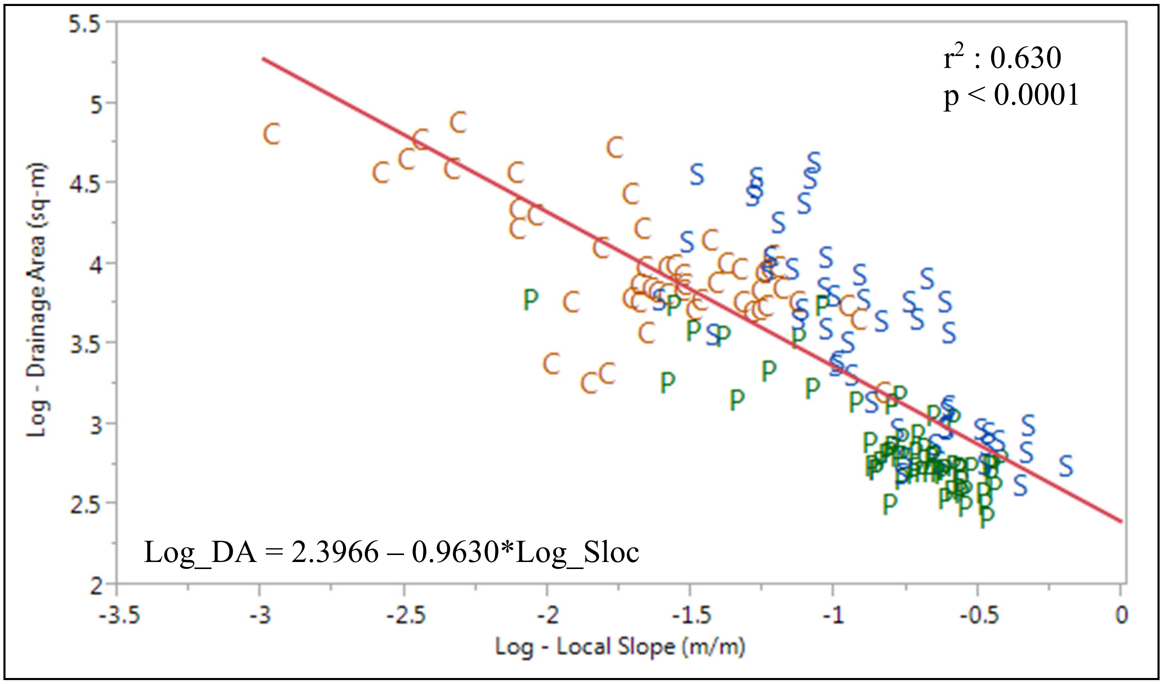

Figure 2.7: The slope-area scatterplot of entire study sites across the state of Alabama (C: CP Region, P: P/RV Region, and S: SWA Region)

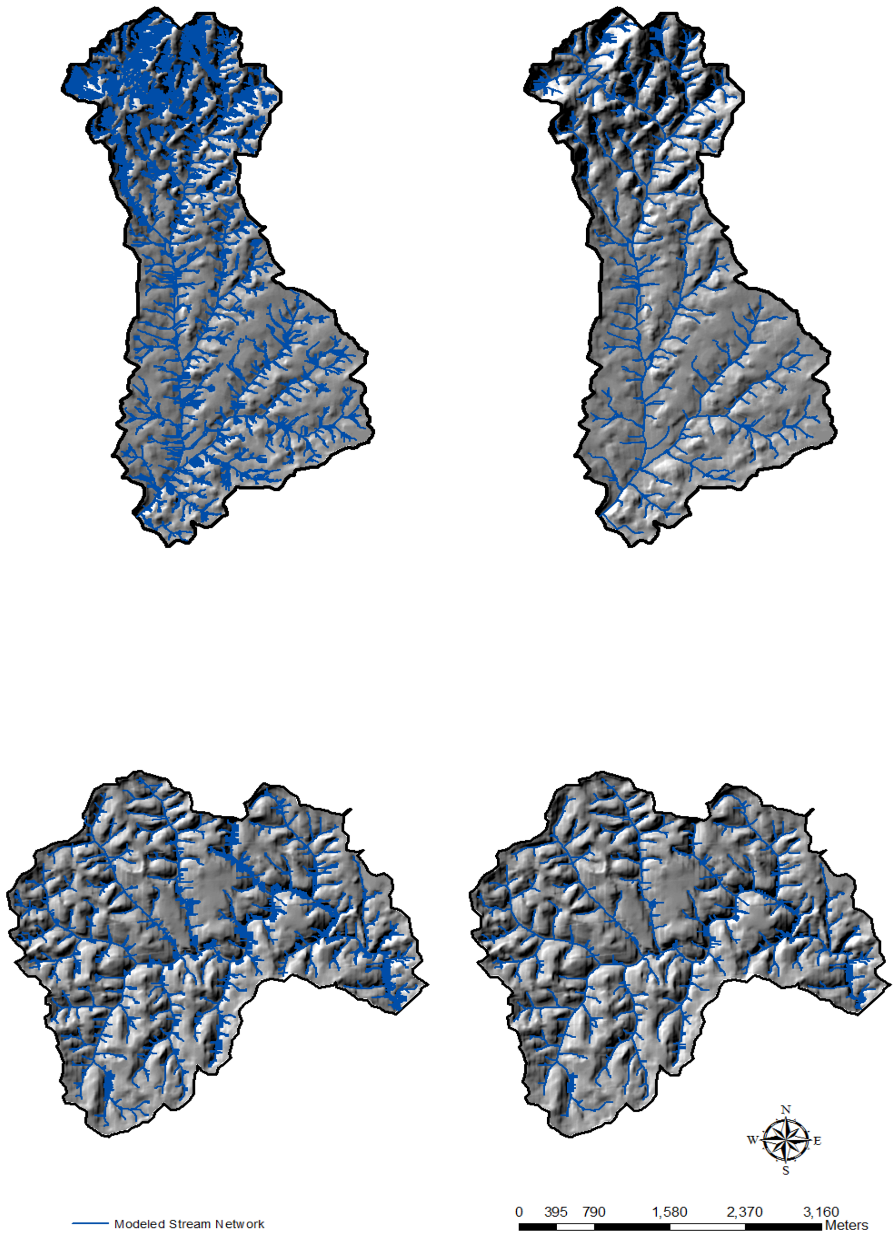

Figure 2.8: Modeled stream networks of the P/RV (top) and SWA (bottom) regions. Feathering effect was observed in these regions when the thresholds resulted from regression equations ($c_{P/RV}$=165 and c_{SWA}=230) were used (left maps). An acceptable stream networks were derived when adjusted thresholds ($c_{P/RV}$=500 and c_{SWA}=425) were used.

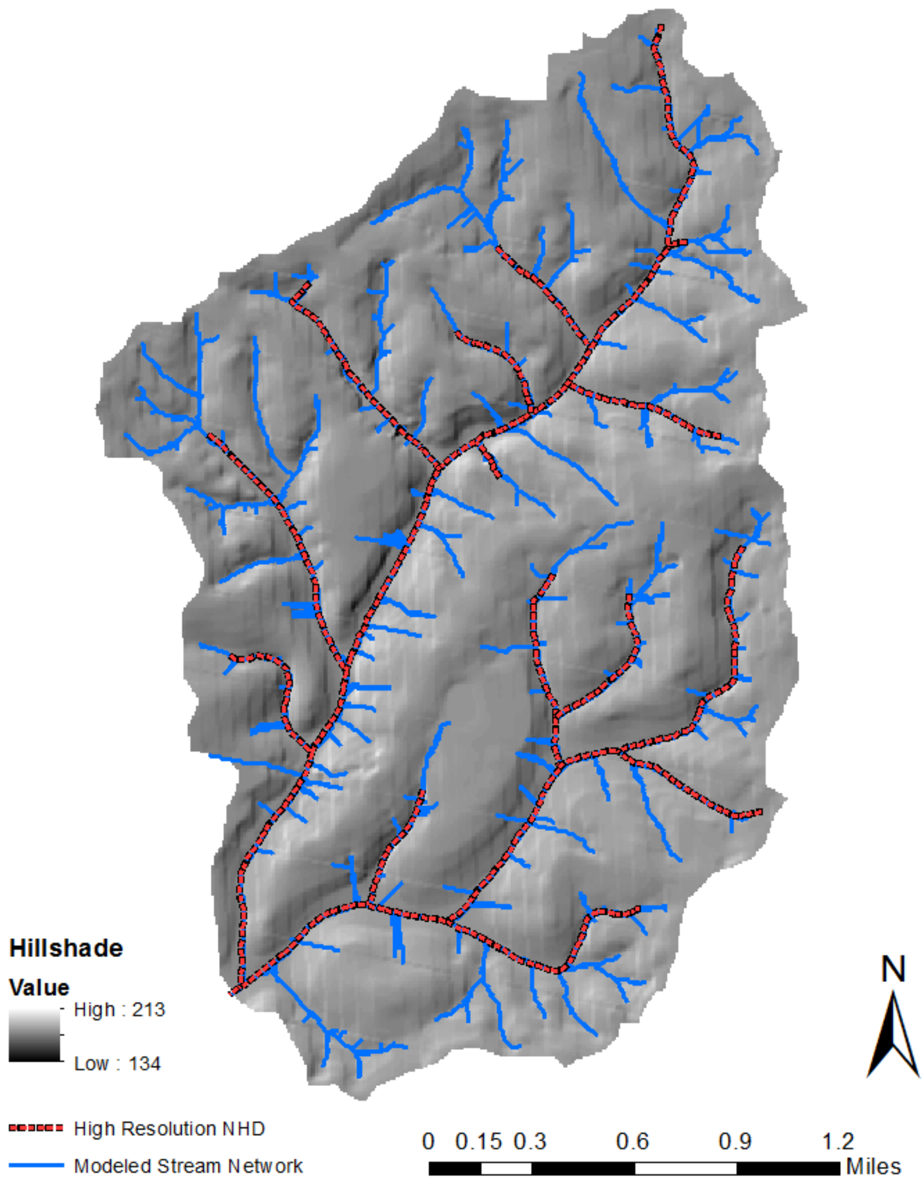

Figure 2.9: Comparison of streams shown on the NHD (1:24,000 scale) to the predicted stream network - CP Region

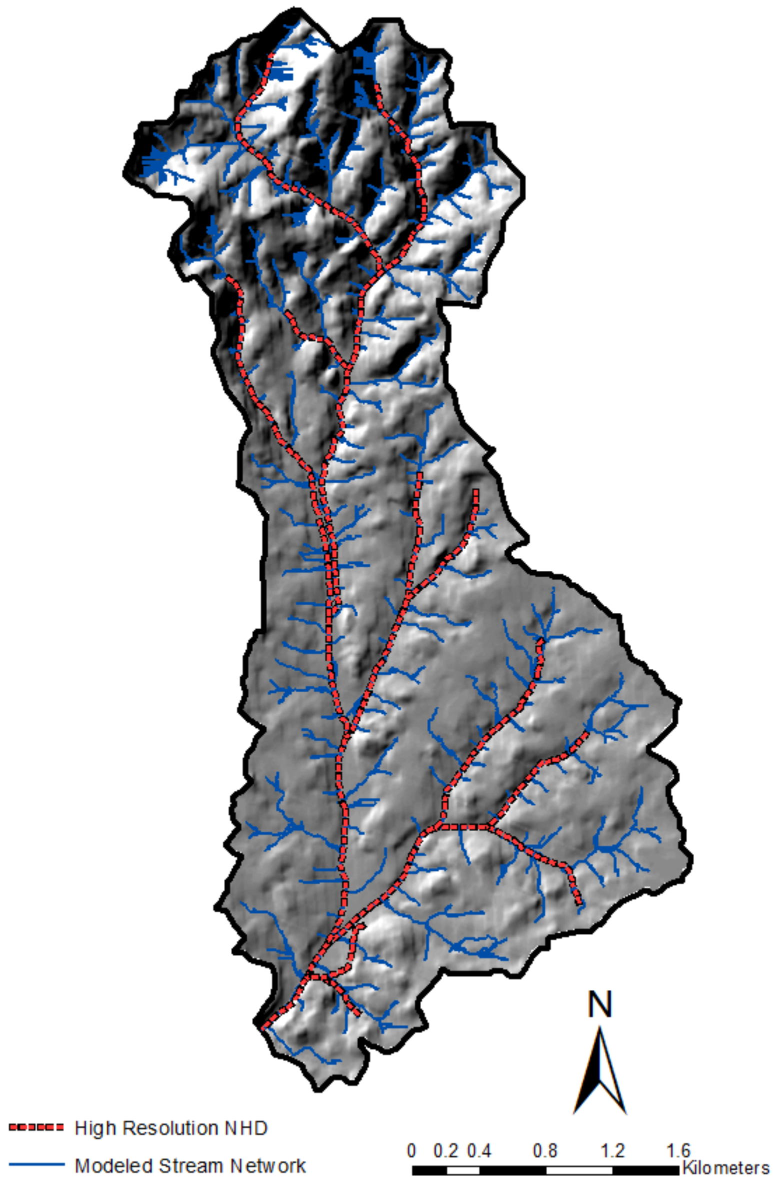

Figure 2.10: Comparison of streams shown on the NHD (1:24,000 scale) to the predicted stream network – P/RV Region

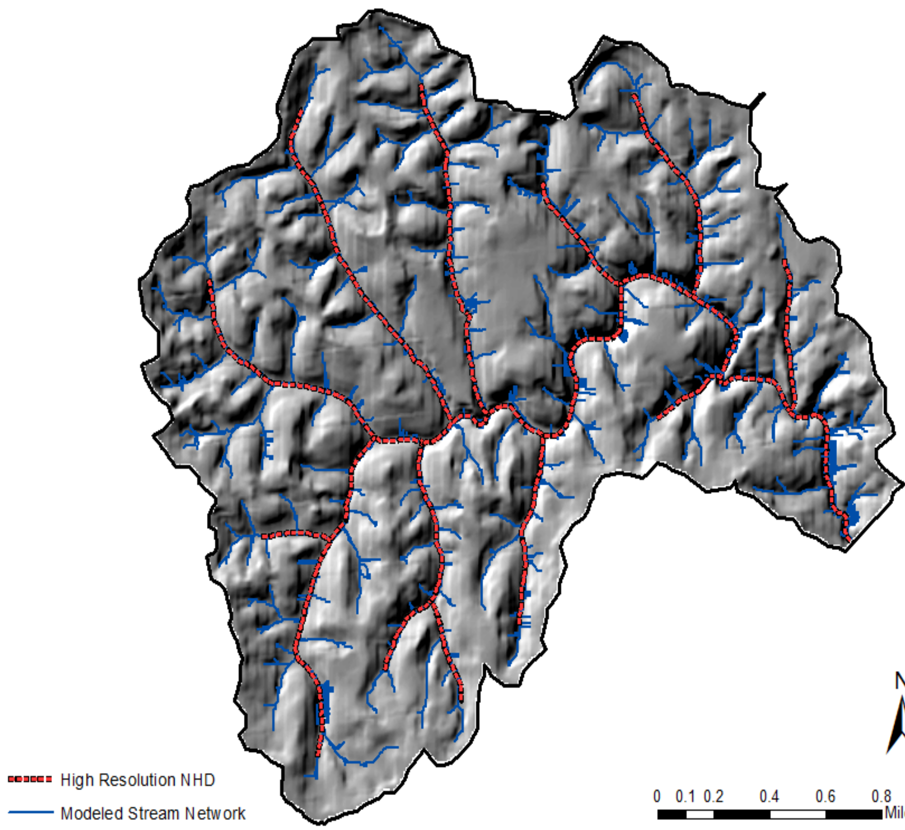

Figure 2.11: Comparison of streams shown on the NHD (1:24,000 scale) to the predicted stream network – SWA Region

Table 2.1: Topographical characteristics of the study areas based on a 10-m DEM.

	Elevation (m)				Slope (Degree)			
	Min	**Max**	**Mean**	**SD**	**Min**	**Max**	**Mean**	**SD**
Conecuh National Forest	24	104	64.51	13.38	0	29.69	2.48	1.92
Talladega National Forest	115	734	304.65	73.21	0	71.82	11.86	7.51
William B. Bankhead National Forest	154	331	229.06	34.96	0	61.46	9.78	6.79

Table 2.2: Variation of the source area and local slope for the field mapped channel heads in each physiographic region.

Site	Number of channel head	Source area (m^2)				Local slope (m/m)			
		Min	Max	Average	SD	Min	Max	Average	SD
CP region	51	1,588	76,308	15,392	17,779	0.001	0.148	0.035	0.029
P/RV region	60	264	5,969	1,085	1,291	0.009	0.377	0.198	0.094
SWA region	51	425	43,378	8,100	10,901	0.025	0.644	0.177	0.136

Table 2.3: Summary of linear regression model results for relationships between local slope and drainage area. Differences in letters denote significant differences among the physiographic regions (ANCOVA)

Study Area	n	Slope	Intercept	r^2	P value
CP region	51	-0.593	3.021	0.45	< .0001 a
P/RV region	60	-0.850	2.211	0.70	< .0001 b
SWA region	51	-1.351	2.364	0.60	< .0001 c
Entire Data	162	-0.963	2.397	0.63	< .0001

Table 2.4 : Assessment of model performance for each of the study sites. “*r*” is the reliability index, and “*s*” is the sensitivity index.

Index	CP Region	P/RV Region	SWA Region
r	0.32	0.70	0.45
s	0.35	0.42	0.41

Table 2.5: Comparison of stream length and drainage density between the predicted stream network and the NHD for the trial watersheds in the three physiographic regions of Alabama

Study Site	Area (km^2)	Modeled Stream Network		National Hydrography Dataset		Underestimation (%)
		Stream Length (km)	Drainage Density (km^{-1})	Stream Length (km)	Drainage Density (km^{-1})	
CP region	11.78	76.67	6.51	18.90	1.60	75
P/RV region	11.47	110.72	9.65	18.61	1.62	83
SWA region	10.67	88.22	8.27	18.10	1.70	80

LITERATURE CITED

Arave, N., 2008. Locating channel heads with digital elevation models, geology, soils, and spectral data in a geographic information systems. Thesis in Idaho State University.

Bischetti, G.B., C. Gandolfi, and M.J. Whelan, 1998. The definition of stream channel head location using digital elevation data. IAHS Publications-Series of Proceedings and Reports-Intern Assoc Hydrological Sciences, 248, 545-552.

Clubb, F.J., S.M. Mudd, D.T. Milodowski, M.D. Hurst, and L.J. Slater, 2014. Objective extraction of channel heads from high-resolution topographic data. Water Resour. Res., 50, 4283–4304, doi: 10.1002/ 2013WR015167.

Colson, T., J. Gregory, J. Dorney, and P. Russell, 2008. Topographic and soil maps do not accurately depict headwater stream networks. National Wetlands Newsletter 30(3):25–28.

Costa-Cabral, M. and S.J. Burges, 1994. Digital elevation model networks (DEMON): A model of flow over hillslopes for computation of contributing and dispersal areas, Water Resour. Res., 30(6), 1681– 1692.

Dietrich, W.E. and T. Dunne, 1993. The channel head. In: Channel Network Hydrology, edited by K. Beven and M. J. Kirkby, pp. 175–219, John Wiley, N. Y.

Storey R., S. Parkyn, B. Smith, G. Croker, P. Franklin, 2009. Effects of development on zero-order streams in the Waikato region. Hamilton, National Institute of Water and Atmospheric Research.

Gaines, G.D. and J.W. Creed, 2003. Forest health and restoration project. National forests in Alabama, Bankhead National Forest Franklin, Lawrence, and Winston Counties, Alabama. Final environmental impact statement. Management Bulletin R8-MB 110B

Golden M.S., 1979. Forest vegetation of the lower Alabama Piedmont. Ecology 60: 770-782.

Gomi, T., R.C. Sidle, & J.S. Richardson, 2002. Understanding Processes and Downstream Linkages of Headwater Systems Headwaters differ from downstream reaches by their close coupling to hillslope processes, more temporal and spatial variation, and their need for different means of protection from land use. BioScience, 52(10), 905-916.

Hancock, G.R., K.G. Evans, 2006. Gully position, characteristics and geomorphic thresholds in an undisturbed catchment in Northern Australia. Hydrological Processes.

Hastings, B.E., & S.K. Kampf, 2014. Evaluation of digital channel network derivation methods in a glaciated subalpine catchment. Earth Surface Processes and Landforms, 39(13), 1790-1802.

Heine, R.A., C.L. Lant, and R.R. Sengupta, 2004. Development and comparison of approaches for automated mapping of stream channel networks. Annals of the Association of American Geographers, 94(3), pp. 477-490.

Imaizumi, F., T. Hattanji, and Y.S. Hayakawa, 2010. Channel initiation by surface and subsurface flows in a steep catchment of the Akaishi Mountains, Japan. Geomorphology, 115(1), 32-42.

Istanbulluoglu, E., D.G. Tarboton, R.T. Pack, and C. Luce, 2002. A probabilistic approach for channel initiation. Water Resour. Res., 38(12), 1325, doi: 10.1029/2001WR000782.

Jefferson, A. J. and R. W. McGee, 2013. Channel network extent in the context of historical land use, flow generation processes, and landscape evolution in the North Carolina Piedmont. Earth Surf. Processes Landforms, 38(6), 601–613, doi:10.1002/esp.3308.

Julian J.P., A.J. Elmore, S.M., and Guinn, 2012. Channel head locations in forested watersheds across the mid-Atlantic United States: A physiographic analysis. Geomorphology 177-178, pp. 194-203.

McNamara, J.P., A.D. Ziegler, S.H. Wood, and J.B. Vogler, 2006. Channel head locations with respect to geomorphologic thresholds derived from a digital elevation model: A case study in northern Thailand. Forest Ecology and Management, 224(1), 147-156.

McWilliams, W.H., 1991. Availability of yellow pine sawtimber in Alabama. In: Jones, R.H. (Ed.), Proceedings: Alabama's Forest Resources: Past, Present, and Future. Auburn University, AL, pp. 115–119.

Mitchell C.C., 2008. Soils of Alabama. Alabama Cooperative Extension System ANR-340, USDA-NRCS http://www.aces.edu/pubs/docs/A/ANR-0340/. Accessed 30 August 2015

Montgomery, D.R. and W.E. Dietrich, 1988. Where do channels begin? Nature, 336, 232–234, doi: 10.1038/336232a0.

Montgomery, D.R. and W.E. Dietrich, 1989. Source areas, drainage density and channel initiation. Wat. Res. Res., 25, 1907-18.

Montgomery, D.R. and W.E. Dietrich, 1994. Landscape dissection and drainage slope–area thresholds. In Process Models I Theoretical Geomorphology, Kirkby M (ed.). Wiley: Chichester; 221–246.

Montgomery, DR and E. Foufoula-Georgiou, 1993. Channel network source representation using digital elevation models. Water Resources Research 29: 3925–3934.

Montgomery, D.R. and W.E. Dietrich, 1992. Channel initiation and the problem of landscape scale. Science, 255(5046), 826-830.

O'Callaghan, J.F. and D.M. Mark, 1984. The extraction of drainage networks from digital elevation data. Comput. Vis. Graph. Image Process, 28(3), 323–344, doi: 10.1016/S0734-189X (84)80011-0.

Orlandini, S. and G. Moretti, 2009. Determination of surface flow paths from gridded elevation data. Water resources research, 45(3).

Orlandini, S., P. Tarolli, G. Moretti, and D.G. Fontana, 2011. On the prediction of channel heads in a complex alpine terrain using gridded elevation data. Water Resour. Res., 47(2), W02538, doi: 10.1029/2010WR009648.

Peterson, B.J., W.M. Wollheim, P.J. Mulholland, J.R. Webster, J.L. Meyer, J.L. Tank, E. Marti, W.B. Bowden, H.M. Valett, A.E. Hershey, W.H. McDowell, W.K. Dodds, S.K. Hamilton, S. Gregory, and D.D. Morrall, 2001. Control of nitrogen export from watersheds by headwater streams. Science 292 (5514): 86-90.

PRISM Climate Group, Oregon State University, http://prism.oregonstate.edu, created 4 Feb 2004.

Prosser IP and B. Abernethy, 1996. Predicting the topographic limits to a gully network using a digital elevation and process thresholds. Water Resources Research 32(7): 2289–2298.

Senevirathne, N. and G.A. Willgoose, 2013. Comparison of the Performance of Digital Elevation Model Pit Filling Algorithms for Hydrology. 20th International Congress on Modeling and Simulation, Adelaide, Australia, 1–6 December 2013

Simley, J., 2007. Statistics of the nationwide high resolution national hydrography dataset: U.S. Geological Survey National Hydrography Dataset Newsletter, 6(11), September 2007. Accessed September 4, 2015 at: http://nhd.usgs.gov/newsletters/ News_Sept_07.pdf.

Sofia, G., P. Tarolli, F. Cazorzi, and D.G. Fontana, 2011. An objective approach for feature extraction: Distribution analysis and statistical descriptors for scale choice and channel network identification. Hydrol. Earth Syst. Sci., 15(5), 1387–1402, doi: 10.5194/hess-15-1387-2011.

Tarboton D.G., 1997. A new method for the determination of flow directions and upslope areas in grid digital elevation models. Water Resources Research 33: 309–319.

U.S. Geological Survey (USGS), 2000. The National Hydrography Dataset Concepts and Contents [Online]. Available at http://nhd.usgs.gov/ chapter1/index.html.

Vannote, R.L., G.W. Minshall, K.W. Cummins, J.R. Sedell, and C.E. Cushing, 1980. The river continuum concept. Canadian journal of fisheries and aquatic sciences, 37(1), 130-137

Yang, T.H., Y.C. Chen, Y.C. Chang, S.C. Yang, and J.Y. Ho, 2015. Comparison of Different Grid Cell Ordering Approaches in a Simplified Inundation Model. Water, 7(2), 438-454.

Chapter 3: Improving the slope-area method for placing channel head locations in the state of Alabama

ABSTRACT

Channel heads act as a bridge that connects hillslopes to downstream ecosystems and are the primary source of water, sediment, and nutrients in a drainage basin. Because of the number and extent of channel heads on the landscape, field identification for mapping their locations would be extremely time-consuming and labor intensive. Therefore, methods for automatic mapping of stream channel head locations using Geographic Information Systems (GIS) and associated datasets have been developed. A total of 162 field mapped stream channel head locations across three physiographic regions of Alabama were analyzed along with their topographical, soil, and climatic data to develop a region-specific GIS model for each area. These data were also used to develop a comprehensive state GIS model for locating stream channel heads. The study objectives were to investigate the value of these landscape variables to accurately predict stream channel head locations in the Coastal Plain (CP), Piedmont/Ridge and Valley (P/RV) and Southwest Appalachian (SW) regions of Alabama and to compare the results with the traditional slope-area method. The region-specific multi-variable models provided the best predictions of stream channel head locations mapped in the field at each region. The comprehensive model was less accurate at locating the actual stream channel head locations compared to the region-specific models. However, the comprehensive model was comparable to region-specific slope-area models,

showing that it could be applied in regions where no field mapped stream channel head location data is available.

INTRODUCTION

Stream channel heads, defined as the upstream boundary of concentrated water flow and sediment transport between definable banks (Dietrich and Dunne, 1993), are the primary source of water in a drainage basin since they connect unchanneled flow paths, called zero-order basins, and stream channels (Dietrich et al., 1987). Stream channel head locations play an important role in water, sediment, and pollutant transport from hillslopes to downstream of a drainage basin (Montgomery and Dietrich, 1988; Clarke et al., 2008). They normally represent the origin of drainage networks that includes streams, rivers, lakes, and coastal waters.

Agencies, planners, and land managers often identify streams for management and planning purposes according to the USGS 1:24,000 scale topographic map blue lines yet these maps are, in most cases, incomplete and outdated (Heine et al., 2004; Colson et al., 2008; see Chapter 2). Nevertheless, these maps are commonly used for conducting studies, planning and managing water resources and water quality programs. This is concerning because these maps were not created for technical and regulatory applications and do not accurately reflect all the streams on the ground (Vannote et al., 1980); however, they are often the best information available.

Up to 85% of the stream network in a drainage basin is composed of first-order streams (Peterson et al., 2001), which drain a substantial portion of a basin. Accurately identifying areas where these stream channels begin on the hillslope has been a challenge for predicting flow, controlling pollution, managing water bodies, and conducting remediation and stream restoration. Drainage density and stream order are two measures commonly used in fluvial geomorphological studies (Henkle et al., 2004). In terms of hydrologic modeling, drainage density has a direct influence on a watershed's hydrograph. Drainage density also has a significant role in the estimation and modeling of sediment and stream discharge since it is directly linked to peak discharge and sediment transport in a drainage basin (Kalin et al., 2003). It has been shown that the source area and drainage density are often strongly dependent on the location of stream channel heads (Gomi et al., 2002). Varying climatic regimes, land use impacts, and soil properties also have an effect on the location of the stream channel head locations (Montgomery and Dietrich, 1988; Prosser and Abernethy, 1996; McGlynn and McDonnel, 2003). Drainage density, therefore, can vary between physiographic regions because these areas often have distinct climatic, topographic, and geologic characteristics (Tucker and Bras, 1998; Chapter 2).

Because of the importance of stream channel head locations, several researchers have focused on identifying and mapping these landscape features (O'Callaghan and Mark, 1984, Montgomery and Dietrich, 1988, 1989; Montgomery and Foufoula-Georgiou, 1993; Henkle et al., 2004, Orlandini et al., 2011). Because there are so many, field mapping all stream channel heads would be unpractical due to the time and labor required. As a result, tecniques for automated identification and mapping of stream channel heads have been developed using DEM and related spatial data (e.g. slope, plan and profile curvature) (O'Callaghan and Mark, 1984; Montgomery and Dietrich 1988, 1989, 1992, 1994; Dietrich and Dunne, 1993; Montgomery and Foufoula-Georgiou; Henkle et al, 2004; Sofia et al., 2011; Orlandini et al., 2011; Clubb et al., 2014). Including these data can help produce more accurate drainage networks that better approximate the spatial extent of streams in the field. The improvement in DEM resolution and availability has advanced various methods to automatically and accurately map stream channel head locations.

Flow routing algorithms are often used with DEMs to determine the paths of water and sediment transport (Tarboton, 1997). Most of the stream extraction methodologies are traditionally based on flow routing algorithms (Sofia et al., 2011), and several have been proposed, such as the

D8 and D∞ flow algorithm (O'Callaghan and Mark 1984; Tarboton, 1997). These methods have been used to convert the drainage flow path to a meaningful stream network and include both the unique source area threshold method (O'Callaghan and Mark, 1984; Tarboton et al., 1991) and the slope-area method (Montgomery and Dietrich, 1988, 1989, 1992, 1994; Montgomery and Foufoula-Georgiou, 1993; Dietrich et al., 1993). However, previous studies show variable reliability and sensitivity of these methods when applied over different drainage basins (Bischetti et al., 1998; Orlandini et al., 2011; Sofia et al., 2011; see also Chapter 2). This is likely because channel incision is not only dependent on topographic features. Climate, land use, and soil also affect the origin of channel heads (Montgomery and Dietrich, 1988; Prosser and Abernethy, 1996; McGlynn and McDonnel, 2003). The drainage area, for instance, tends to increase when an area is more arid or with increasing infiltration capacity, hydraulic conductivity, or critical shear stress (Montgomery and Dietrich, 1994).

Some studies have found the slope-area method to be suitable for determining the stream channel head locations from DEM (Montgomery and Dietrich, 1989, 1992, 1994; Hancock and Evans, 2006;) but others have not (Heine et al., 2004, McNamara et al., 2006). Montgomery and Dietrich (1988) studied channel heads in basins across the western U.S. and found a strong inverse relationship between local slope and drainage area. Where the slope-area method is insufficient, the location of the channel head may also be heavily affected by climate, with wetter regions generating smaller drainage areas even if the slopes could be the same (Montgomery and Dietrich 1988). Other studies have demonstrated that additional factors are sometimes needed when predicting channel head locations. In their study, Heine et al. (2004) compared five existing methods and two new methods for delineating the stream channel networks. They demonstrated that using the variable flow accumulation method calculated by logistic regression resulted in the most accurate stream channel network delineation (especially in low-order stream channels). It outperformed the existing USGS topographic maps and other flow accumulation area methods, including the slope-area and unique source area method. The updated method developed by Heine et al. (2004) generates a variable flow accumulation area estimated by multiple linear regression. The method considers flow accumulation area as a function of other independent variables (i.e., slope, plan and profile curvature) that can be derived from DEMs. However, land use, soil, and climate variables were not included in the model even though they have an effect on the flow accumulation area. They also concluded that this method performed better than all the existing methods. In another study, Russell (2008) studied 23 watersheds across five physiographic regions in North Carolina to develop a map of the state that precisely depicted the headwater streams (first-order and second-order streams). Terrain features derived from DEM (i.e. weighted/local slope, curvature, contributing drainage area) were used in a logistic regression model to locate headwater streams. The model yielded accurate results in predicting the location of headwater streams with 83% accuracy and stream length with 77% accuracy. Russell noted that additional variables, such as soil and climate, other than terrain variables might yield even more accurate results.

Some evidence suggests that local slope and drainage area may be even less important than other related topographic variables used. Julian et al. (2012) studied the channel head locations across five physiographic regions in Maryland and Virginia in the mid-Atlantic US. They compared topographic, geologic, climatic, and land cover variables to demonstrate the significant factors that initiate stream channel heads and the statistical relationship between these variables with each other in each physiographic region. They found no relationship between the local slope and the drainage area in any of their study sites. They noted that local plan curvature was actually the best parameter to predict source area if all the landscape variables were weakly correlated to channel head location. The best correlations to the drainage area of the stream channel head were found for other landscape variables such as topographic attributes, i.e., local plan curvature in a site, average profile curvature in tree sites, and local slope in a site.

Literature shows that there are few studies that have examined all the possible variables for precisely determining the stream channel head locations across a variety of physiographic regions (Julian et al., 2012). This chapter investigated what other landscape variables could improve the accuracy of stream channel head location predictions in three physiographic regions of Alabama. In order to demonstrate which variables could best improve the determination of the stream channel head's location, the stream channel heads mapped across the state of Alabama from the previous chapter (Chapter 2) were evaluated further.

METHODOLOGY

Study Areas

This part of the study was conducted, like the previous chapter, in three physiographic regions of Alabama: the Coastal Plain (CP), the Piedmont/Ridge and Valley (P/RV) and the Southwestern Appalachians (SWA) (Figure 3.1).

Conecuh National Forest was the primary study area in the CP region. The CP covers a massive portion of the state of Alabama extending over most of central and southern Alabama. Annual precipitation across Alabama is highest in this region with a mean annual rate of 1550 mm (PRISM, 2004). Soils in the CP are generally described as being well-drained and having loamy subsoils with sandy loam or loam surface layers (Mitchel, 2008). Our study area was generally less than 100 m above sea level and the slope ranges from 0 to 30 degrees (Table 2.1).

Talladega National Forest was used to map stream channel head locations in the P/RV region, and is located in both the Piedmont and Rindge and Valley regions. The Piedmont is a transitional area between the Ridge and Valley region and the Coastal Plain region. Even though field sites visited in Talladega National Forest were mapped as the Piedmont, the area was considered a transitional zone between the Piedmont and the Ridge and Valley. Average annual precipitation in this region is about 1400 mm (PRISM, 2004). Soils in this region often consist of some clayey subsoils with a sandy loam to clay loam surface layer (Mitchell, 2008). Elevation ranges from 115 to 734 m, and slope also varies between 0 - 72 degrees (Table 2.1).

For the SWA region, the William B. Bankhead National Forest was used to map stream channel head locations. This national forest is located in the northwest section of Alabama, and is characterized by mountains with abrupt, deeply incised cliffs. Average annual precipitation is approximately 1450 mm (PRISM, 2004). The soil of this region is often moderately deep, well drained, and permeable and consists mostly of loamy subsoils and sandy loam surface layers (Mitchell, 2008). Elevation in this region is, in general, less than 330 m above sea level, and slopes range between 0 - 62 degrees (Table 2.1).

Field Mapped Stream Channel Head Locations

Stream channel heads were field identified using guidelines provided by Dietrich and Dunne (1993). Field identification consisted of a multi-step process. First, the main stream channel was identified in the field. Then, we walked upstream until the stream channel origin was reached, and a GPS location was collected. Next, we walked back down the stream to a convergence, and then walked up to the next stream channel head origin. This was continued until all channel heads were mapped in the selected catchment. Between February and May 2015, a total of 162 stream channel head locations were identified across the three physiographic regions of Alabama, including CP region (n=51), P/RV region (n=60), SWA region (n=51). Each stream channel head was mapped using a map-grade GPS - Forge 912 F4 device. For each channel head location, photographs were taken to better interpret the field data and notes taken on the form of stream initiation (i.e., gradual or abrupt), apparent bedrock condition, and flow conditions (dry or wet) during the visit.

Stream Channel Head Variables

In this study, multiple variables were used to generate a model to accurately delineate the stream channel head locations. The most commonly used variables were selected based on previous studies (Dietrich and Dunne, 1993; Heine et al., 2004; Julian et al., 2012) to develop a model and compare the important variables for each physiographic region (Table 3.1). The topographic, climatic, and soil variables are briefly explained below.

Topographic Variables

Topographic variables used in this study included drainage area (*DA*), local slope (S_{loc}), average upstream slope (S_{avr}), local plan curvature (PL_{loc}), average upstream plan curvature (PL_{avr}), local profile curvature (PR_{loc}), and average upstream profile curvature (PR_{avr}). All these variables were derived from Digital Elevation Model (DEM) with 10-m resolution acquired from the USGS National Elevation Dataset (NED). TauDEM, an ArcGIS toolset, was used to create drainage area and slope raster datasets. For drainage area calculation, the D∞ flow algorithm method (Tarboton, 1997) was used to determine flow direction and flow accumulation. Each cell in the raster dataset was assigned to their drainage area (m^2) calculated as the upstream cells draining into the cell plus its own area, then multiplied by the DEM cell size. The slope (m/m) was calculated as the steepest outward slope between one of the eight surrounding cells centered at each grid cell (Tarboton, 1997). ArcGIS, spatial analyst - surface toolset, was used to extract curvature rasters. Curvature is the second derivative of the surface, or known as the slope of the slope (Evans, 1972) and helps to interpret if an area is concave or convex. Profile curvature is calculated parallel to the maximum slope, with positive values indicating that a surface is upwardly concave, negative values indicating that a surface is upwardly convex, and a value of zero indicating that the surface is linear. These measures can affect the speed/rate of flow across the surface. Plan curvature, on the other hand, is calculated perpendicular to the maximum slope, with positive values indicating that a surface is sidewardly convex, negative values indicating that a surface is sidewardly concave, and a value of zero indicating that the surface is linear. They determine the convergence or divergence of flow across the surface. Local plan and profile curvature values were calculated at the channel head while the average values were the mean of the plan and profile curvatures of upstream drainage area. The units for all curvature values are 1/100 of a z-unit.

Climatic Variables

Climatic variables used in this study included 30-yr average annual precipitation (P_{annual}) for the period of 1981-2010 and 30-min rainfall depth with two years recurrence interval (I_{30}) (Julian et al., 2012). For the P_{annual} data, PRISM dataset with 800-m resolution was downloaded (http://prism.oregonstate.edu) and extracted for each stream channel head location using GIS. The 30-min rainfall depth data were also extracted for each stream channel head locations from National Oceanic and Atmospheric Administration (NOAA) Precipitation Frequency Data Server (PFDS).

Soil Variables

Soil variables consisted of hydraulic conductivity (K_{sat}), soil erodibility factor (K_{fac}), sand percentage (*%Sand*), clay percentage (*%Clay*) and soil depth to bedrock (D_{bdr}). The maximum soil depth (D_{bdr}) is limited to 201 cm in SSURGO dataset. In order to obtain these values for each stream channel head location, Soil Survey Geographic Database (SSURGO) and Soil Data Viewer tool (an ArcGIS extension) were used. SSURGO dataset, available across the US, was downloaded from http://www.nrcs.usda.gov.

Statistical Analysis and Assessment of Model Performance

The 162 stream channel head locations along with their characteristics (topographic, climatic and soil) were statistically analyzed to develop a model that best predicted stream channel head locations in each physiographic region, as well as across the state of Alabama. For all stream channel head locations across the three physiographic regions, mean and standard deviations of all variables were summarized. Data used for analyses were tested for normality and homogeneity and then examined between regions using a one-way ANOVA with Tukey's HSD (Honestly Significantly Different) test. All statistical test results were considered significant at <0.05.

A Pearson product moment correlation coefficient was computed to assess the relationship between the log of drainage area and each variable for providing an initial understanding of the effective variables that could be related to channel initiation for each study site. The correlations were considered to be effectively correlated when $r > 0.5$ and $p < 0.05$. The topographic, climatic, and soil variables were then analyzed using Akaike Information Criterion (AIC) to select the most appropriate model for each physiographic region and the whole dataset. AIC was selected for this study because it is more suitable than other information criteria (e.g. Bayesian) when there is low number of sample sizes (Soltani, 2014 and Emiliano et al., 2009). Stepwise regression using the forward method, in which each variable was entered into the model step by step according to *p*-values until the lowest AIC value was reached, was used to identify the most suitable variables for each model. JMP® Pro 11 (JMP User Guide, 2007) was used for all statistical analysis.

Using the selected variables based on AIC, region specific models for each physiographic region and a comprehensive state model were developed to locate stream channel head locations.

An assessment method (Orlandini, 2011) for quantifying model reliability and sensitivity indices was used to compare the model performance between the physiographic regions and to demonstrate model improvement compared to only using the slope-area method (examined in the previous chapter, Table 2.4). Around each mapped channel head, a 10-m buffer zone was created to define a reasonable neighborhood. Channel head locations were classified into three classes: true positives (*TP*), false positives (*FP*), and false negatives (*FN*). *TPs* were defined as occurring when a predicted channel head was found inside one of the circles around a mapped channel head location. *FPs* occurred when a predicted channel head fell outside of the circle drawn around the mapped channel head. *FNs* were defined when the buffer drawn around the observed channel heads do not include any of the predicted channel heads. Examples of each scenario are provided in Figure 2.3.

Using these classifications, the reliability (*r*) of the slope-area method was calculated as:

$$\mathbf{r} = \frac{\sum \mathbf{TP}}{\sum \mathbf{TP} + \sum \mathbf{FP}} \tag{2.1}$$

where $\sum$ TP and $\sum$ FP were the total numbers of true and false positives. This measured the model's capacity not to generate channel heads when there is no observed channel head.

The sensitivity (*s*) of the method was calculated as:

$$\mathbf{s} = \frac{\sum \mathbf{TP}}{\sum \mathbf{TP} + \sum \mathbf{FN}} \tag{3.2}$$

where $\sum$ TP and $\sum$ FN were the total numbers of true positives and false negatives. This measured the model's ability not to generate *FNs*, or to predict all mapped channel heads. The *r* and *s* indices were calculated for each region and a comprehensive state model to demonstrate the suitability of each model. Scores closer to 1 were considered a better performed model, and the values were compared among the study sites and the models used.

RESULTS

Characteristics of Stream Channel Head Locations

Descriptive statistics for the topographic, climatic, and soil characteristics for the stream channel head locations at each study site are presented in Table 3.2. The variables analyzed in this study were compared between the physiographic regions. Physiographic regions showed significant differences in drainage area even though the local slope was not always significantly different (e.g. in the P/RV and SWA regions) (Figure 3.2; Table 3.2). The highest mean drainage area was found in the CP region, and was approximately 15,400 m^2. As expected, the lowest mean local and mean average slopes were in this region too, and were 0.035 and 0.041 (m/m), respectively (Table 3.2). On the other hand, the steepest slopes were calculated in the P/RV and SWA regions along with the smallest drainage areas. The drainage areas in the P/RV region were as low as 264 m^2 and as high as 6000 m^2. The local slopes at the channel heads did not significantly differ in the P/RV and the SWA; whereas, the average upstream slopes were significantly different among the three physiographic regions. Box-plots (Figure 3.2) indicate the statistical differences in drainage area and local slope for each physiographic region and showed that the P/RV region had a substantially narrower range in drainage area than the CP region and the SWA region. In consideration of the local slope, the P/RV region and the SWA region showed a similar pattern, with a wider range of local slope values than the CP region.

The deepest soil depth to bedrock (201 cm) was in the CP region. The SWA and the P/RV region soils were relatively shallow, 81.5 cm and 48.5 cm, respectively. The erodibility indexes were not substantially different among the physiographic regions (Table 3.2). The highest erosion susceptibility was found in the CP region, and the lowest was found in SWA region. The CP region soils had the highest sand percentage (73%) while P/RV had the highest clay percentage (52%).

Both of the climate parameters, average annual precipitation and the 30-min rainfall depth, also significantly differed across the physiographic regions of Alabama (Table 3.2). The CP region received the highest average annual precipitation (1570 mm), as opposed the P/RV and SWA regions where the average annual precipitations were 1400 mm and 1485 mm, respectively. Correspondingly, the 30-min rainfall depth was the highest in the CP region and respectively lower in the SWA and P/RV regions.

Model Parameters Selection

There was a strong negative correlation between the log of drainage area (log-*DA*) and log of local slope (log-S_{loc}) for all the three physiographic regions and the entire dataset (r_{CP} = -0.67, $r_{P/RV}$ = -0.84, r_{SWA} = -0.78, and r_{entire} = -0.79); however, log of average slope (log-Savr) was significantly correlated with the log-DA for only the SWA region and the entire dataset (r_{SWA} = -0.50 and r_{entire} = -0.70). Scatterplots of the drainage area and the local slope summarizes the results (Figure 3.3). Overall, the log-Sloc had the strongest correlation with the log-DA (Table 3.3), supporting the concept that drainage area deacreases as the slope at the channel head increases.

Among the individual study sites, the P/RV region had the strongest correlations between the log-DA and the PLloc, PLavr, and PRloc variables (*r*=-0.65, *r*=-0.56, and *r*=0.58, respectively), with a relatively weaker correlation to the PRavr (*r*= 0.45). A positive correlation between the log-DA and PRavr were observed for all the three study sites and the entire dataset (r_{CP}=0.32, $r_{P/RV}$=0.45, r_{SWA}=0.64, and r_{entire}=0.62), resulting in higher drainage areas in more convex drainage catchments. The soil and climate variables had no significant correlations with the log-DA when the study sites were analyzed within the individual regions (Table 3.3). However, local and average slope, soil depth to bedrock, sand and clay percentages, and climate parameters were all found to have strong correlations with the log-DA when the entire stream channel head locations were pooled across the state of Alabama (n=162) (Table 3.3). Among the soil variables, clay and sand percentages and soil depth to bedrock had strong correlations with log-DA for the entire dataset (r_{clay} = -0.67, r_{sand} = 0.62, and r_{dbdr} = 0.65), indicating that more clayey stream channel heads tended to have smaller drainage areas, and increasing sand percentage and soil depth related to a larger drainage area for stream channel head locations.

According to AIC results, topographic variables (local slope and local plan curvature) were found to be the primary explanatory variables of stream channel head locations for each individual study site (Table 3.4). On the contrary, topographic, soil, and climatic variables were found to have a strong correlation with the log-DA and were the primary explanatory variables for the entire dataset. Log of local slope and surprisingly local plan curvature were the primary explanatory variables for all of the regional study sites and the entire dataset.

Assessment of Model Performance

For each physiographic region, the *r*- and the *s*-indices were calculated to compare model performance between physiographic regions and to indicate the improvement of predicted stream channel head locations when other landscape variables were modeled instead of just relying on the slope-area model. The *r*- and *s*-indices for the region specific multi-variable model, the comprehensive multi-variable model, and the slope-area model (Chapter 2) for each physiographic region were calculated and compared (Figure 3.4).

According to the *r*- and *s*-indices, there was an overall increase in the model performance for all physiographic regions once the region specific multiple variables were used to locate the stream channel head locations (Figure 3.4). However, the slope-area model's performance was slightly better than the comprehensive multi-variable model in all physiographic regions. The region specific and comprehensive multi-variable model were still the most sensitive and reliable in the P/RV region compared to the other regions (the CP and SWA regions).

In the CP and the SWA regions, the region specific multi-variable model tended to show less reliability and more sensitivity. In other words, the model had a tendency to generate more FPs, but satisfactorily do not to generate too many FNs in these physiographic regions. In contrast, the region specific multi-variable model for the P/RV region resulted in slightly higher reliability and less sensitivity, and performed relatively higher reliability and sensitivity scores among the physiographic regions.

The region specific multi-variable model for the P/RV region provided the most reliable prediction of field mapped stream channel heads ($r_{(P/RV)}$ = 0.77). The P/RV multi-variable model was the best at not generating channel heads that were not actually located in the field compared to the CP region and SWA region ($r_{(CP)}$ = 0.43 and $r_{(SWA)}$ = 0.52, respectively). Although the region specific model for the P/RV region was also the most sensitive ($s_{(P/RV)}$ = 0.67), the CP and SWA regions models also had relatively high scores ($s_{(CP)}$ = 0.51 and $s_{(SWA)}$ = 0.61, respectively). Higher sensitivity means that the models were fairly accurate at identifying the field mapped stream channel head locations.

DISCUSSION

In this study, a total of 162 stream channel heads across three physiographic regions of Alabama were mapped and related data used to develop and evaluate models for stream channel head locations. The stream channel heads reported in this study had drainage areas ranging from 0.03 ha to 7.63 ha (mean of 1.54 ha in CP region, 0.11 ha in P/RV region and 0.81 ha in SWA region). Additionally, the mean local slope at the channel head was 0.04 m/m in CP, 0.20 in P/RV, and 0.18 in SWA. These drainage areas and slopes were substantially smaller than others reported in similar studies (Montgomery and Dietrich, 1989; Bischetti et al., 1998; Julian et al., 2012; Villines et al., 2015), yet this is likely a result of the fact that our study areas could be categorized as wet regions.

Distinct characteristics were detected between our study sites regarding topographic, climatic, and soil variables. The local slopes at the channel heads did not significantly differ between the P/RV and SWA regions, but were significantly different from the CP region. Surprisingly, drainage areas of all three physiographic regions significantly differed from each other. This was somewhat surprising given the steep topography present at the P/RV and SWA regions. This may be partially explained by the high clay percentage in soils in the P/RV region compared to the SWA region, which had a measurable sand percentage. Sandy soils tend to have a higher infiltration capacity that may increase water storage and increase the effective drainage area needed to accumulate enough water to initiate stream channel head. Clayey soils tend to create a less permeable layer that causes more runoff and eventually smaller drainage areas (Critchley and Siegert, 1991). In the CP region, stream channel heads initiated at a considerably flatter slope range with larger drainage areas needed to accumulate enough water and sediment aggregation for channel head initiation. All the stream channel head locations were concave in plan and profile, indicating that the stream channel heads occurred in valleys, consistent with others studies (Heine et al., 2004; Julian et al. 2012).

In all of the study sites, the drainage area increased with decreasing local slope, which is also consistent with earlier studies (Montgomery and Dietrich, 1988, 1989, 1992; Montgomery and Foufoula-Georgiou, 1993; Villines et al., 2015). For all study sites and the entire dataset, the local slope was found to have the strongest correlation with the log of drainage area and therefore was the primary explanatory variable. In the P/RV region, local plan and local profile curvature were also strongly correlated with the log of drainage area. It should be noted that because of the study design, topographic variables were likely significant parameters in each physiographic region because stream channel head locations were normally collected in a fairly close range from each other. Since they were close, the soil and the climate parameters did not show significant variation between the channel head locations within regions, but did across physiographic regions. Results demonstrated that soil and climate variables also had a strong correlation with the log of drainage area when the entire dataset was pooled. It was not surprising to see a strong positive correlation between the drainage area and the soil depth and the sand percentage because deeper soils with more sand tend to have higher infiltration and storage capacities. Thus, a larger drainage area is needed to generate concentrated surface runoff. Due to these reasons, differences in the drainage area between the P/RV and SWA regions would expected, in spite of the similar topography.

Consistent with Julian et al. (2012), local plan curvature was also a primary explanatory variable in all four models created for the three physiographic regions, including the comprehensive statewide model. For streams evaluated in Alabama, all channel heads occurred in flow convergent areas. Where all the variables are poorly correlated with the log-DA, the local plan curvature should be considered a primary explanatory variable to locate stream channel head locations.

In all of the physiographic regions, the region specific multi-variable model satisfactorily located the stream channel head locations observed in the field. There was an increasing trend in the overall region specific multivariable model performance (r and s analysis) at all study sites compared to the performance of just using the slope-area model (see Chapter 2). However, using the comprehensive multi variable model did not improve performance compared to the slope-area model (Figure 3.4). These results suggest that the comprehensive model was an inadequate substitute for a multivariable stream channel head model developed specifically for the physiographic regions we examined. The field mapped stream channel head location data showed that each region had its own characteristics that significantly differed from each other and the formation of the stream channel heads varied between the regions because of the variation in explanatory variables. However, the comprehensive model resulted in similar reliability and sensitivity scores for individual regions compared to just using the slope-area model (Figure 3.4), indicating that the comprehensive model developed in this study would be useful in regions where channel head location data is not already available to develop a slope-area model.

According to the reliability and sensitivity indices, the region specific multi-variable model performed the best in the P/RV region. The model, however, resulted in lower reliability scores than sensitivity scores in the CP and SWA regions (Figure 3.4) while the reliability was higher than sensitivity in the P/RV region. In other words, in the CP and SWA regions, the model tended to produce more stream channel head locations than the ones observed in the field. Generating more reliable predictions of stream networks usually results in less sensitive stream networks, and vise-versa. In other words, producing a less dense stream network would increase the reliability of the model performance, but it would, meanwhile, reduce the model's sensitivity. The balance between the reliability and the sensitivity scores should be considered when selecting the best method to locate stream channel head locations. Additionally, more effective accuracy assessment methods are needed to properly decide which method performs better than others.

In conclusion, the region specific multi-variable models developed for three physiographic regions of Alabama (the CP, P/RV, and SWA regions) provided the best predictions of stream channel head locations that were previously mapped in the field. Our study also generated a comprehensive model that was less accurate for locating the actual stream channel head locations. However, the comprehensive model was comparable to the slope-area model, concluding that it could be applied in physiographic regions of Alabama where there is no available field mapped stream channel head location data. The advantage of this method is that all the data used in this study are publicly available datasets that cover the entire United States. This means that with some field mapped stream channel head locations, the region specific model can be easily applied anywhere to have a better representation of the actual stream network. Our data indicates that the field mapped stream channel head locations with a wider range of spatial locations (i.e., with more variations in soil and climate within a region) would increase the ability of the model for accurately locate stream channel head locations.

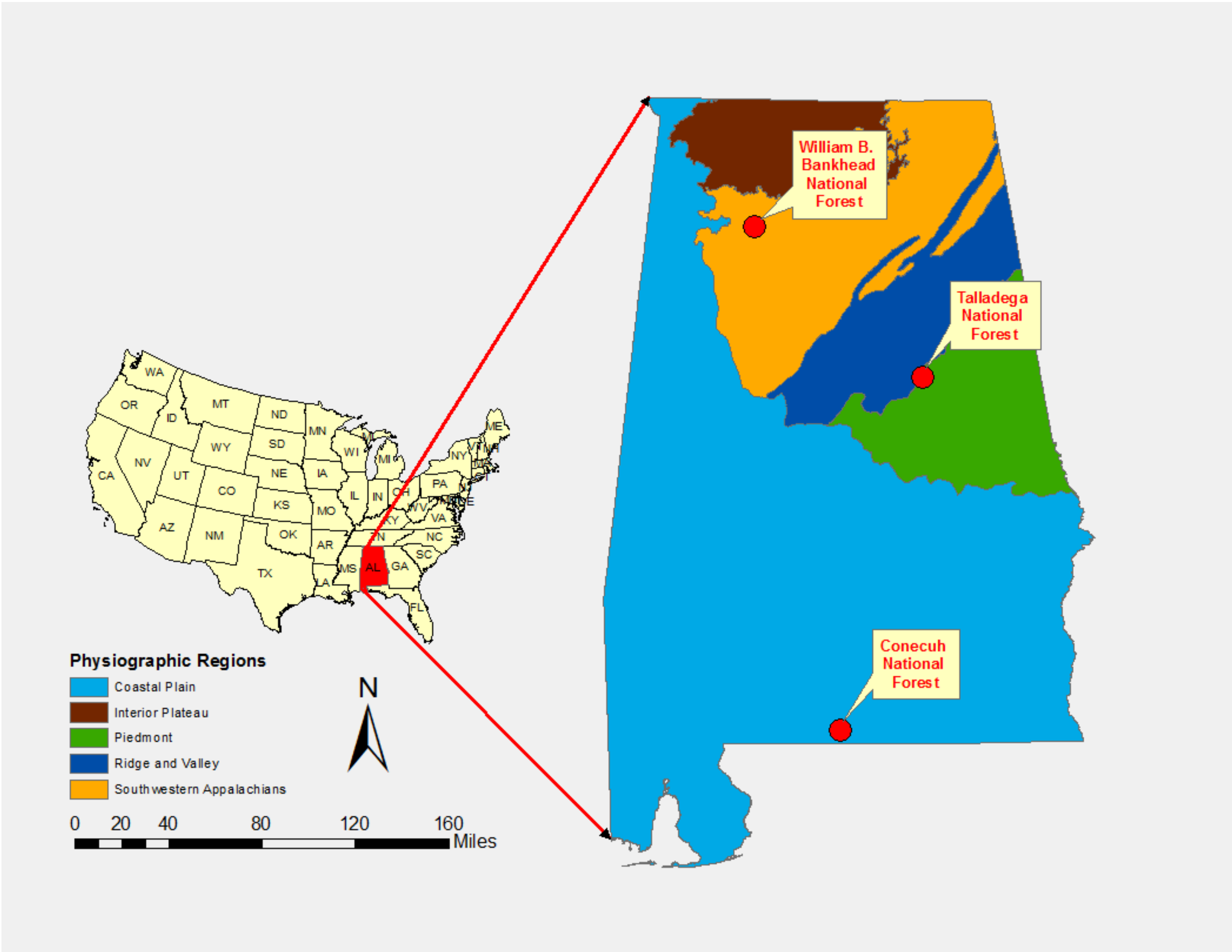

Figure 3.1: Locations of channel heads mapped in the watersheds across the physiographic regions of Southwestern Appalachian, Piedmont/Ridge and Valley, and Coastal Plain.

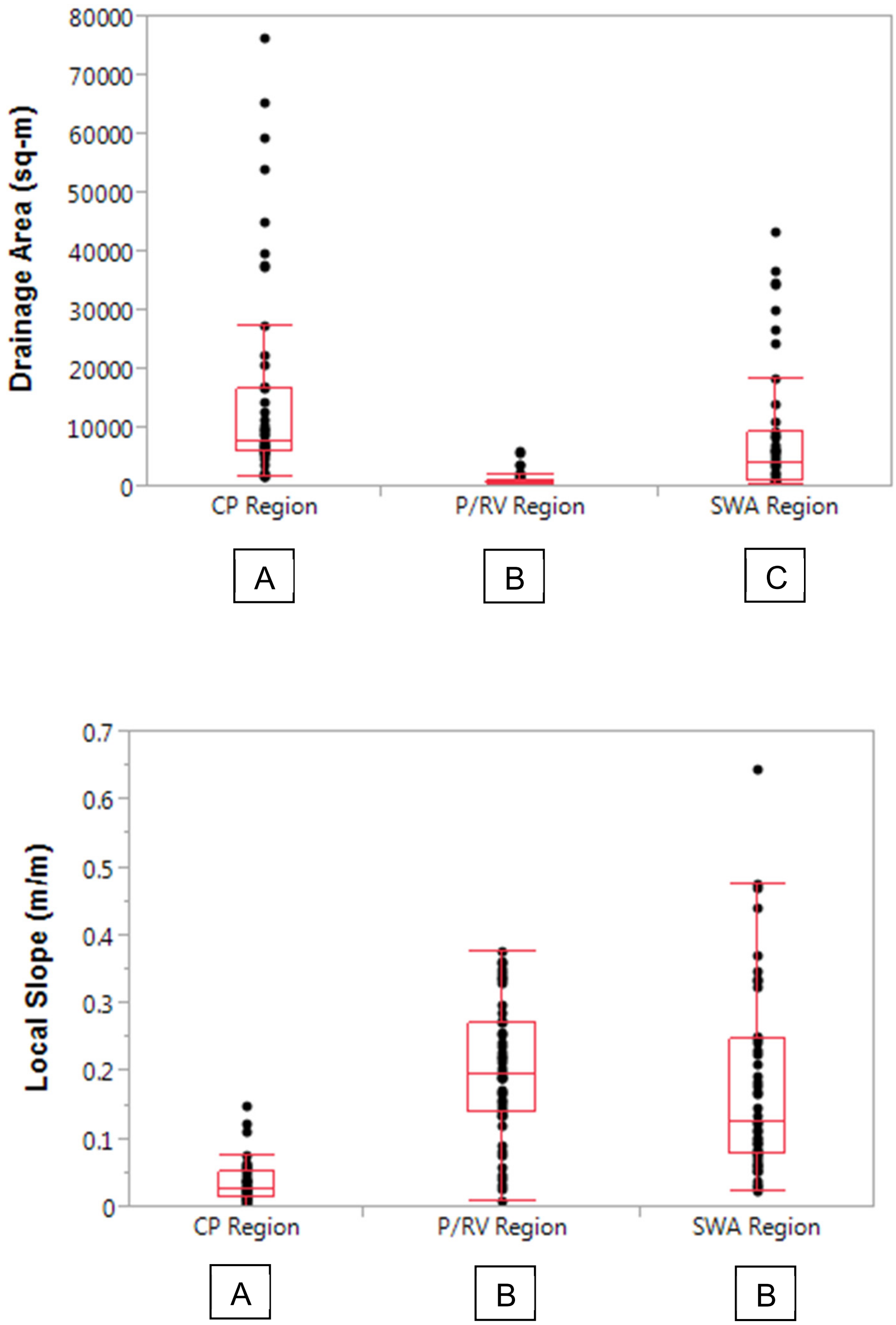

Figure 3.2: Drainage area and slope variations in each physiographic region. CP: Coastal Plain, P/RV: Piedmont/Ridge and Valley, SWA: Southwestern Appalachians. Different boxed letters indicate that the regions differ significantly (One-way ANOVA Tukey's HSD test, α = 0.05).

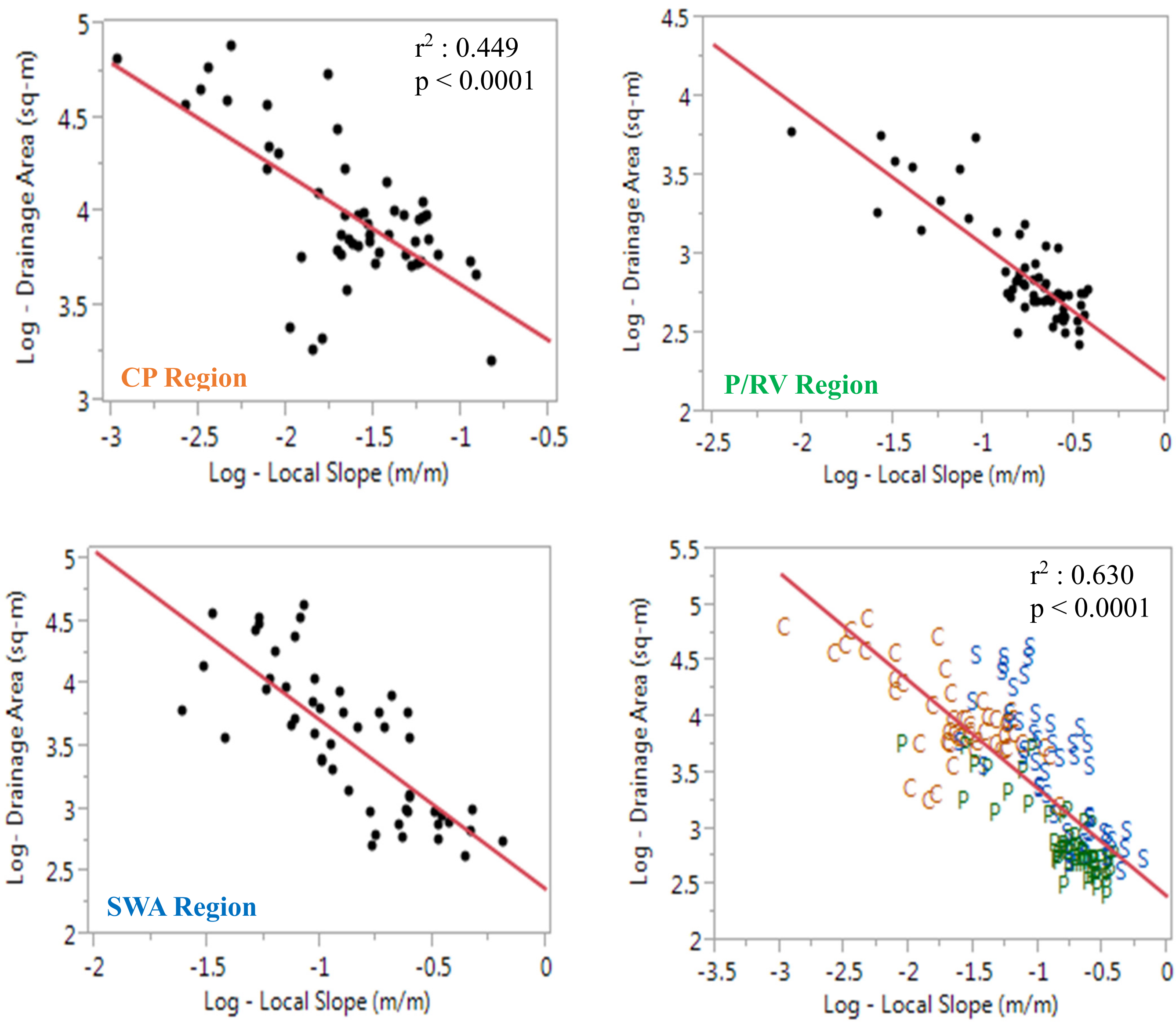

Figure 3.3: Scatterplots and regression results of log-drainage area and log-local slope for each physiographic region and the entire dataset (C: CP region, P: P/RV region, and S: SWA region).

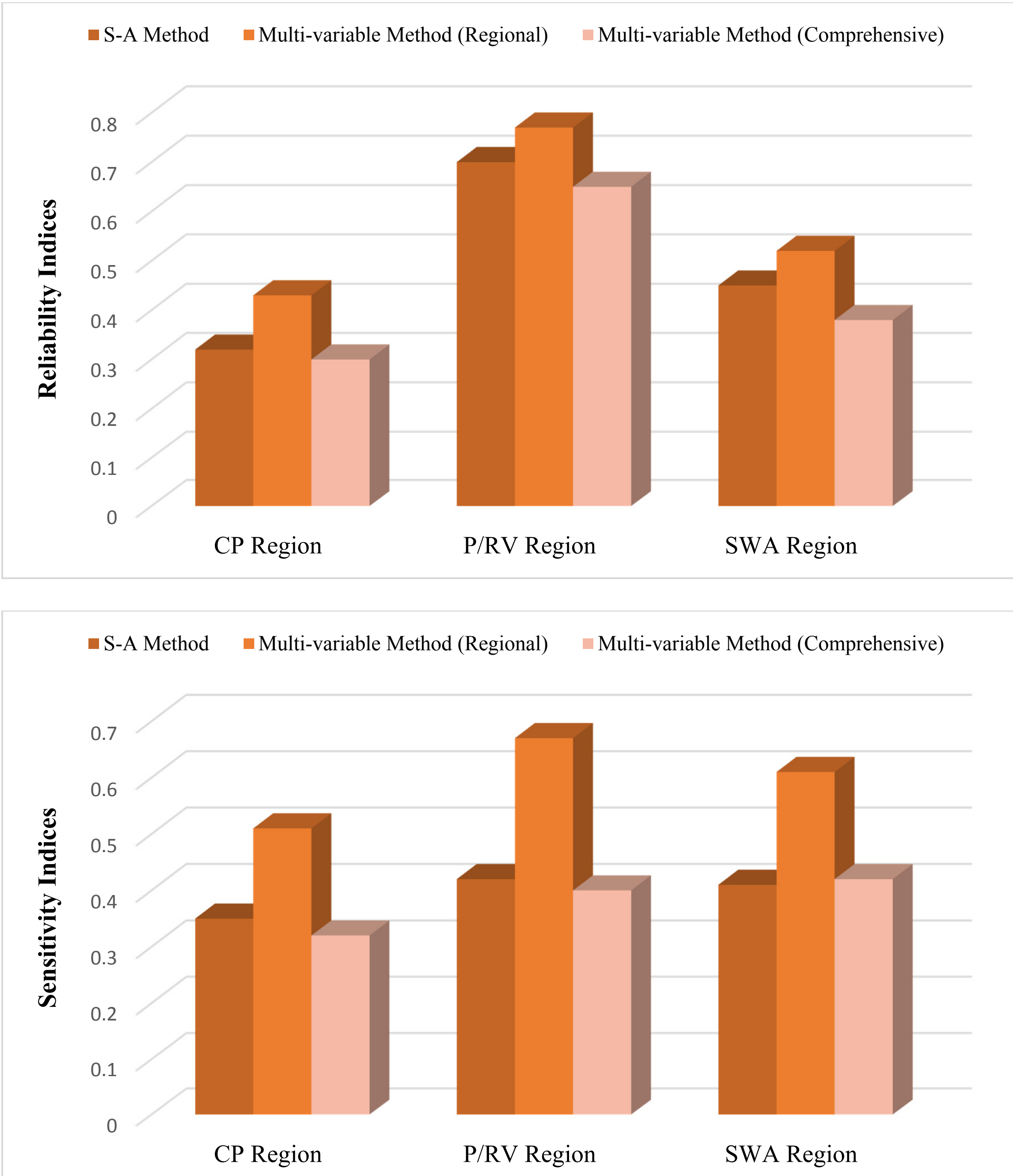

Figure 3.4: Reliability and sensitivity indices of slope-area (S-A) method and multi-variable method (regional and comprehensive) for the three physiographic regions.

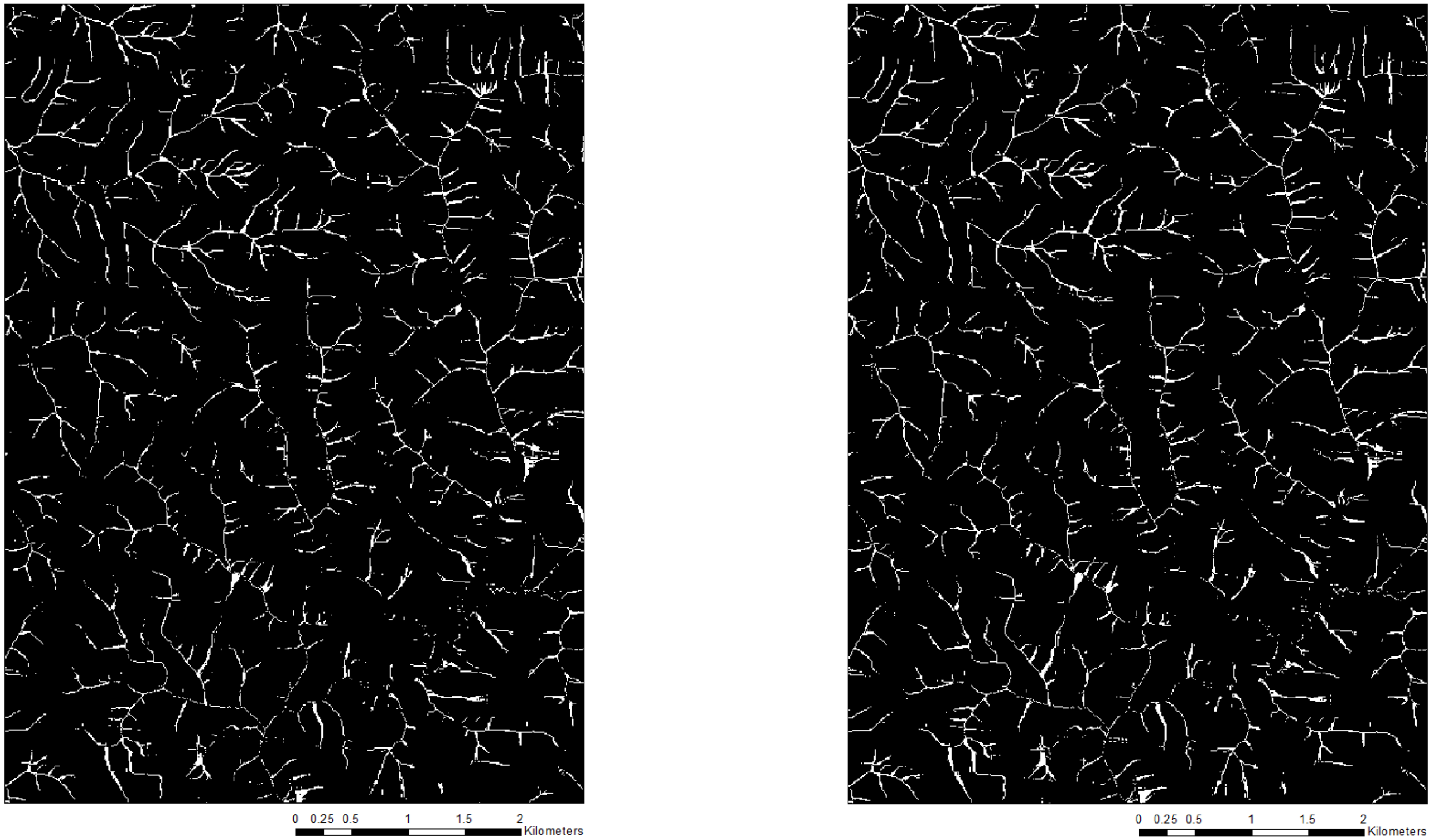

Figure 3. 5: Example of simulated stream network in the CP region using comprehensive multi-variable model (left) and region-specific multi-variable model (right)

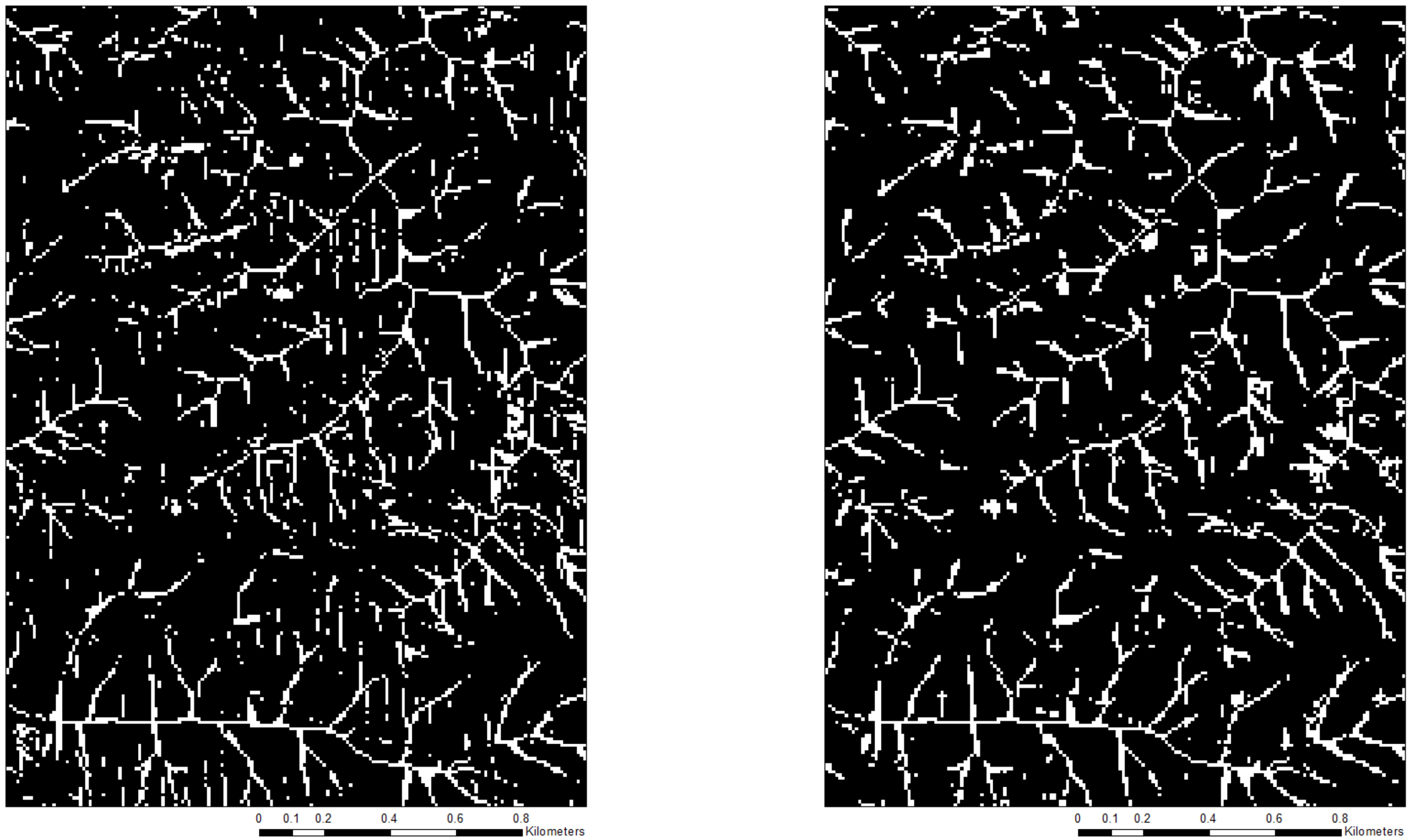

Figure 3. 6: Example of simulated stream network in the P/RV region using comprehensive multi-variable model (left) and region-specific multi-variable model (right)

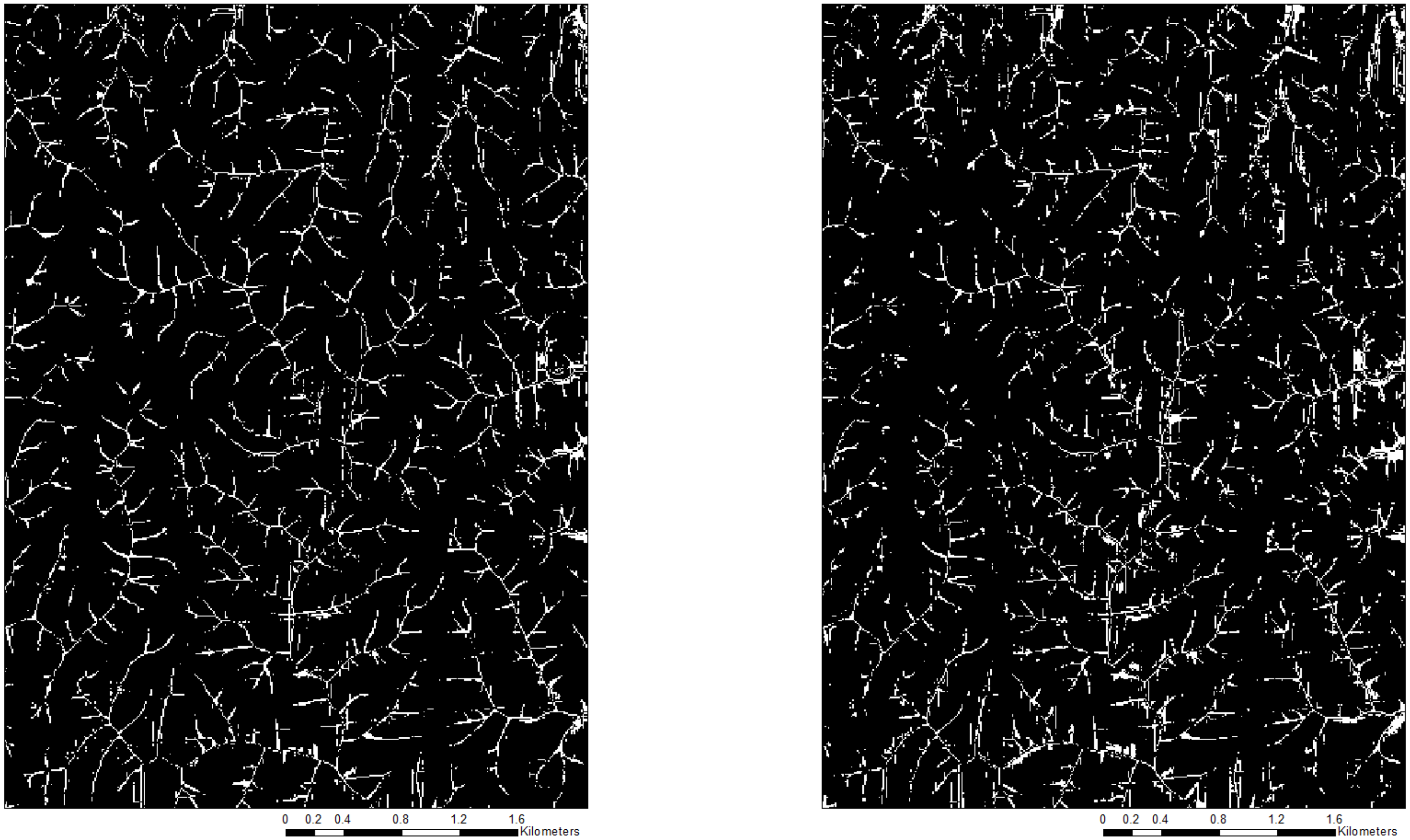

Figure 3. 7: Example of simulated stream network in the SWA region using comprehensive multi-variable model (left) and region-specific multi-variable model (right)

Table 3. 1: Topographic, climatic, and soil variables used in this study

Variables	Definition	Source
DA	Source area draining to channel head (m^2)	10-m DEM
$\boldsymbol{S_{loc}}$ / $\boldsymbol{S_{avr}}$	Local / average upstream slope (m/m)	10-m DEM
$\boldsymbol{PL_{loc}}$ / $\boldsymbol{PL_{avr}}$	Local / average upstream plan curvature perpendicular to the slope	10-m DEM
$\boldsymbol{PR_{loc}}$ / $\boldsymbol{PR_{avr}}$	Local / average upstream profile curvature parallel to the slope	10-m DEM
$\boldsymbol{K_{sat}}$	Saturated Hydraulic Conductivity (µm/sec)	SSURGO
$\boldsymbol{K_{fac}}$	Soil Erodibility Factor	SSURGO
$\boldsymbol{D_{bdr}}$	Depth to restricted layer (bedrock) (cm)	SSURGO
%Sand	Percentage of sand (%)	SSURGO
%Clay	Percentage of clay (%)	SSURGO
$\boldsymbol{P_{annual}}$	30-yr average annual precipitation (1981 – 2010) (mm)	PRISM
$\boldsymbol{I_{30}}$	30-min rainfall depth with 2-yr recurrence interval (mm)	NOAA-PFDS

Table 3. 2: Mean and standard deviation (SD) of the variables in each physiographic region. Regions with different letters indicate significant differences.

Variables	STAT	CP	P/RV	SWA
***DA* (m²)**	Mean	15,392 (a)	1,092 (b)	8,100 (c)
	SD	17,464	1,300	10,901
S_{loc} (m/m)	Mean	0.04 (a)	0.20 (b)	0.18 (b)
	SD	0.03	0.09	0.14
S_{avr} (m/m)	Mean	0.04 (a)	0.20 (b)	0.13 (c)
	SD	0.02	0.07	0.07
PL_{loc}	Mean	-0.30 (a)	-0.65 (b)	-0.97 (b)
	SD	0.32	0.72	0.97
PL_{avr}	Mean	-0.02 (a)	0.05 (b)	-0.05 (a)
	SD	0.03	0.20	0.12
PR_{loc}	Mean	0.16 (a)	0.36 (a)	0.37 (a)
	SD	0.32	0.93	1.06
PR_{avr}	Mean	-0.03 (a)	-0.27 (b)	-0.20 (b)
	SD	0.03	0.23	0.23
K_{sat} (µm/sec)	Mean	18.13 (a)	5.99 (b)	61.78 (c)
	SD	13.70	0.13	35.52
K_{fac}	Mean	0.23 (a)	0.21 (ab)	0.19 (b)
	SD	0.03	0.05	0.11
D_{bdr} (cm)	Mean	201 (a)	48 (b)	82 (c)
	SD	0	14	17
***%Sand* (%)**	Mean	73 (a)	30 (b)	66 (c)
	SD	11	3	18
***%Clay* (%)**	Mean	10 (a)	52 (b)	10 (a)
	SD	3	3	4
P_{annual} (mm)	Mean	1569 (a)	1398 (b)	1484 (c)
	SD	5	4	17
I_{30} (mm)	Mean	42 (a)	32 (b)	32 (c)
	SD	0.1	0	0.1

Table 3. 3: Correlation of each variable to the log of the drainage area in each physiographic region. Significant correlations were highlighted in the table.

Variables	**CP Log_*DA***	**P/RV Log_*DA***	**SWA Log_*DA***	**Comprehensive Log_*DA***
Log_*Sloc*	**-0.67**	**-0.84**	**-0.78**	**-0.79**
Log_*Savr*	0.01	-0.34	**-0.50**	**-0.70**
PLloc	-0.08	**-0.65**	-0.42	-0.17
PLavr	0.25	**-0.56**	-0.27	-0.37
PRloc	0.25	**0.58**	0.45	0.24
PRavr	0.32	0.45	**0.64**	**0.62**
Ksat	0.07	-0.16	0.10	0.23
Kfac	-0.17	-0.07	0.09	0.05
Dbdr	0.00	-0.09	0.06	**0.65**
%Sand	0.14	-0.07	0.01	**0.62**
%Clay	-0.07	0.07	-0.18	**-0.67**
Pannual	-0.18	0.09	0.25	**0.73**
I_{30}	-0.17	0.00	0.27	**0.59**

Table 3. 4: Stepwise regression model results along with their Akaike Information Criterion (AIC) value, *p*-value and consecutive R^2 values. (AIC increased beyond these when other parameters were added).

Study Area	Variables	AIC	p-value	R^2
CP Region	Log-S_{loc}	25.04	<0.0001	0.45
	PL_{loc}	21.05	0.0150	0.52
P/RV Region	Log-S_{loc}	-31.03	<0.0001	0.70
	PL_{avr}	-39.92	0.0014	0.75
	PL_{loc}	-41.22	0.0456	0.77
	PR_{avr}	-42.90	0.0519	0.79
SWA Region	Log-S_{loc}	49.11	<0.0001	0.60
	I_{30}	40.88	0.0069	0.68
	PL_{loc}	37.03	0.0165	0.72
Entire Dataset	Log-S_{loc}	161.06	<0.0001	0.63
(Comprehensive)	*%Clay*	90.32	0.0773	0.76
	PL_{loc}	63.14	0.0036	0.80
	PR_{avr}	55.90	0.0016	0.81
	PL_{avr}	55.13	0.0477	0.82
	Log-S_{avr}	54.98	0.0327	0.82
	P_{annual}	54.58	0.0055	0.82
	I_{30}	53.23	0.0074	0.83

LITERATURE CITED

Bischetti, G. B., Gandolfi, C., & Whelan, M. J., 1998. The definition of stream channel head location using digital elevation data. IAHS Publications-Series of Proceedings and Reports-Intern Assoc Hydrological Sciences, 248, 545-552.

Clubb, F. J., Mudd, S. M., Milodowski, D. T., Hurst, M. D., and Slater, L. J., 2014. Objective extraction of channel heads from high-resolution topographic data. Water Resour. Res., 50, 4283–4304, doi: 10.1002/ 2013WR015167.

Colson, T., J. Gregory, J. Dorney, and P. Russell., 2008. Topographic and soil maps do not accurately depict headwater stream networks. National Wetlands Newsletter 30(3):25–28.

Dietrich, W. E., and Dunne T., 1993. The channel head. In: Channel Network Hydrology, edited by K. Beven and M. J. Kirkby, pp. 175–219, John Wiley, N. Y.

Dietrich, W.E., Reneau, S.L., Wilson, C.J., 1987. Overview: "zero-order basins" and problems of drainage density, sediment transport and hillslope morphology. Int. Assoc. Hydrol. Sci. Bull. 165, 27–37.

Emiliano, P. C., Vivanco, M. J. F., Menezes, F. S. D., & Avelar, F. G., 2009. Foundations and comparison of information criteria: Akaike and Bayesian. Revista Brasileira de Biometria, São Paulo, 27(3), 394-411.

Evans, I. S., 1972: General geomorphology, derivatives of altitude and descriptive statistics. In: Spatial Analysis in Geomorphology, edited by: Chorley, R. J., Methuen&Co. Ltd, London, 17–90.

Gomi, T., Sidle, R. C., & Richardson, J. S., 2002. Understanding Processes and Downstream Linkages of Headwater Systems Headwaters differ from downstream reaches by their close coupling to hillslope processes, more temporal and spatial variation, and their need for different means of protection from land use. BioScience, 52(10), 905-916.

Hancock GR, Evans KG., 2006. Gully position, characteristics and geomorphic thresholds in an undisturbed catchment in Northern Australia. Hydrological Processes.

Heine, R.A., Lant, C.L., and Sengupta, R.R., 2004. Development and comparison of approaches for automated mapping of stream channel networks. Annals of the Association of American Geographers, 94(3), pp. 477-490.

Henkle, J. E., Wohl, E., and Beckman, N., 2011. Locations of channel heads in the semiarid Colorado Front Range, USA. Geomorphology, 129(3–4), 309–319, DOI:10.1016/j.geomorph.2011.02.026.

JMP User Guide, Release 7 Copyright ©, 2007. SAS Institute Inc., Cary, NC, USA ISBN 978-1-59994-408-1

Julian J.P., Elmore A.J., Guinn S.M., 2012. Channel head locations in forested watersheds across the mid-Atlantic United States: A physiographic analysis. Geomorphology 177-178, pp. 194-203.

Kalin, L., Govindaraju, R.S., Hantush, M.M., 2003. Effect of geomorphologic resolution on runoff hydrograph and sedimentograph. Journal of Hydrology, 276:89-111.

McGlynn, B. L., McDonnell, J. J., 2003. Role of discrete landscape units in controlling catchment dissolved organic carbon dynamics. Water Resources Research, 39(4).

McNamara, J. P., Ziegler, A. D., Wood, S. H., & Vogler, J. B., 2006. Channel head locations with respect to geomorphologic thresholds derived from a digital elevation model: A case study in northern Thailand. Forest Ecology and Management, 224(1), 147-156.

Mitchell CC, 2008. Soils of Alabama. Alabama Cooperative Extension System ANR-340, USDA-NRCS http://www.aces.edu/pubs/docs/A/ANR-0340/. Accessed 30 August 2015.

Montgomery D. R., Dietrich W. E., 1988. Where do channels begin? Nature, 336, 232–234, doi: 10.1038/336232a0.

Montgomery D. R., Dietrich W. E., 1989. Source areas, drainage density and channel initiation. Wat. Res. Res., 25, 1907-18.

Montgomery D. R., Dietrich W. E., 1994. Landscape dissection and drainage slope–area thresholds. In Process Models I Theoretical Geomorphology, Kirkby M (ed.). Wiley: Chichester; 221–246.

Montgomery DR, Foufoula-Georgiou E., 1993. Channel network source representation using digital elevation models. Water Resources Research 29: 3925–3934.

Montgomery, D. R., Dietrich, W. E., 1992. Channel initiation and the problem of landscape scale. Science, 255(5046), 826-830.

O'Callaghan, J. F., and Mark, D. M., 1984. The extraction of drainage networks from digital elevation data. Comput. Vis. Graph. Image Process, 28(3), 323–344, doi: 10.1016/S0734-189X (84)80011-0.

Orlandini, S., Tarolli, P., Moretti, G., and Fontana D.G., 2011. On the prediction of channel heads in a complex alpine terrain using gridded elevation data. Water Resour. Res., 47(2), W02538, doi: 10.1029/2010WR009648.

Peterson, B.J., W.M. Wollheim, P.J. Mulholland, J.R. Webster, J.L. Meyer, J.L. Tank, E. Marti, W.B. Bowden, H.M. Valett, A.E. Hershey, W.H. McDowell, W.K. Dodds, S.K. Hamilton, S. Gregory, and D.D. Morrall, 2001. Control of nitrogen export from watersheds by headwater streams. Science 292 (5514): 86-90.

PRISM Climate Group, Oregon State University, http://prism.oregonstate.edu, created 4 Feb 2004.

Prosser IP, Abernethy B., 1996. Predicting the topographic limits to a gully network using a digital elevation and process thresholds. Water Resources Research 32(7): 2289–2298.

Russell, P., 2008. Mapping headwater streams: intermittent and perennial headwater stream model development and spatial application. Final Report for Federal Highway Administration Contract Feasibility Study WBS: 36486.4.2. January 28, 2008.

Sofia, G., Tarolli, P., Cazorzi, F., and Fontana, D.G., 2011. An objective approach for feature extraction: Distribution analysis and statistical descriptors for scale choice and channel network identification. Hydrol. Earth Syst. Sci., 15(5), 1387–1402, doi: 10.5194/hess-15-1387-2011.

Soltani, A. A., 2014. A Greedy, Flexible Algorithm to Learn an Optimal Bayesian Network Structure. arXiv preprint arXiv: 1411.6651.

Tarboton D. G., 1997. A new method for the determination of flow directions and upslope areas in grid digital elevation models. Water Resources Research 33: 309–319.

Tarboton, D. G., Bras, R. L., and Rodriguez-Iturbe, I., 1991. On the extraction of channel networks from digital elevation data. Hydrol. Processes, 5(1), 81–100, doi:10.1002/hyp.3360050107.

Tucker, G. E., & Bras, R. L. (1998). Hillslope processes, drainage density, and landscape morphology. Water Resources Research, 34(10), 2751-2764.

Vannote, R. L., Minshall, G. W., Cummins, K. W., Sedell, J. R., & Cushing, C. E., 1980. The river continuum concept. Canadian journal of fisheries and aquatic sciences, 37(1), 130-137.

Villines, Jonathan A., Carmen T. Agouridis, Richard C. Warner, and Christopher D. Barton, 2015. Using GIS to Delineate Headwater Stream Origins in the Appalachian Coalfields of Kentucky. Journal of the American Water Resources Association (JAWRA) 1-21. DOI: 10.1111/1752-1688.12350

CHAPTER 4: Summary

The main goal of this study was to develop a GIS model to automatically and accurately place stream channel head locations across different physiographic regions of Alabama, U.S. The specific objectives to achieve this goal were to assess the slope-area model and its ability to locate channel heads under a variety of physiographic regions and to explore what other topographic variables may improve the model's explanatory capability in each physiographic region. For this purpose, a total of 162 stream channel head locations were mapped across the three physiographic region of Alabama, including Coastal Plain (*n*=51), Piedmont/Ridge and Valley (*n*=60), and Southwestern Appalachians (*n*=51), and were evaluated along with their topographic, climatic, and soil characteristics.

For the first part of this study, the slope-area models derived from strictly topographic parameters (i.e. drainage area and local slope) were developed for each physiographic region, and the results were compared to the National Hydrographic Dataset (NHD). Increasing drainage area size with decreasing local valley gradient was a trend observed in all of the study sites. The slope-area scatterplots of the three study sites demonstrated an inverse correlation between the local slope and the drainage area; however, the model resulted in excessively small drainage areas where highly dissected topography were observed, such as the Piedmont/Ridge and Valley and Southwestern Appalachians regions. The model reliability and sensitivity were also calculated as low to moderate in the study sites; however, the model had advantages for depicting headwater streams compared to topographic maps or NHD.

In the following study, other variables related to channel initiation (e.g., curvature, soil, and climate) for each field mapped stream channel head locations were obtained from readily available GIS datasets and were statistically analyzed to develop a multi-variable model for each physiographic region and a comprehensive state multi-variable model. The topographic variables were highly correlated with drainage area and were the primary explanatory variables of stream channel head initiation within regions; however, soil and climatic variables had a strong correlation with drainage area when the entire dataset was pooled. The region specific multi-variable model satisfactorily located stream channel head locations with relatively higher reliability and sensitivity scores compared to the slope-area and comprehensive multi-variable models. The comprehensive multi-variable model resulted in a similar performance with the slope-area model in all of the study sites. Thus, it can be concluded that this method could be used to automatically locate stream channel head locations across the state of Alabama if field mapped stream channel head location data is not available. The advantage of this method is that all the data used in this study can be generated from publicly available datasets that cover the entire United States. This means that with some field mapped stream channel head locations, the region specific model can be easily developed anywhere to have a better representation of the actual stream network.

The stream channel head locations evaluated in this thesis study were mapped in national forests of Alabama to demonstrate forest conditions. Thus, they do not represent the entire region, which has variety of land cover types. Expansion of a project such as this may better elucidate the importance of various factors. For instance, the field mapped stream channel head locations in each study sites were too close to each other; therefore, little spatial variation in soil and climate variables was observed within regions.

Suggestions for future work include mapping and evaluating stream a larger number of stream channel head locations with a wider range of slope and spatial variation to fully demonstrate the effects of soil and climatic variables within a physiographic region. Since stream channel head initiation is affected by different runoff processes, assessing the performance of slope-area method and developing the multi-variable model with a larger sample size including all runoff processes could provide better insight as to whether or not these models can be generalized to the entire U.S.

Future work may also include development of a model that can be applied to the entire U.S. for accurately locating stream channel heads. To do so, the stream channel head location data used in earlier studies across the United States might be gathered and evaluated using meta-analysis. A GIS toolbox would be created to provide a user-friendly interface to easily delineate stream channel head locations. By evaluating a wide range of studies and combining these data, a broader comprehensive model may be achieved for better stream mapping and watershed management.

Appendix 1: Coordinates of field mapped stream channel head locations

Point Number	Location	Longitude (UTM Zone-16)	Latitude (UTM Zone-16)
1	Conecuh	87° 14' 47.640" W	34° 16' 33.039" N
2	Conecuh	87° 22' 54.006" W	34° 13' 4.656" N
3	Conecuh	87° 22' 24.690" W	34° 13' 3.772" N
4	Conecuh	87° 14' 14.391" W	34° 16' 31.157" N
5	Conecuh	87° 14' 39.041" W	34° 16' 35.004" N
6	Conecuh	87° 14' 0.699" W	34° 16' 29.885" N
7	Conecuh	87° 14' 23.804" W	34° 16' 40.554" N
8	Conecuh	87° 14' 49.983" W	34° 16' 31.736" N
9	Conecuh	87° 14' 10.079" W	34° 16' 27.594" N
10	Conecuh	87° 14' 26.932" W	34° 16' 40.223" N
11	Conecuh	87° 14' 0.323" W	34° 16' 35.080" N
12	Conecuh	87° 22' 34.479" W	34° 13' 7.963" N
13	Conecuh	87° 14' 0.716" W	34° 16' 36.053" N
14	Conecuh	87° 14' 14.817" W	34° 16' 43.493" N
15	Conecuh	87° 14' 55.054" W	34° 16' 27.505" N
16	Conecuh	87° 22' 34.896" W	34° 13' 13.806" N
17	Conecuh	87° 23' 4.138" W	34° 12' 58.131" N
18	Conecuh	87° 14' 17.179" W	34° 16' 49.008" N
19	Conecuh	87° 14' 42.165" W	34° 16' 33.375" N
20	Conecuh	87° 14' 30.831" W	34° 16' 35.995" N
21	Conecuh	87° 14' 23.436" W	34° 16' 48.671" N
22	Conecuh	87° 14' 53.092" W	34° 16' 25.236" N
23	Conecuh	87° 14' 19.083" W	34° 16' 30.823" N
24	Conecuh	87° 14' 8.581" W	34° 16' 51.297" N
25	Conecuh	87° 22' 46.148" W	34° 12' 55.590" N
26	Conecuh	87° 14' 12.077" W	34° 16' 42.525" N
27	Conecuh	87° 22' 54.702" W	34° 12' 45.823" N
28	Conecuh	87° 22' 47.693" W	34° 12' 51.364" N
29	Conecuh	87° 14' 10.146" W	34° 16' 51.619" N
30	Conecuh	87° 14' 33.959" W	34° 16' 35.664" N
31	Conecuh	87° 22' 18.047" W	34° 13' 4.117" N
32	Conecuh	87° 22' 31.377" W	34° 13' 13.492" N
33	Conecuh	87° 23' 8.013" W	34° 12' 50.976" N
34	Conecuh	87° 22' 53.174" W	34° 12' 53.620" N
35	Conecuh	87° 14' 13.267" W	34° 16' 48.691" N
36	Conecuh	87° 13' 56.007" W	34° 16' 30.218" N
37	Conecuh	87° 22' 40.344" W	34° 13' 8.594" N

Point Number	Location	Longitude (UTM Zone-16)	Latitude (UTM Zone-16)
38	Conecuh	87° 22' 36.355" W	34° 12' 50.425" N
39	Conecuh	87° 14' 22.646" W	34° 16' 45.751" N
40	Conecuh	87° 22' 30.121" W	34° 12' 54.665" N
41	Conecuh	87° 22' 47.677" W	34° 12' 47.793" N
42	Conecuh	87° 23' 8.445" W	34° 13' 0.066" N
43	Conecuh	87° 14' 5.814" W	34° 16' 40.913" N
44	Conecuh	87° 23' 0.653" W	34° 13' 5.285" N
45	Conecuh	87° 14' 10.898" W	34° 16' 40.579" N
46	Conecuh	87° 23' 10.738" W	34° 12' 48.695" N
47	Conecuh	87° 14' 15.935" W	34° 16' 23.687" N
48	Conecuh	87° 22' 50.910" W	34° 13' 11.484" N
49	Conecuh	87° 22' 43.374" W	34° 12' 46.832" N
50	Conecuh	87° 14' 6.950" W	34° 16' 27.600" N
51	Conecuh	87° 14' 47.230" W	34° 16' 26.547" N
52	Talladega	86° 5' 27.604" W	33° 20' 37.666" N
53	Talladega	86° 5' 49.846" W	33° 20' 56.661" N
54	Talladega	86° 5' 41.944" W	33° 20' 35.173" N
55	Talladega	86° 5' 25.979" W	33° 20' 45.122" N
56	Talladega	86° 5' 53.735" W	33° 20' 54.741" N
57	Talladega	86° 6' 15.125" W	33° 20' 43.856" N
58	Talladega	86° 5' 20.530" W	33° 20' 48.329" N
59	Talladega	86° 5' 36.848" W	33° 20' 41.630" N
60	Talladega	86° 6' 13.961" W	33° 20' 44.172" N
61	Talladega	86° 5' 56.063" W	33° 20' 54.108" N
62	Talladega	86° 6' 5.794" W	33° 20' 48.334" N
63	Talladega	86° 5' 46.678" W	33° 21' 3.781" N
64	Talladega	86° 5' 34.137" W	33° 20' 41.935" N
65	Talladega	86° 5' 24.398" W	33° 20' 48.357" N
66	Talladega	86° 5' 33.353" W	33° 20' 42.903" N
67	Talladega	86° 6' 4.614" W	33° 20' 50.274" N
68	Talladega	86° 5' 56.813" W	33° 20' 56.387" N
69	Talladega	86° 5' 52.558" W	33° 20' 56.356" N
70	Talladega	86° 5' 38.436" W	33° 20' 37.745" N
71	Talladega	86° 5' 21.288" W	33° 20' 12.618" N
72	Talladega	86° 5' 13.230" W	33° 20' 6.389" N
73	Talladega	86° 6' 4.594" W	33° 20' 52.222" N
74	Talladega	86° 5' 24.089" W	33° 20' 40.887" N
75	Talladega	86° 5' 49.386" W	33° 21' 3.801" N
76	Talladega	86° 6' 5.397" W	33° 20' 49.305" N

Point Number	Location	Longitude (UTM Zone-16)	Latitude (UTM Zone-16)
77	Talladega	86° 6' 8.899" W	33° 20' 47.382" N
78	Talladega	86° 5' 20.190" W	33° 20' 43.781" N
79	Talladega	86° 5' 35.011" W	33° 20' 32.200" N
80	Talladega	86° 5' 8.514" W	33° 20' 13.498" N
81	Talladega	86° 6' 11.207" W	33° 20' 48.698" N
82	Talladega	86° 5' 38.412" W	33° 20' 40.018" N
83	Talladega	86° 5' 25.674" W	33° 20' 37.327" N
84	Talladega	86° 5' 23.275" W	33° 20' 44.777" N
85	Talladega	86° 5' 40.363" W	33° 20' 38.408" N
86	Talladega	86° 5' 35.321" W	33° 20' 39.670" N
87	Talladega	86° 5' 39.283" W	33° 20' 30.608" N
88	Talladega	86° 5' 9.695" W	33° 20' 11.558" N
89	Talladega	86° 5' 23.956" W	33° 20' 16.534" N
90	Talladega	86° 5' 33.050" W	33° 20' 34.783" N
91	Talladega	86° 5' 38.103" W	33° 20' 32.547" N
92	Talladega	86° 6' 12.781" W	33° 20' 46.112" N
93	Talladega	86° 5' 27.927" W	33° 20' 43.837" N
94	Talladega	86° 5' 46.762" W	33° 20' 55.664" N
95	Talladega	86° 5' 15.426" W	33° 20' 18.419" N
96	Talladega	86° 5' 44.367" W	33° 21' 2.790" N
97	Talladega	86° 6' 11.190" W	33° 20' 50.321" N
98	Talladega	86° 5' 29.562" W	33° 20' 35.407" N
99	Talladega	86° 5' 13.203" W	33° 20' 8.987" N
100	Talladega	86° 5' 16.196" W	33° 20' 18.750" N
101	Talladega	86° 5' 40.430" W	33° 20' 31.915" N
102	Talladega	86° 5' 8.551" W	33° 20' 9.926" N
103	Talladega	86° 5' 34.611" W	33° 20' 33.496" N
104	Talladega	86° 5' 20.841" W	33° 20' 18.459" N
105	Talladega	86° 5' 43.081" W	33° 20' 37.454" N
106	Talladega	86° 5' 56.056" W	33° 20' 54.758" N
107	Talladega	86° 5' 24.873" W	33° 20' 39.919" N
108	Talladega	86° 5' 42.748" W	33° 20' 32.257" N
109	Talladega	86° 6' 4.217" W	33° 20' 51.245" N
110	Talladega	86° 5' 30.655" W	33° 20' 41.909" N
111	Talladega	86° 6' 6.531" W	33° 20' 51.911" N
112	William	87° 14' 47.640" W	34° 16' 33.039" N
113	William	87° 22' 54.006" W	34° 13' 4.656" N
114	William	87° 22' 24.690" W	34° 13' 3.772" N
115	William	87° 14' 14.391" W	34° 16' 31.157" N

Point Number	Location	Longitude (UTM Zone-16)	Latitude (UTM Zone-16)
116	William	87° 14' 39.041" W	34° 16' 35.004" N
117	William	87° 14' 0.699" W	34° 16' 29.885" N
118	William	87° 14' 23.804" W	34° 16' 40.554" N
119	William	87° 14' 49.983" W	34° 16' 31.736" N
120	William	87° 14' 10.079" W	34° 16' 27.594" N
121	William	87° 14' 26.932" W	34° 16' 40.223" N
122	William	87° 14' 0.323" W	34° 16' 35.080" N
123	William	87° 22' 34.479" W	34° 13' 7.963" N
124	William	87° 14' 0.716" W	34° 16' 36.053" N
125	William	87° 14' 14.817" W	34° 16' 43.493" N
126	William	87° 14' 55.054" W	34° 16' 27.505" N
127	William	87° 22' 34.896" W	34° 13' 13.806" N
128	William	87° 23' 4.138" W	34° 12' 58.131" N
129	William	87° 14' 17.179" W	34° 16' 49.008" N
130	William	87° 14' 42.165" W	34° 16' 33.375" N
131	William	87° 14' 30.831" W	34° 16' 35.995" N
132	William	87° 14' 23.436" W	34° 16' 48.671" N
133	William	87° 14' 53.092" W	34° 16' 25.236" N
134	William	87° 14' 19.083" W	34° 16' 30.823" N
135	William	87° 14' 8.581" W	34° 16' 51.297" N
136	William	87° 22' 46.148" W	34° 12' 55.590" N
137	William	87° 14' 12.077" W	34° 16' 42.525" N
138	William	87° 22' 54.702" W	34° 12' 45.823" N
139	William	87° 22' 47.693" W	34° 12' 51.364" N
140	William	87° 14' 10.146" W	34° 16' 51.619" N
141	William	87° 14' 33.959" W	34° 16' 35.664" N
142	William	87° 22' 18.047" W	34° 13' 4.117" N
143	William	87° 22' 31.377" W	34° 13' 13.492" N
144	William	87° 23' 8.013" W	34° 12' 50.976" N
145	William	87° 22' 53.174" W	34° 12' 53.620" N
146	William	87° 14' 13.267" W	34° 16' 48.691" N
147	William	87° 13' 56.007" W	34° 16' 30.218" N
148	William	87° 22' 40.344" W	34° 13' 8.594" N
149	William	87° 22' 36.355" W	34° 12' 50.425" N
150	William	87° 14' 22.646" W	34° 16' 45.751" N
151	William	87° 22' 30.121" W	34° 12' 54.665" N
152	William	87° 22' 47.677" W	34° 12' 47.793" N
153	William	87° 23' 8.445" W	34° 13' 0.066" N
154	William	87° 14' 5.814" W	34° 16' 40.913" N

Point Number	Location	Longitude (UTM Zone-16)	Latitude (UTM Zone-16)
155	William	87° 23' 0.653" W	34° 13' 5.285" N
156	William	87° 14' 10.898" W	34° 16' 40.579" N
157	William	87° 23' 10.738" W	34° 12' 48.695" N
158	William	87° 14' 15.935" W	34° 16' 23.687" N
159	William	87° 22' 50.910" W	34° 13' 11.484" N
160	William	87° 22' 43.374" W	34° 12' 46.832" N
161	William	87° 14' 6.950" W	34° 16' 27.600" N
162	William	87° 14' 47.230" W	34° 16' 26.547" N

Appendix 2: Supplementary Data

Point Number	DA	Sloc	Savr	PLloc	PLavr	PRloc	PRavr	Ksat	Kfac	Dbdr	%Sand	%Clay	Pannual	Pint
CP-1	1588	0.1477	0.1241	-0.7949	-0.1414	0.0050	-0.2151	7.27	0.32	201	63.9	9.5	1565	41.79
CP-2	1822	0.0141	0.0119	-0.0639	-0.0105	0.0732	-0.0080	8.51	0.24	201	74.1	10.4	1569	41.91
CP-3	2089	0.0162	0.0411	-0.0184	0.0173	0.0276	0.0116	8.51	0.24	201	74.1	10.4	1558	41.72
CP-4	2388	0.0104	0.0193	-0.1444	-0.0222	0.0863	-0.0212	41.87	0.17	201	93.2	5.5	1577	41.93
CP-5	3781	0.0223	0.0417	-0.2348	0.0033	0.0282	0.0035	10.95	0.24	201	66.1	14	1559	41.72
CP-6	4617	0.1222	0.0558	-0.1156	-0.0204	-0.4858	-0.0496	10.95	0.24	201	66.1	14	1574	41.91
CP-7	5126	0.0518	0.0338	-0.0126	-0.0192	-0.0550	-0.0304	12.93	0.24	201	63.5	10	1574	41.93
CP-8	5238	0.0328	0.0430	-0.4459	-0.0458	0.8289	-0.0467	41.87	0.17	201	93.2	5.5	1572	41.90
CP-9	5268	0.0555	0.0302	-0.1789	-0.0170	0.0417	-0.0218	41.87	0.17	201	93.2	5.5	1572	41.90
CP-10	5486	0.1119	0.0614	-0.5470	-0.0479	-0.1565	-0.0558	10.95	0.24	201	66.1	14	1570	41.86
CP-11	5505	0.0583	0.0720	-0.8632	-0.0413	0.7281	-0.0485	10.95	0.24	201	66.1	14	1565	41.81
CP-12	5802	0.0121	0.0264	-0.1461	-0.0294	0.0620	-0.0262	12.93	0.24	201	63.5	10	1571	41.91
CP-13	5857	0.0208	0.0243	-0.0630	0.0069	0.0419	0.0046	12.93	0.24	201	63.5	10	1572	41.93
CP-14	5867	0.0479	0.0300	-0.1312	-0.0134	0.0511	-0.0245	10.95	0.24	201	66.1	14	1569	41.87
CP-15	5878	0.0745	0.0411	-0.5435	-0.0600	-0.0996	-0.0633	44.46	0.17	201	84.9	6	1575	41.94
CP-16	6102	0.0341	0.0404	-0.1846	-0.0294	0.0777	-0.0302	12.93	0.24	201	63.5	10	1575	41.96
CP-17	6156	0.0197	0.0577	-0.2323	-0.0032	-0.0110	-0.0098	10.95	0.24	201	66.1	14	1574	41.90
CP-18	6529	0.0261	0.0591	-0.1892	-0.0724	0.3223	-0.0867	12.93	0.24	201	63.5	10	1572	41.91
CP-19	6756	0.0242	0.0228	-0.0862	-0.0095	0.0250	-0.0160	8.51	0.24	201	74.1	10.4	1569	41.90
CP-20	6974	0.0553	0.0400	-0.1527	-0.0555	-0.0513	-0.0600	12.93	0.24	201	63.5	10	1574	41.93
CP-21	6996	0.0297	0.0176	-0.0030	-0.0178	0.1147	-0.0210	10.95	0.24	201	66.1	14	1568	41.84
CP-22	7076	0.0652	0.0443	-0.4422	-0.0363	0.2772	-0.0391	41.87	0.17	201	93.2	5.5	1572	41.88
CP-23	7203	0.0231	0.0139	-0.0088	-0.0098	-0.0320	-0.0132	8.51	0.24	201	74.1	10.4	1574	41.94
CP-24	7479	0.0208	0.0334	-0.2081	-0.0184	0.1742	-0.0166	12.93	0.24	201	63.5	10	1574	41.97
CP-25	7571	0.0299	0.0333	-0.1290	0.0034	0.0242	0.0019	8.51	0.24	201	74.1	10.4	1569	41.87

CP-26	7629	0.0389	0.0211	-0.1346	-0.0063	-0.0435	-0.0058	8.51	0.24	201	74.1	10.4	1567	41.85
CP-27	8595	0.0297	0.0437	-0.4807	-0.0340	0.2629	-0.0332	44.46	0.17	201	84.9	6	1575	41.96
CP-28	9002	0.0569	0.0641	-0.4552	-0.0516	0.2026	-0.0549	10.95	0.24	201	66.1	14	1570	41.85
CP-29	9440	0.0601	0.0435	-0.5031	-0.0309	0.2471	-0.0332	41.87	0.17	201	93.2	5.5	1572	41.88
CP-30	9479	0.0468	0.0302	-0.3428	-0.0409	-0.1719	-0.0399	8.51	0.24	201	74.1	10.4	1567	41.83
CP-31	9551	0.0262	0.0411	-0.1614	-0.0055	-0.0400	-0.0100	10.95	0.24	201	66.1	14	1568	41.86
CP-32	9595	0.0640	0.0598	-0.4366	-0.0387	-0.0103	-0.0432	12.93	0.24	201	63.5	10	1575	41.92
CP-33	9663	0.0219	0.0437	-0.1500	-0.0281	-0.1048	-0.0268	10.95	0.24	201	66.1	14	1570	41.84
CP-34	9829	0.0278	0.0490	-0.0813	-0.0005	-0.0215	-0.0042	10.95	0.24	201	66.1	14	1560	41.73
CP-35	10255	0.0420	0.0573	-0.5074	-0.0556	0.3467	-0.0556	12.93	0.24	201	63.5	10	1575	41.92
CP-36	11292	0.0610	0.0392	-0.6584	-0.0420	0.8010	-0.0425	40.43	0.2	201	84.3	6.5	1565	41.81
CP-37	12714	0.0155	0.0324	-0.2871	0.0058	0.1299	0.0070	10.95	0.24	201	66.1	14	1568	41.84
CP-38	14282	0.0373	0.0594	-0.5041	-0.0134	0.7269	-0.0234	10.95	0.24	201	66.1	14	1568	41.82
CP-39	16785	0.0215	0.0335	-0.6097	-0.0291	0.4600	-0.0276	12.93	0.24	201	63.5	10	1575	41.96
CP-40	17005	0.0079	0.0340	-0.1117	-0.0030	0.3028	-0.0039	41.87	0.17	201	93.2	5.5	1572	41.91
CP-41	20657	0.0091	0.0214	-0.0588	-0.0113	0.0024	-0.0097	44.46	0.17	201	84.9	6	1569	41.89
CP-42	22400	0.0079	0.0471	-0.1806	-0.0102	0.2291	-0.0109	8.51	0.24	201	74.1	10.4	1562	41.73
CP-43	27435	0.0195	0.0620	-1.9963	-0.0497	1.4456	-0.0529	10.95	0.24	201	66.1	14	1567	41.80
CP-44	37325	0.0026	0.0362	-0.1085	-0.0233	0.1258	-0.0245	12.93	0.24	201	63.5	10	1574	41.95
CP-45	37503	0.0078	0.0461	-0.1544	-0.0110	0.1924	-0.0116	10.95	0.24	201	66.1	14	1558	41.71
CP-46	39553	0.0047	0.0562	-0.2218	-0.0226	0.1099	-0.0242	8.51	0.24	201	74.1	10.4	1558	41.71
CP-47	44899	0.0033	0.0281	-0.1434	-0.0078	0.0827	-0.0061	8.51	0.24	201	74.1	10.4	1569	41.86
CP-48	53869	0.0172	0.0315	-0.1369	-0.0105	0.0029	-0.0098	8.51	0.24	201	74.1	10.4	1567	41.84
CP-49	59316	0.0036	0.0341	-0.1508	-0.0142	-0.0105	-0.0155	41.87	0.17	201	93.2	5.5	1571	41.91
CP-50	65478	0.0011	0.0360	-0.3574	-0.0160	0.7375	-0.0154	41.87	0.17	201	93.2	5.5	1565	41.79
CP-51	76308	0.0049	0.0315	-0.3263	0.0017	0.1141	0.0017	8.51	0.24	201	74.1	10.4	1569	41.87
P/RV-1	264	0.3393	0.2536	0.6356	0.5225	-1.1429	-0.6049	6.00	0.2	46	29.7	52.3	1399	32
P/RV-2	313	0.2844	0.2666	-0.3457	0.0078	0.5655	-0.9659	6.00	0.2	46	29.7	52.3	1393	32
P/RV-3	321	0.1552	0.2048	0.1387	0.3502	0.3699	-0.2841	6.00	0.2	46	29.7	52.3	1399	32
P/RV-4	321	0.3356	0.2987	-1.2668	-0.0485	-0.6865	-1.1061	5.85	0.2	43	29.7	52.3	1395	32

P/RV-5	345	0.2409	0.2123	-0.5572	0.3370	-0.1682	-0.4074	6.00	0.2	46	29.7	52.3	1393	32
P/RV-6	380	0.3300	0.2863	-0.2486	0.4127	-0.3860	-0.5789	6.00	0.2	46	29.7	52.3	1393	32
P/RV-7	381	0.2748	0.3084	0.0263	0.2282	-0.5166	-0.4815	5.85	0.2	43	29.7	52.3	1395	32
P/RV-8	389	0.2534	0.1223	-0.2999	0.1254	-1.3819	-0.1430	6.00	0.2	46	29.7	52.3	1399	32
P/RV-9	393	0.2846	0.1992	-0.0713	0.0971	-0.3856	-0.4492	6.00	0.2	46	29.7	52.3	1396	32
P/RV-10	400	0.2705	0.2416	-0.9163	-0.2268	0.2347	-0.5301	5.85	0.2	43	29.7	52.3	1393	32
P/RV-11	407	0.3604	0.2315	0.1326	-0.1403	-0.6069	-0.5217	6.00	0.2	46	29.7	52.3	1393	32
P/RV-12	456	0.1707	0.1661	-0.2284	0.1099	0.3438	-0.2166	5.85	0.2	43	29.7	52.3	1399	32
P/RV-13	479	0.3496	0.3152	-1.5729	0.0143	1.1177	-0.5957	6.00	0.2	46	29.7	52.3	1395	32
P/RV-14	500	0.1886	0.1787	-1.1078	0.0376	0.1233	-0.3483	6.00	0.2	46	29.7	52.3	1399	32
P/RV-15	502	0.2367	0.2861	-0.3376	0.1661	0.7134	-0.2069	6.00	0.2	46	29.7	52.3	1393	32
P/RV-16	506	0.1992	0.2073	-0.1772	0.0512	0.1385	-0.2358	6.00	0.2	46	29.7	52.3	1393	32
P/RV-17	508	0.2140	0.2294	-0.1198	0.2171	0.7822	-0.1489	6.00	0.2	46	29.7	52.3	1393	32
P/RV-18	509	0.2271	0.1769	0.4552	0.3075	-0.4991	-0.1681	5.85	0.2	43	29.7	52.3	1399	32
P/RV-19	529	0.1400	0.1040	-0.3352	0.1379	-0.1932	-0.1050	5.85	0.2	43	29.7	52.3	1404	32
P/RV-20	529	0.1388	0.0992	0.0154	0.2332	-0.1147	-0.0704	5.85	0.2	43	29.7	52.3	1408	32
P/RV-21	530	0.2698	0.2677	0.0989	0.1518	0.6494	-0.3792	5.85	0.2	43	29.7	52.3	1393	32
P/RV-22	531	0.2409	0.2733	-0.0077	0.0915	-0.2065	-0.3581	6.00	0.2	46	29.7	52.3	1399	32
P/RV-23	543	0.2985	0.3435	-1.2866	-0.0003	2.0945	-0.3896	6.00	0.2	46	29.7	52.3	1393	32
P/RV-24	547	0.2699	0.1786	-0.0900	0.0657	0.0307	-0.3655	6.00	0.2	46	29.7	52.3	1393	32
P/RV-25	548	0.1903	0.2634	-0.1185	0.2104	0.6161	-0.0515	6.00	0.2	46	29.7	52.3	1399	32
P/RV-26	557	0.1353	0.1599	-0.9355	0.0060	0.0419	0.0951	6.00	0.2	46	29.7	52.3	1399	32
P/RV-27	557	0.2567	0.1578	0.1185	0.1756	-0.8991	-0.2015	6.00	0.2	46	29.7	52.3	1408	32
P/RV-28	561	0.3450	0.3248	0.2610	0.1888	-0.0248	-0.2016	6.00	0.2	46	29.7	52.3	1393	32
P/RV-29	562	0.3580	0.2168	-0.1119	-0.0909	-1.1220	-0.6136	6.00	0.2	46	29.7	52.3	1399	32
P/RV-30	596	0.1431	0.2080	-1.4470	0.4564	1.6658	-0.0354	5.85	0.2	43	29.7	52.3	1399	32
P/RV-31	599	0.3773	0.3874	0.0588	0.4612	0.0836	-0.3387	6.00	0.2	46	29.7	52.3	1399	32
P/RV-32	618	0.2174	0.2132	-1.0701	0.1118	0.3842	-0.2359	6.00	0.2	46	29.7	52.3	1399	32
P/RV-33	636	0.1704	0.2519	-0.8828	0.2689	2.0443	-0.0183	6.00	0.2	46	29.7	52.3	1399	32
P/RV-34	640	0.2203	0.1058	-0.3051	-0.2502	-1.2182	-0.5000	6.00	0.2	46	29.7	52.3	1399	32

P/RV-35	647	0.1665	0.1487	-1.7987	0.2008	0.8075	-0.1405	6.00	0.2	46	29.7	52.3	1408	32
P/RV-36	662	0.1501	0.1063	0.3120	0.0454	-0.2275	-0.0771	6.00	0.2	46	29.7	52.3	1399	32
P/RV-37	681	0.1552	0.1735	-0.3827	0.0539	1.9883	-0.0869	6.00	0.2	46	29.7	52.3	1399	32
P/RV-38	684	0.1902	0.2216	-0.6272	0.0730	0.2391	-0.1436	6.00	0.2	46	29.7	52.3	1399	32
P/RV-39	717	0.2040	0.2707	-0.2553	-0.1619	0.5588	-0.3138	6.00	0.2	46	29.7	52.3	1393	32
P/RV-40	745	0.1587	0.2769	-1.2636	-0.2481	1.2288	-0.2081	5.85	0.2	43	29.7	52.3	1399	32
P/RV-41	781	0.1329	0.1311	-0.8874	-0.0909	0.6800	-0.2765	6.00	0.2	46	29.7	52.3	1393	32
P/RV-42	826	0.1711	0.1310	-0.6678	-0.0527	0.0493	-0.0936	6.00	0.2	46	29.7	52.3	1399	32
P/RV-43	1091	0.2572	0.2164	-0.9519	-0.1305	0.5147	-0.3561	6.00	0.2	46	29.7	52.3	1393	32
P/RV-44	1138	0.2216	0.1980	-1.1203	0.0557	0.2571	-0.2197	6.00	0.2	46	29.7	52.3	1399	32
P/RV-45	1345	0.1583	0.1614	-1.0223	-0.0238	-0.0654	-0.1444	6.00	0.2	46	29.7	52.3	1408	32
P/RV-46	1376	0.1193	0.1273	-0.6832	-0.0953	0.0203	-0.0689	6.00	0.2	46	29.7	52.3	1399	32
P/RV-47	1426	0.0453	0.1144	-1.7663	0.0155	1.9033	0.1001	6.00	0.2	46	29.7	52.3	1399	32
P/RV-48	1519	0.1686	0.0653	-0.7832	-0.0993	-0.5410	-0.1342	6.00	0.2	46	29.7	52.3	1408	32
P/RV-49	1692	0.0829	0.1289	-0.5346	-0.2511	0.4015	-0.2084	6.00	0.2	46	29.7	52.3	1399	32
P/RV-50	1838	0.0261	0.1251	-1.5637	-0.1558	1.1912	-0.1082	6.00	0.2	46	29.7	52.3	1399	32
P/RV-51	2169	0.0586	0.0746	-1.4080	0.0112	0.7205	0.0230	5.85	0.2	43	29.7	52.3	1399	32
P/RV-52	3437	0.0748	0.1903	-1.5904	-0.2072	1.9087	-0.1645	5.85	0.2	43	29.7	52.3	1393	32
P/RV-53	3583	0.0405	0.1963	-1.6716	-0.3355	1.5667	-0.2864	6.00	0.2	46	29.7	52.3	1399	32
P/RV-54	3830	0.0322	0.1296	-1.5440	0.0097	1.2354	-0.0181	5.85	0.2	43	29.7	52.3	1399	32
P/RV-55	5499	0.0902	0.2113	-2.5993	-0.1304	1.7032	-0.1180	6.00	0.2	46	29.7	52.3	1393	32
P/RV-56	5566	0.0274	0.2004	-0.3881	-0.1890	1.9420	-0.1850	5.85	0.2	43	29.7	52.3	1399	32
P/RV-57	5969	0.0087	0.1876	-2.7505	-0.2412	2.4162	-0.2092	5.85	0.2	43	29.7	52.3	1393	32
P/RV-58	445	0.2742	0.2042	-0.2034	-0.1196	-0.2706	-0.3705	6.47	0.43	107	42.4	38.1	1393	32
P/RV-59	533	0.2396	0.1799	-0.1707	0.1201	-0.9485	-0.2745	6.47	0.43	107	42.4	38.1	1393	32
P/RV-60	872	0.1932	0.1458	-0.6279	0.0239	-0.4356	-0.1011	6.47	0.43	107	42.4	38.1	1395	32
SWA-1	425	0.4418	0.2920	-0.0507	0.1517	-0.7332	-0.9372	28.00	0.1	66	74.1	10.9	1471.2	32.01
SWA-2	505	0.1705	0.0794	-0.1931	0.0237	-0.1030	-0.2325	28.00	0.1	66	74.1	10.9	1503.9	32.13
SWA-3	559	0.6438	0.2693	1.2128	0.3329	-1.3810	-0.7147	28.00	0.1	66	74.1	10.9	1502.21	32.14
SWA-4	567	0.3331	0.1922	0.3558	0.0852	-0.7157	-0.2848	92.00	0.15	91	65.2	14.7	1469.58	32.02

SWA-5	595	0.2306	0.0794	-0.1318	0.0502	-1.4088	-0.3226	92.00	0.15	91	69.9	10	1470.33	32.01
SWA-6	627	0.1774	0.2444	-0.7956	0.1856	0.1627	-0.2823	92.00	0.15	91	65.2	14.7	1469.58	32.02
SWA-7	683	0.4683	0.2717	-1.2210	-0.4091	-0.5365	-1.1026	28.00	0.1	66	74.1	10.9	1470.33	32.01
SWA-8	750	0.2239	0.1042	-0.1983	0.0742	-1.2893	-0.1723	28.00	0.1	66	74.1	10.9	1471.2	32.01
SWA-9	757	0.3367	0.1424	-0.1986	-0.0857	-0.9327	-0.3196	92.00	0.15	91	65.2	14.7	1469.58	32.02
SWA-10	788	0.3707	0.1574	-0.2335	0.0772	-0.5752	-0.2471	28.00	0.1	66	74.1	10.9	1470.33	32.01
SWA-11	893	0.3464	0.1874	0.2663	0.0443	-1.4900	-0.3185	92.00	0.15	91	65.2	14.7	1469.58	32.02
SWA-12	940	0.3227	0.2388	-0.7022	-0.0681	1.1672	-0.4799	92.00	0.15	91	69.9	10	1502.21	32.13
SWA-13	943	0.2471	0.1879	-0.3931	0.0214	1.2515	-0.2224	92.00	0.15	91	65.2	14.7	1469.58	32.01
SWA-14	946	0.1665	0.1061	0.0557	0.0338	-0.1518	-0.1303	9.00	0.49	119	19	14	1469.58	32.01
SWA-15	974	0.2419	0.1164	-1.2412	-0.0334	0.8736	-0.3143	9.00	0.28	53	46.8	14.3	1471.2	32.02
SWA-16	990	0.4758	0.2885	-2.2146	-0.0957	0.6795	-0.4687	28.00	0.24	66	66.8	12	1502.21	32.13
SWA-17	1253	0.2481	0.2002	-1.2610	-0.3157	-0.3091	-0.4837	92.00	0.17	79	77.1	3.9	1503.9	32.13
SWA-18	1316	0.2514	0.2624	-0.9725	-0.1031	3.0380	-0.2661	92.00	0.17	79	77.1	3.9	1469.01	32.00
SWA-19	1396	0.1344	0.0322	0.0533	0.0056	-0.7861	-0.0731	92.00	0.15	91	69.9	10	1470.33	32.01
SWA-20	2063	0.1147	0.0795	-0.5668	0.0347	0.0015	-0.0027	92.00	0.15	91	69.9	10	1470.33	32.01
SWA-21	2374	0.1010	0.3034	-0.8704	-0.2545	-0.0533	-0.3118	28.00	0.1	66	74.1	10.9	1469.01	32.00
SWA-22	2492	0.1024	0.1284	-3.4741	-0.2032	2.3140	-0.2688	9.00	0.28	53	46.8	14.3	1471.2	32.02
SWA-23	3252	0.1114	0.1330	-1.8654	-0.1233	1.0279	-0.1817	92.00	0.15	91	65.2	14.7	1470.33	32.01
SWA-24	3648	0.0379	0.0975	-1.1266	-0.0127	0.8492	0.0003	9.00	0.49	119	16	16.5	1468.24	32.00
SWA-25	3737	0.2514	0.1080	-1.6891	-0.1764	0.0121	-0.1990	92.00	0.17	79	77.1	3.9	1503.9	32.14
SWA-26	3983	0.0938	0.1335	0.1183	-0.0085	0.3693	-0.0255	9.00	0.49	119	16	16.5	1469.58	32.01
SWA-27	4475	0.1464	0.0550	-0.8235	-0.0343	0.6697	-0.0746	92.00	0.17	79	77.1	3.9	1503.9	32.14
SWA-28	4507	0.1933	0.0683	-1.0124	-0.0560	0.7590	-0.0575	92.00	0.17	79	77.1	3.9	1503.9	32.14
SWA-29	4617	0.0746	0.1112	-0.3372	0.0445	-0.2029	0.0000	9.00	0.49	119	16	16.5	1468.24	32.00
SWA-30	5262	0.0775	0.0773	-0.3651	0.0219	0.2578	0.0131	28.00	0.1	66	74.1	10.9	1470.33	32.01
SWA-31	5841	0.1831	0.1089	-1.1363	-0.0788	0.3710	-0.0895	92.00	0.17	79	77.1	3.9	1502.21	32.14
SWA-32	5858	0.2431	0.1434	-2.3322	-0.1667	0.1734	-0.2111	28.00	0.24	66	66.8	12	1502.21	32.13
SWA-33	5951	0.1265	0.0672	-1.8356	-0.0487	0.3337	-0.0741	92.00	0.17	79	77.1	3.9	1503.9	32.14
SWA-34	6070	0.0245	0.0860	-0.6435	-0.0697	0.1012	-0.0711	92.00	0.17	79	77.1	3.9	1503.9	32.14

SWA-35	6321	0.0992	0.0987	-1.5536	-0.0514	0.9971	-0.0327	92.00	0.17	79	77.1	3.9	1468.24	32.00
SWA-36	7070	0.0921	0.1183	-0.9423	-0.1489	0.8137	-0.1463	92.00	0.15	91	65.2	14.7	1469.58	32.02
SWA-37	8169	0.2094	0.1219	-2.0787	-0.1075	0.7688	-0.1521	28.00	0.1	66	74.1	10.9	1502.21	32.13
SWA-38	8714	0.1220	0.0667	-1.1622	-0.1537	-0.2184	-0.1427	92.00	0.15	91	69.9	10	1502.21	32.15
SWA-39	9224	0.0578	0.2092	-1.0334	-0.1461	0.2003	-0.1465	28.00	0.1	66	74.1	10.9	1469.01	32.01
SWA-40	9388	0.0709	0.0446	-0.5639	-0.0637	-0.0363	-0.0643	92.00	0.17	79	77.1	3.9	1502.21	32.15
SWA-41	11030	0.0598	0.1157	-2.6052	-0.1130	2.8426	-0.1188	92.00	0.17	79	77.1	3.9	1503.9	32.15
SWA-42	11054	0.0938	0.1244	-2.7094	-0.1010	1.2370	-0.1115	92.00	0.17	79	77.1	3.9	1503.9	32.13
SWA-43	13910	0.0304	0.1229	-0.2977	-0.0973	0.8328	-0.0878	92.00	0.15	91	65.2	14.7	1469.58	32.01
SWA-44	18425	0.0636	0.0638	-2.2482	-0.0263	1.5021	-0.0223	28.00	0.1	66	74.1	10.9	1503.9	32.13
SWA-45	24245	0.0781	0.1197	-0.3046	-0.0415	-0.0589	-0.0476	9.00	0.49	119	16	16.5	1469.58	32.01
SWA-46	26569	0.0519	0.0797	-0.6396	-0.0289	0.1624	-0.0246	92.00	0.17	79	77.1	3.9	1503.9	32.14
SWA-47	30144	0.0537	0.1361	-0.4506	-0.0757	1.3759	-0.0694	92.00	0.15	91	65.2	14.7	1470.33	32.02
SWA-48	34324	0.0825	0.0242	-0.3445	0.0054	-0.1610	0.0043	28.00	0.24	66	66.8	12	1503.9	32.13
SWA-49	34588	0.0535	0.0630	-0.7949	-0.0219	-0.1275	-0.0185	92.00	0.17	79	77.1	3.9	1502.21	32.15
SWA-50	36501	0.0331	0.0983	-2.1108	-0.0734	3.1969	-0.0704	92.00	0.15	91	65.2	14.7	1469.58	32.02
SWA-51	43378	0.0848	0.0860	-3.5455	-0.0786	1.6492	-0.0799	28.00	0.1	66	74.1	10.9	1471.2	32.02

Appendix 3: Stream channel heads mapped in the Coastal Plain Region.

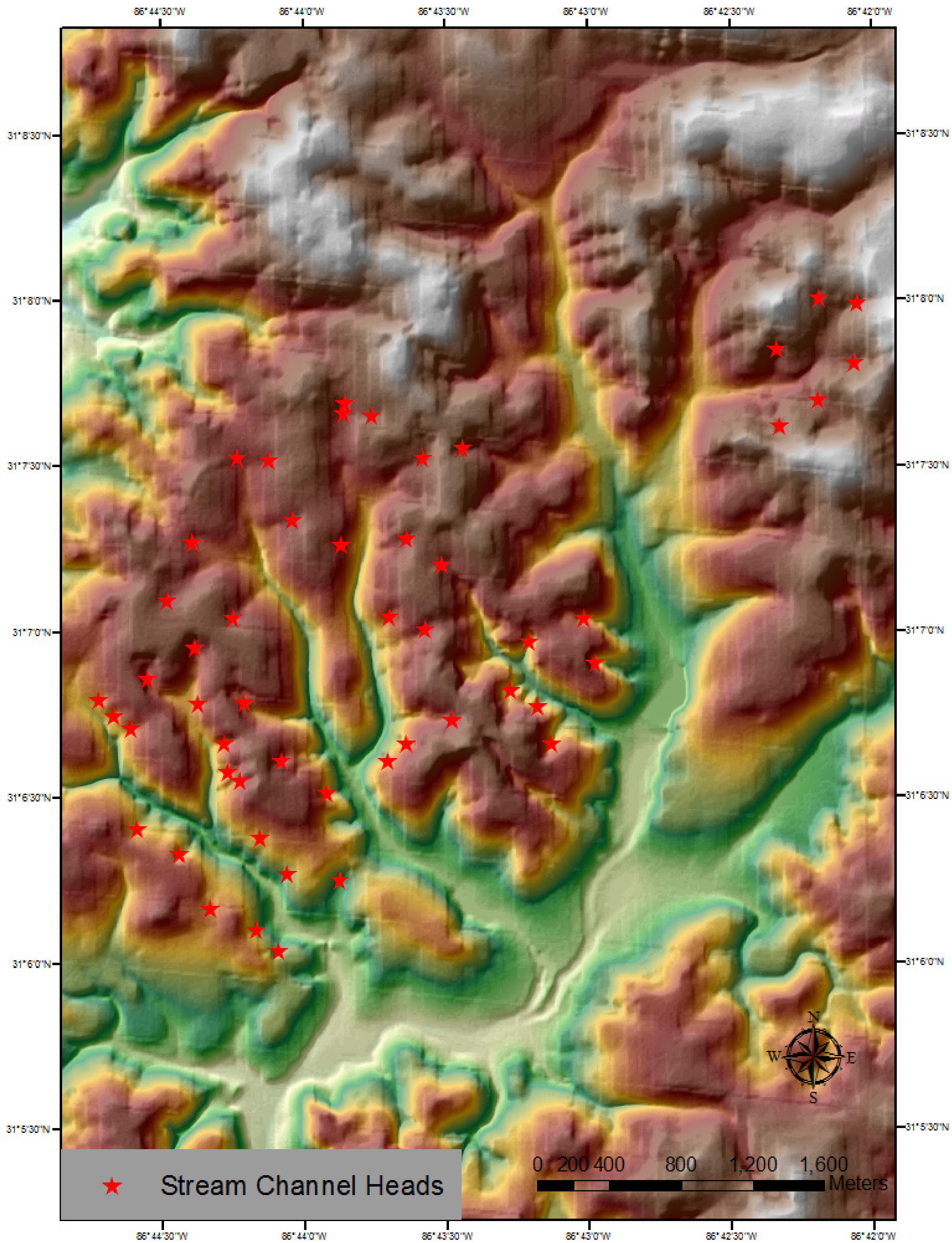

Appendix 3: Stream channel head mapped in the Piedmont/Ridge and Valley Region.

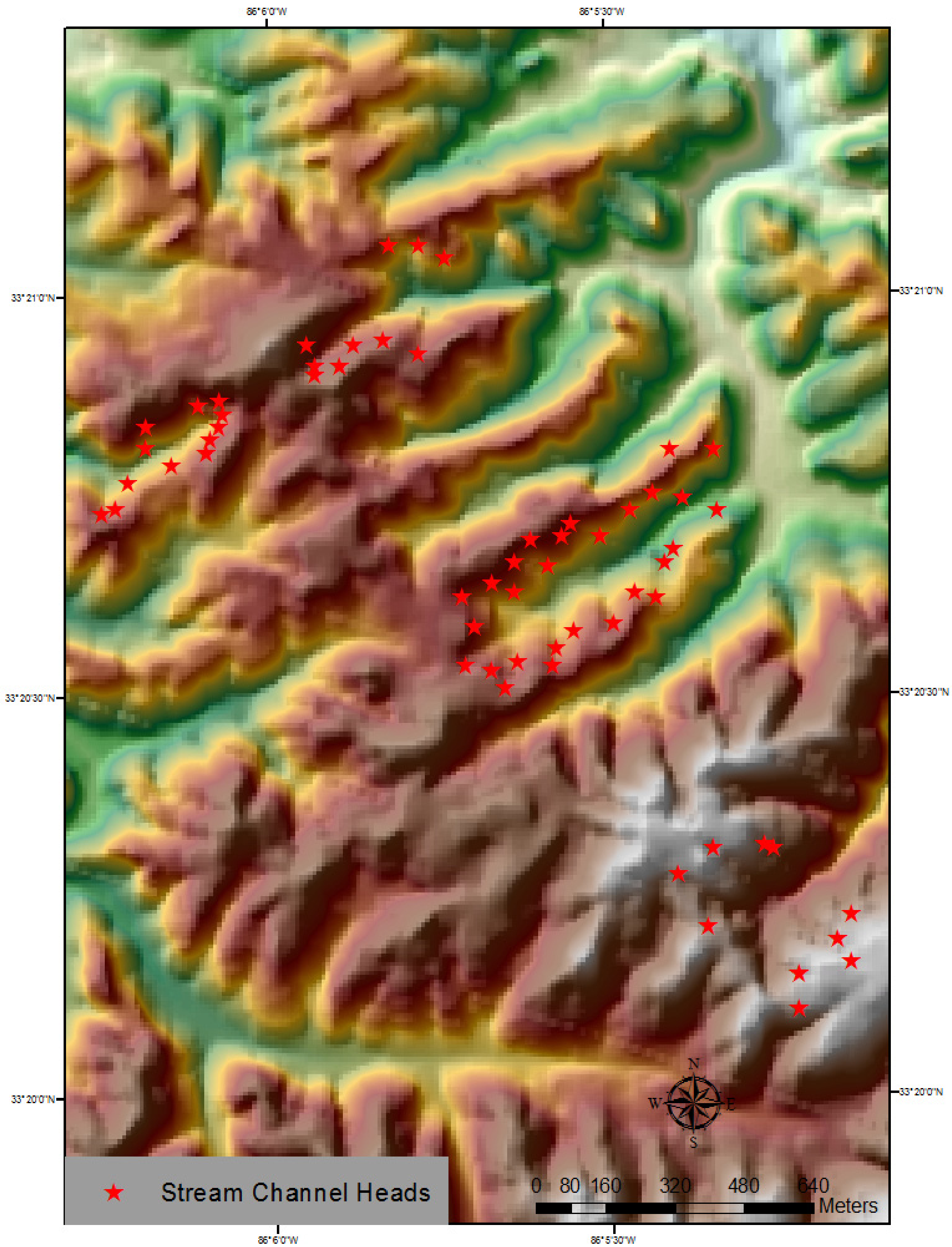

Appendix 3: Stream channel head mapped in the Southwestern Appalachians Region.

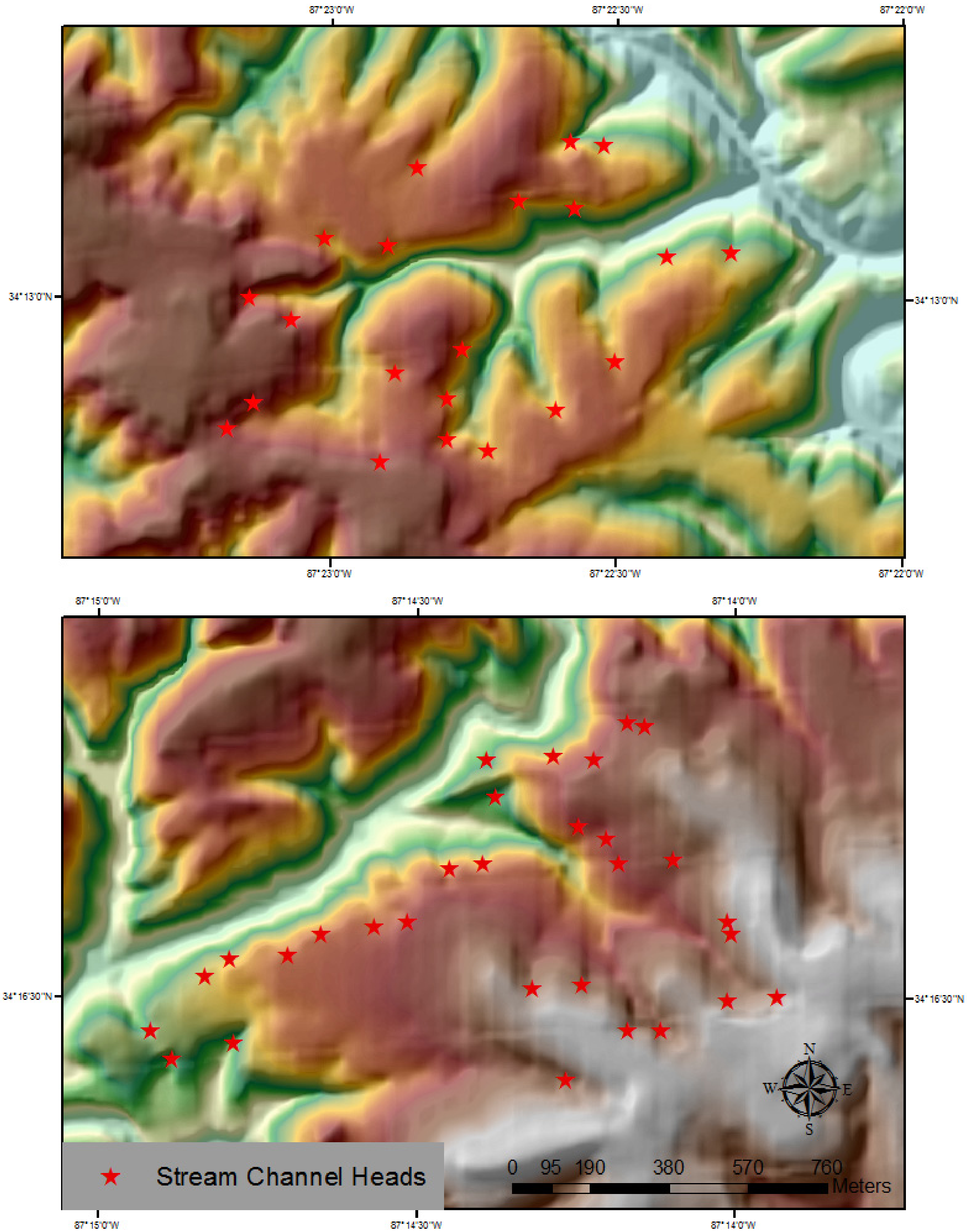

Appendix 4: GIS processing flow chart for Chapter 2

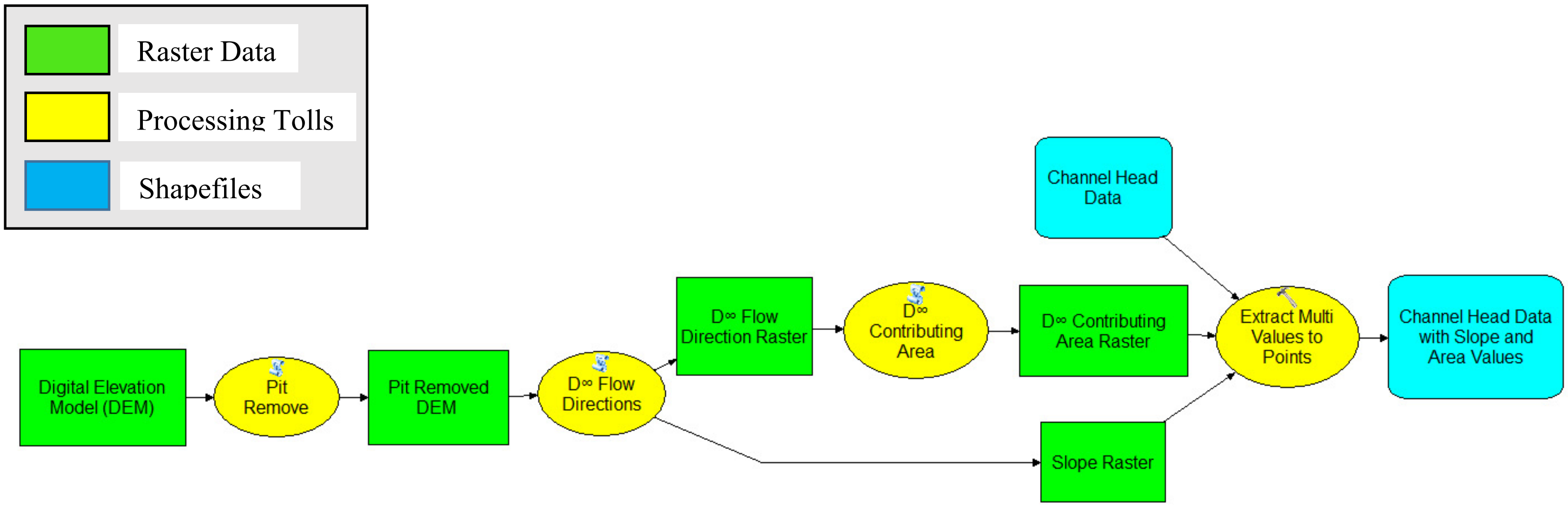

Appendix 5: GIS processing flow chart for Chapter 3

<u>Generating the topographic variables:</u>

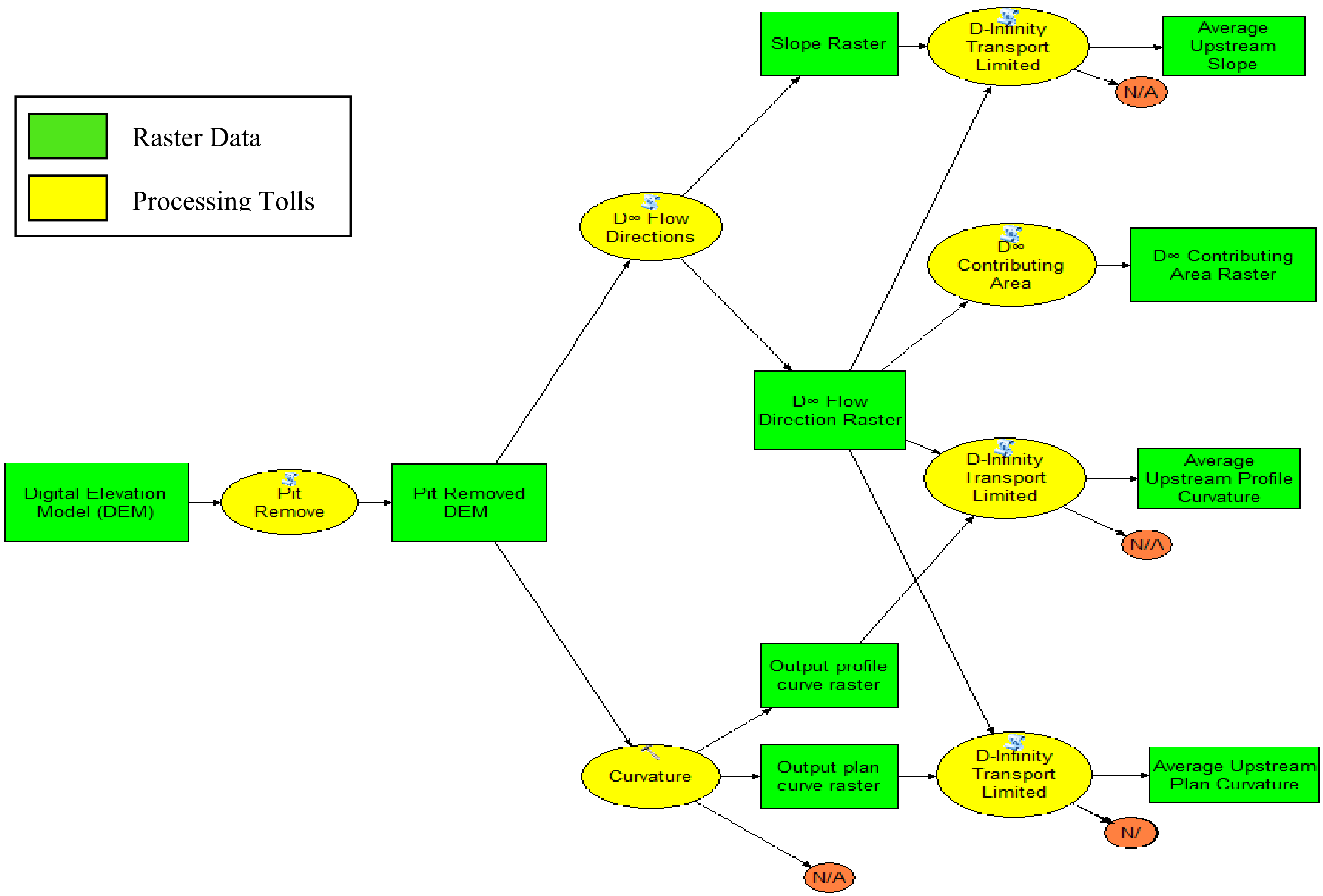

Extracting all values to stream channel head location data